การดัดแปรยางธรรมชาติดีโปรติไนซ์ด้วยการกราฟต์กับมาเลอิกแอนไฮไดรด์โดย
เทคนิคดิฟเฟอเรนเชียลไมโครอิมัลชันพอลิเมอไรเซชัน

นายภิญโญ วงษ์ทอง

วิทยานิพนธ์นี้เป็นส่วนหนึ่งของการศึกษาตามหลักสูตรปริญญาวิทยาศาสตรดุษฎีบัณฑิต
สาขาวิชาปิโตรเคมี
คณะวิทยาศาสตร์ จุฬาลงกรณ์มหาวิทยาลัย
ปีการศึกษา 2557

MODIFICATION OF DEPROTEINIZED NATURAL RUBBER BY GRAFTING WITH MALEIC ANHYDRIDE VIA DIFFERENTIAL MICROEMULSION POLYMERIZATION TECHNIQUE

Mr. Pinyo Wongthong

A Dissertation Submitted in Partial Fulfillment of the Requirements
for the Degree of Doctor of Philosophy Program in Petrochemistry
Faculty of Science
Chulalongkorn University
Academic Year 2014

Thesis Title	MODIFICATION OF DEPROTEINIZED NATURAL RUBBER BY GRAFTING WITH MALEIC ANHYDRIDE VIA DIFFERENTIAL MICROEMULSION POLYMERIZATION TECHNIQUE
By	Mr. Pinyo Wongthong
Field of Study	Petrochemistry
Thesis Advisor	Professor Suda Kiatkamjornwong, Ph.D.
Thesis Co-Advisor	Professor Garry L. Rempel, Ph.D.
	Professor Qinmin Pan, Ph.D.
	Associate Professor Charoen Nakason, Ph.D.

Accepted by the Faculty of Science, Chulalongkorn University in Partial Fulfillment of the Requirements for the Doctoral Degree

.....Dean of the Faculty of Science
(Professor Supot Hannongbua, Dr.rer.nat.)

THESIS COMMITTEE

.....Chairman
(Professor Pattarapan Prasassarakich, Ph.D.)

.....Thesis Advisor
(Professor Suda Kiatkamjornwong, Ph.D.)

.....Thesis Co-Advisor
(Professor Garry L. Rempel, Ph.D.)

.....Thesis Co-Advisor
(Professor Qinmin Pan, Ph.D.)

.....Thesis Co-Advisor
(Associate Professor Charoen Nakason, Ph.D.)

.....Examiner
(Associate Professor Nuanphun Chantarasiri, Ph.D.)

.....Examiner
(Assistant Professor Varawut Tangpasuthadol, Ph.D.)

.....External Examiner
(Wiyong Kangwansupamonkon, Ph.D.)

ภิญโญ วงษ์ทอง : การดัดแปรยางธรรมชาติดีโปรติไนซ์ด้วยการกราฟต์กับมาเลอิกแอนไฮไดรด์โดยเทคนิคดิฟเฟอเรนเชียลไมโครอิมัลชันพอลิเมอไรเซชัน (MODIFICATION OF DEPROTEINIZED NATURAL RUBBER BY GRAFTING WITH MALEIC ANHYDRIDE VIA DIFFERENTIAL MICROEMULSION POLYMERIZATION TECHNIQUE) อ.ที่ปรึกษาวิทยานิพนธ์หลัก: ศ. ดร. สุดา เกียรติกำจรวงศ์, อ.ที่ปรึกษาวิทยานิพนธ์ร่วม: Prof. Dr. Garry L. Rempel, Prof. Dr. Qinmin Pan, รศ. ดร. เจริญ นาคะสรรค์, 173 หน้า.

งานวิจัยนี้เสนอเทคนิคใหม่ในการสังเคราะห์กราฟต์โคพอลิเมอร์ของมาเลอิกแอนไฮไดรด์ (MA) บนยางธรรมชาติ (NR) เพื่อให้ได้ประสิทธิภาพการกราฟต์ (G.E) สูงและมีเจลต่ำ ด้วยการแยกโปรตีนออกจากน้ำยางธรรมชาติ (DPNR) ก่อน แล้วกราฟต์กับ MA โดยใช้และไม่ใช้สไตรีน (ST) เป็นโคมอนอเมอร์ และกราฟต์ด้วยเทคนิคดิฟเฟอเรนเชียลไมโครอิมัลชันพอลิเมอไรเซชัน (DMP) ตัวแปรที่ศึกษาคือ ความเข้มข้นของสารริเริ่มและมอนอเมอร์ อุณหภูมิของปฏิกิริยา เวลาการเกิดปฏิกิริยา อัตราการหยดมอนอเมอร์ และอัตราส่วนของ ST/MA ศึกษาจลนพลศาสตร์การ กราฟต์ภายใต้อิทธิพลของสไตรีนโคมอนอเมอร์ พบว่า การกราฟต์ MA กับ DPNR ให้ค่า G.E สูงและเกิดเจลต่ำกว่าการกราฟต์กับ NR เทคนิค DMP ให้ค่า G.E สูงกว่าเทคนิคอิมัลชันแบบดั้งเดิม การเติม STในระบบช่วยเพิ่มค่า G.E และเร่งอัตราการเกิดปฏิกิริยาการกราฟต์ งานวิจัยนี้ได้นำกราฟต์โคพอลิเมอร์ไปใช้เป็นสารเสริมสภาพเข้ากันได้ของ NR และอะคริโลไนไทรล์-บิวทาไดอีน- สไตรีน (ABS) วัลคาไนซ์เบลนด์ ศึกษาผลของอัตราส่วนของ NR/ABS ปริมาณฟินอลิกเรซิน และกราฟต์โคพอลิเมอร์ ต่อสมบัติเชิงกล สมบัติพลวัติ สมบัติเชิงความร้อน และสัณฐานวิทยา พบว่า การเพิ่มสัดส่วนของ ABS ในเบลนด์ส่งผลให้ความต้านทานต่อแรงดึงและความแข็งเพิ่มขึ้นแต่ความสามารถในการยืดจนขาดลดลง การตอบสนองแบบอิลาสติกของเบลนด์สูงกว่า ABS และ ความเสถียรทางความร้อนเพิ่มเมื่อปริมาณของ ABS เพิ่มขึ้น สัณฐานวิทยาของ NR/ABS เบลนด์เป็นแบบสองวัฏภาค การเติมกราฟต์โคพอลิเมอร์ใน NR/ABS เบลนด์ทำให้ได้สัณฐานวิทยาไม่เป็นระเบียบซึ่งมีผลกระทบต่อสมบัติเชิงกล

สาขาวิชา ปิโตรเคมี
ปีการศึกษา 2557

ลายมือชื่อนิสิต .....
ลายมือชื่อ อ.ที่ปรึกษาหลัก .....
ลายมือชื่อ อ.ที่ปรึกษาร่วม .....
ลายมือชื่อ อ.ที่ปรึกษาร่วม .....
ลายมือชื่อ อ.ที่ปรึกษาร่วม .....

5273838223 : MAJOR PETROCHEMISTRY
KEYWORDS: DEPROTEINIZED NATURAL RUBBER / STYRENE / MALEIC ANHYDRIDE / GRAFTING / DIFFERENTIAL MICROEMULSION POLYMERIZATION / POLYMER BLENDS

PINYO WONGTHONG: MODIFICATION OF DEPROTEINIZED NATURAL RUBBER BY GRAFTING WITH MALEIC ANHYDRIDE VIA DIFFERENTIAL MICROEMULSION POLYMERIZATION TECHNIQUE. ADVISOR: PROF. SUDA KIATKAMJORNWONG, Ph.D., CO-ADVISOR: PROF. GARRY L. REMPEL, Ph.D., PROF. QINMIN PAN, Ph.D., ASSOC. PROF. CHAROEN NAKASON, Ph.D., 173 pp.

This work involves a novel technical route for synthesizing graft copolymers of maleic anhydride (MA) onto natural rubber (NR). To improve the grafting efficiency (G.E) and reduce gel content in the grafts, deproteinizing the rubber latex (DPNR) was conducted before the grafting reaction. Styrene as a comonomer was used to increase the G.E, and a differential microemulsion polymerization (DMP) technique was applied for the grafting reaction. The effects of initiator and monomer amount, reaction temperature, reaction time, monomer addition rate, and ST/MA ratio on the G.E and gel content were investigated. Grafting kinetics under the influences of styrene comonomer were investigated. The MA grafting onto DPNR provided higher G.E and a lower gel content than grafting onto NR. The graft copolymers obtained by the DMP method provided much better results with respect to G.E compared to those provided by the conventional method. Adding copolymerizing styrene to the grafting process improves the efficiency of MA grafting and also enhances the graft copolymerization rate. The graft copolymer so obtained was used as a compatibilizer for vulcanized NR/acrylonitrile-butadiene-styrene (ABS) blends. The effects of blend proportions, phenolic curative content, and graft copolymer on mechanical, dynamic, thermal and morphological properties of the blends were investigated. Tensile strength and hardness of the blends increased with increasing ABS content while elongation at break decreased. These blends showed a greater elastic response than that of neat ABS. Thermal stability of the blends increased with increasing ABS content. SEM micrographs of the blends showed a two-phase morphology system. Adding the graft copolymer as a blend compatibilizer produced non-uniform vulcanized NR and ABS phase morphology that affected the mechanical properties.

Field of Study: Petrochemistry	Student's Signature .....
Academic Year: 2014	Advisor's Signature .....
	Co-Advisor's Signature .....
	Co-Advisor's Signature .....
	Co-Advisor's Signature .....

ACKNOWLEDGEMENTS

I would like to express my sincerest gratitude to my advisor, Professor Dr. Suda Kiatkamjornwong for her kindness, encouragement, supervision, and helpful suggestions throughout the course of the research. This dissertation would have not been realized without her help, tireless reviews and corrections of the dissertation, and great help in the preparation of three manuscripts. I also would like to acknowledge my co-advisors, Professor Dr. Garry L. Rempel and Professor Dr. Qinmin Pan for their helpful guidance, valuable discussions, reviewing the dissertation and manuscript corrections.

Special thanks to Associate Professor Dr. Charoen Nakason for his kind permission to use the rubber processing facility in Pattani, and his suggestions about rubber blending. I wish to express my thankfulness to Professor Dr. Pattarapan Prasassarakich for serving as the dissertation chairman, Associate Professor Dr. Nuanphun Chantarasiri, Assistant Professor Dr. Varawut Tangpasuthadol, and Dr. Wiyong Kangwansupamonkon for serving on the dissertation committee.

I gratefully acknowledge the co-support of the Thailand Research Fund (TRF) and Chulalongkorn University under the Royal Golden Jubilee (RGJ) Project (Grant No. PHD/0304/2550). The support from the Natural Sciences and Engineering Research Council of Canada (NSERC) and the Canada Foundation for Innovation (CFI) during my one-year of research study in Canada are sincerely appreciated.

Sincere thanks and appreciation go to the Department of Imaging and Printing Technology, Chulalongkorn University for provision of the research facilities. I am also gratefulness to the Advanced Rubber Technology and Applied Catalysis Laboratory in Chemical Engineering, University of Waterloo, Canada for provision of the research facilities during my short-term research during the period of September, 2011 to August, 2012. Sincere thanks go to Associate Professor Azizon Kaesaman of the Department of Rubber Technology and Polymer Science, Prince of Songkla University, Pattani Campus for use of the rubber blending laboratory facilities during the period of November, 2012 to February, 2013.

Finally, I wish to express my deep gratitude to my parents for their unconditional love, encouragement, and great moral support during my Ph.D. studies.

CONTENTS

Page

Page

LIST OF TABLES

Table **Page**

LIST OF TABLES (Continued)

Table **Page**

LIST OF FIGURES

Figure **Page**

LIST OF FIGURES (Continued)

Figure **Page**

LIST OF FIGURES (Continued)

Figure **Page**

LIST OF FIGURES (Continued)

Figure **Page**

LIST OF FIGURES (Continued)

Figure **Page**

LIST OF FIGURES (Continued)

Figure **Page**

LIST OF FIGURES (Continued)

Figure **Page**

LIST OF FIGURES (Continued)

Figure **Page**

LIST OF FIGURES (Continued)

Figure **Page**

LIST OF ABBREVIATIONS

Abbreviation		Name
ABS	:	Acrylonitrile-butadiene-styrene
AIBN	:	2,2'-azoisobutyronitrile
AFM	:	Atomic force microscopy
APS	:	Ammonium persulfate
BPO	:	Benzoyl peroxide
CHPO	:	Cumene hydroperoxide
CNR	:	Chlorinated natural rubber
CRI	:	Cure rate index
CTC	:	Charge transfer complex
DCP	:	Dicumyl peroxide
DLS	:	Dynamic light scattering
DMA	:	Dynamic mechanical analysis
DMAEA	:	Dimethylaminoethyl acrylate
DMAEMA	:	Dimethylaminoethyl methacrylate
DMMMP	:	Dimethyl(methacryloyloxymethyl)phosphonate
DMP	:	Differential microemulsion polymerization
DPNR	:	Deproteinized natural rubber
DRC	:	Dried rubber content
DSC	:	Differential scanning calorimetry
EDMO	:	Ethylene-diene copolymers
ENR	:	Expoxidized natural rubber

LIST OF ABBREVIATIONS (Continued)

Abbreviation		Name
EPDM	:	Ethylene-propylene diene terpolymer rubber
EVA	:	Ethylene-vinyl acetate copolymer
FTIR	:	Fourier transform infrared spectroscopy
G.E	:	Grafting efficiency
GMA	:	Glycidyl methacrylate
HDPE	:	High-density polyethylene
HNR	:	Hydrogenated natural rubber
^{1}H NMR	:	Proton nuclear magnetic resonance spectroscopy
iPB-1	:	Isotactic polybutene-1
LVE	:	Linear viscoelastic
MA	:	Maleic anhydride
m-EPM	:	maleated ethylene propylene rubber
MFI	:	Melt flow index
M_H	:	Maximum torque
M_L	:	Minimum torque
MMA	:	Methyl methacrylate
MNR	:	Maleated natural rubber
NBR	:	Nitrile butadiene rubber
NR	:	Natural rubber
PA6	:	Polyamide 6
PE	:	Polyethylene

LIST OF ABBREVIATIONS (Continued)

Abbreviation		Name
phr	:	Parts per hundred
PMMA	:	Poly(methyl methacrylate)
POE	:	Polyolefin elastomer
PP	:	Polypropylene
PTA	:	Phosphotungstic acid
PVC	:	Poly(vinyl chloride)
R_p	:	Rate of graft copolymerization
R^2	:	Coefficient of correlation
SAN	:	styrene-*co*-acrylonitrile
SDS	:	Sodium dodecyl sulfate
SEM	:	Scanning electron microscopy
ST	:	Styrene
t-BHP	:	*tert*-butyl hydroperoxide
T_{c90}	:	Optimum cure time
TEPA	:	tetraethylenepentamine
TEM	:	Transmission electron microscopy
TGA	:	Thermal gravimetric analysis
T_d	:	Decomposition temperature
T_g	:	Glass transition temperature
THF	:	Tetrahydrofuran
TMQ	:	2,2,4-trimethyl-1,2-dihydroquinoline

LIST OF ABBREVIATIONS (Continued)

Abbreviation		Name
TPEs	:	Thermoplastic elastomers
TPU	:	Thermoplastic polyurethane
TPVs	:	Thermoplastic vulcanizates
T_{S2}	:	Scorch time
TSH	:	Toluene sulfonylhydrazide
XPS	:	X-ray photoelectron spectroscopy

CHAPTER I: INTRODUCTION

1.1 Motivation

In recent years, there has been increasing attention of searching for new materials which are widely used in a variety of industrial applications. Because of increasing environmental concerns, this attention has particularly concentrated on environmentally friendly materials that are renewable, recyclable, sustainable and biodegradable [1, 2]. Biopolymers provide an interesting material to replace some petroleum-based polymers which are obtained from non-renewable resources. There are various kinds of biopolymers from biomaterials such as natural polymers (i.e., starch, protein and cellulose), synthetic polymers from natural monomers (i.e., poly(lactic acid)), and polymers from microbial fermentation (i.e., polyhydroxybutyrate). Among a variety of renewable materials, natural rubber (NR) obtained from *Hevea brasiliensis* is classified as one of the most valuable renewable resources. NR has attracted great interest in many fields, such as in transportation, industrial, consumer, and medical sectors, mainly due to its outstanding elasticity and good mechanical properties [3]. The world's annual NR production during the period of 2000 to 2013 has been constantly increasing from 6.76 up to 11.70 million tons and the consumption has also been rising from 7.34 up to 11.30 million tons [4]; hence, NR is an important sustainable material and the market for it can be expected to grow more in the future.

Although NR possesses many superior properties it lacks some properties such as oil resistance and weather resistance. The presence of the unsaturation of the carbon-carbon double bonds (C=C) in the NR backbone causes easy degradation when NR is exposed to sunlight, ozone, UV radiation and air, especially at increased temperature. Consequently, modification of NR is justified to overcome its disadvantages and result in a material with more desirable physical and chemical properties. Many types of modifications have been used to modify the NR structure such as chlorination [5, 6], epoxidation [7-10], hydrogenation [11, 12], and grafting

[13-22]. Among these, grafting is one of the most attractive techniques. Various monomers have been used for grafting with NR to improve the properties of NR, such as styrene (ST) [14, 18, 19, 21], methyl methacrylate (MMA) [20, 22], MMA-ST comonomer [13, 15], dimethylaminoethyl acrylate (DMAEA), dimethylaminoethyl methacrylate (DMAEMA) [17], and dimethyl(methacryloyloxymethyl)phosphonate (DMMMP) [16]. Recently, maleic anhydride (MA) has become an attractive monomer for grafting with NR. The improved hydrophilicity of the modified NR by MA grafting (NR-*g*-MA) has found important applications in the area of reactive blending as a blend compatibilizer for NR blended cassava starch [23] and thermoplastic polyurethane (TPU) [24]. The NR-*g*-MA can also be used as a blending composition with NR [25], poly(methyl methacrylate) (PMMA) [26], and polypropylene (PP) [27]. The introduction of the NR-*g*-MA reduces interfacial tension and enhances the adhesion between the two phases of the blends and therefore improves the mechanical properties of the blends.

However, it is very difficult to achieve a favorable efficiency of MA grafting onto NR due to the difficulty of MA homopolymerization and only one MA unit as a maximum is grafted on each active site along the rubber chains [28, 29]. Theoretically, MA is not reactive towards the polymer macroradicals because of their structural symmetry and deficiency of electron density around the carbon-carbon double bond, leading to a low content of grafted MA. An effective way of promoting the activity of MA is by introducing a comonomer which has higher activity toward both the macroradicals and the MA monomer. Recently, styrene (ST) has been used as a comonomer for promoting grafting of MA onto PP [30, 31], NR [32], ethylene-octene copolymer [33], isotactic polybutene-1 (iPB-1) [34], and polyethylene (PE) [35]. It has also been reported that ST can improve the grafting degree of glycidyl methacrylate (GMA) onto PE [36], high-density PE (HDPE) [37], and PP [38]. The addition of styrene not only improves grafting degree of the MA grafting as a result of forming a charge transfer complex (CTC) for graft copolymerization but also by reducing the degradation of the plastics during the mixing process.

Although the grafting of MA onto NR has been successfully carried out in either the molten state [23-26, 39] or solution state [32, 40, 41] some problems still

could not be overcome. The grafting in a molten state by mixing MA and NR was normally realized by an internal mixer at high temperatures (i.e., > 135 °C). Under such a condition, competitive reactions occurred via more than one reaction mechanism, and a low degree of grafted MA with a high gel fraction was obtained, which is undesirable as the gel in the grafts not only causes problems in characterization but also presents difficulties for further processing operations. The grafting in solution has also been carried out by dissolving solid NR in a suitable solvent, of which the drawback is that a large amount of toxic solvent is needed for the reaction medium which has a negative impact on the production cost and the environment. Emulsion polymerization is a more desirable approach as NR is naturally available in latex form and it would be very advantageous to carry out the grafting directly in the latex phase without using any organic solvents. However, it has been discovered that the grafting reaction on the naturally obtained NR latex is not efficient and it may be suppressed by the presence of non-rubber components in the NR such as proteins [14, 18, 20]. The proteins can act as free-radical scavengers and terminate the free-radical species involved in the grafting reaction. Moreover, it also causes formation of a branched network in NR [42-48]. As a result, it is important to remove proteins from the NR latex before the grafting operation.

The removal of proteins from the NR to obtain deproteinized NR (DPNR) can be carried out by various deproteinization methods such as urea treatment [42, 43], saponification, surfactant washing [44], and enzymatic treatment [44, 45]. It has been reported that the DPNR by proteolytic enzyme and urea-deproteinization provided similar residual nitrogen content in DPNR, indicating that both methods gave the same efficiency for removing the proteins from NR. However, the incubation time need for enzymatic treatment was much longer than that of urea treatment [43]. Therefore, urea-deproteinization is a better technique as it can remove proteins from NR latex rapidly and efficiently.

Differential microemulsion polymerization (DMP) is a unique technique for synthesizing the polymer nanoparticles which requires a lower amount of surfactant than conventional microemulsion polymerization [49-54]. The surfactant is not only expensive but also causes water sensitivity of the product. The main difference of

these methods is the monomer feeding operation. The former is provided as a slow addition of monomer with continuous dropping into the reaction system while the latter is incorporated in a single addition. This method provides a new technique for synthesizing nanosize polymer particles. However, the use of DMP technique for synthesizing of graft copolymers of natural rubber has not been reported.

In the literature, few works have been reported on kinetics of graft copolymerization of vinyl monomers onto NR. Kinetics and mechanism of graft copolymerization of ST [21] and MMA-ST [13] onto NR by emulsion polymerization have been reported. The influences of reaction conditions of monomer and initiator concentration, reaction time, and reaction temperature on monomer conversion and grafting efficiency have been well established [13, 21]. However, the reaction kinetics of MA grafting onto DPNR in either the presence or absence of styrene, so far has not been reported in the literature.

It is our understanding that removing the proteins from NR latex could help improve the efficiency of graft copolymerization of vinyl monomers onto NR and the differential microemulsion polymerization (DMP) technique could help minimize the use of the surfactant, and thus it was applied in this work for a study of graft copolymerization of MA onto DPNR in latex form. In addition, styrene as a comonomer was introduced into the grafting system to increase the grafting efficiency. Grafting kinetics of MA onto DPNR latex in the presence and absence of styrene were also investigated.

Blending of a thermoplastic polymer with an elastomeric polymer to provide new polymeric materials called thermoplastic elastomers (TPEs) has been a research and industrial topic of considerable interest for many years. The blended product is a valuable material in the polymer industry because it combines excellent processing characteristics of thermoplastics and outstanding elastic properties of rubbers. A number of reports have carried out on rubber/thermoplastic blends using either a simple blend [27, 55-57] or dynamic vulcanization [58-70]. It has been well reported that thermoplastic vulcanizates (TPVs) obtained by dynamic vulcanization can improve the properties of the blends. This is attributed to the unique morphology in

which small and uniform crosslinked rubber particles are finely dispersed in the thermoplastic matrix [60, 64, 66, 68]. Various parameters that influence the morphology of TPVs are the vulcanization system [59, 61-63], compatibilization [16, 59, 61, 65], and mixing conditions [66]. Among these, curative content is one of the most important parameters. However, few works have been reported on this effect on the mechanical and morphological properties of the blends [64, 67].

Synthetic rubbers such as ethylene propylene diene monomer rubber (EPDM) and nitrile butadiene rubber (NBR) have been reported for blending with thermoplastics for improving the mechanical properties of the blends [65, 67, 68]. Natural rubber (NR) has also been reported for blending with PMMA [57], PP [55, 66], and HDPE [61, 64]. Acrylonitrile-butadiene-styrene (ABS) is one of the most important engineering thermoplastic materials. ABS is an interesting polymer for blending with NR because of the superior properties of both constituents. ABS gives high impact strength, chemical resistance, and easy processing characteristics while NR provides the outstanding elasticity and mechanical properties. Recently, the use of NR and polystyrene grafted NR as modifiers in ABS has been carried out using a simple blend and it has been reported that the strength properties and thermal stability of the blends were improved [71]. Several reports have been carried out the vulcanization of NBR/ABS blends and it has been found that superior mechanical properties were obtained [58, 69, 70]. Studies of mechanical properties of vulcanized NR/ABS blends have also been established [58]. However, the influences of curative content and blend proportions on morphological and other related properties of the vulcanized NR/ABS blends have not been reported in literature.

In the present work, the vulcanization of NR/ABS blends using a phenolic curing agent by a melt mixing process was investigated. The graft copolymer of MA grafting onto DPNR was used as a blend compatibilizer for vulcanized NR/ABS blends. The effects of the blend proportions, phenolic curative content, and graft copolymer on mechanical, dynamic, thermal and morphological properties of the vulcanized NR/ABS blends were elucidated.

1.2 Objective and Scope of Research

Modification of NR via grafting with MA has received wide attention as it could improve the properties of NR and extend its application to a wider field. However, the efficiency of MA grafting onto NR in either the molten state or solution state is low and is accompanied by undesired high gel content in the grafts. This work presents a novel technical route to improve the grafting efficiency and reduce gel content in the grafts in that deproteinization of the NR latex was conducted before the grafting reaction. Styrene (ST) as a comonomer was used to increase the grafting efficiency and a differential microemulsion polymerization (DMP) technique was applied for the grafting reaction. The effects of monomer and initiator amount, reaction temperature, reaction time, monomer addition rate, and ST/MA ratio on grafting efficiency and gel content were elucidated. The effect of the proteins in the NR latex on graft copolymerization was investigated. Two techniques of the conventional microemulsion polymerization and differential microemulsion polymerization were used to carry out the grafting reaction for a comparison of grafting efficiency. The performance of styrene comonomer for promoting grafting of MA onto DPNR was investigated. In addition, grafting kinetics of MA grafting onto DPNR in either the presence or absence of styrene were also studied.

The graft copolymers of MA grafting onto DPNR (DPNR-*g*-MA) and styrene-assisted grafting of MA onto DPNR (DPNR-*g*-(MA-*co*-ST)) were used as compatibilizers for vulcanized NR/ABS blends by a melt mixing process. The effects of the blend proportions, phenolic curative content, and graft copolymer on mechanical, morphological and other related properties of the vulcanized NR/ABS blends were investigated. The scope and overview of this thesis are as follows:

Chapter I presents an introduction of this research work. The motivation, objective and scope of the research are also provided in this chapter.

Chapter II provides the theory and literature review relating to this research work. This chapter presents an overview of NR, DPNR, and chemical modification of the NR backbone. An overview of understanding the preparation methods of DPNR latex and graft copolymerization of vinyl monomers onto NR is provided in this

chapter. This chapter also presents an overview of elastomer and thermoplastic blends.

Chapter III concentrates on the preparation of the DPNR latex by urea-deproteinization. The effect of the amount of urea on efficiency of removing the proteins from NR latex was investigated. The nitrogen content in the NR and DPNR was determined using the Kjeldahl procedure. The gel content of rubber before and after deproteinization was also determined. Confirmation of removing the proteins from NR latex by FTIR analysis is presented and discussed in this chapter.

Chapter IV reports on an investigation of the grafting of MA onto DPNR (DPNR-*g*-MA) using the DMP technique. The effects of monomer and initiator amount, reaction temperature, reaction time, and monomer addition rate on grafting efficiency and gel content in the grafts were investigated. The MA grafting onto NR substrate was also carried out for a comparison of grafting efficiency. Two techniques of conventional microemulsion polymerization and differential microemulsion polymerization for the grafting reaction were compared. Fourier transform infrared (FTIR) and nuclear magnetic resonance (NMR) spectroscopies were used to characterize the chemical structures of graft copolymer. The chemical composition at the surface of the DPNR and DPNR-*g*-MA was investigated by X-ray photoelectron spectroscopy (XPS). The diameters of the rubber and graft copolymer latex particles were measured by dynamic light scattering (DLS). The morphology was investigated by transmission electron microscopy (TEM) and atomic force microscopy (AFM). Thermal properties such as the glass transition temperature (T_g) and decomposition temperature (T_d) for the rubber and graft copolymer were investigated using differential scanning calorimetry (DSC) and thermal gravimetric analysis (TGA), respectively.

Chapter V reports on the styrene-assisted grafting of MA onto DPNR. When the appropriate conditions for MA grafting were found, this condition was applied for the grafting reaction with inclusion of styrene to obtain DPNR-*g*-(MA-*co*-ST). The effect of various ST/MA ratios on grafting efficiency and gel content was investigated. The chemical structures of the graft copolymers were characterized by

FTIR, NMR, and XPS techniques. The diameters of the graft copolymer latex particles were measured by DLS. The morphology was investigated by TEM. Thermal analysis of the graft copolymer was investigated by DSC and TGA. The performance of the styrene comonomer for promoting grafting of MA onto DPNR is discussed and a grafting mechanism for the styrene-assisted grafting reaction is proposed in this chapter.

Chapter VI focuses on the kinetics of graft copolymerization of MA onto DPNR in either the presence or absence of the styrene comonomer. The effect of various ratios of ST/MA on the polymerization kinetics of MA grafting onto DPNR was investigated. The monomer conversion was determined by a gravimetric method. The reaction rate of the graft copolymerization was determined. The initial rate of graft copolymerization was also calculated from the slope of the time-conversion curves during the initial stage of the reaction.

Chapter VII concentrates on the use of graft copolymers of DPNR-*g*-MA and DPNR-*g*-(MA-*co*-ST) as compatibilizers for vulcanized NR/ABS blends by a melt mixing process. The effects of the blend proportions, phenolic curative content, and graft copolymer on mechanical, morphological and other related properties of the vulcanized NR/ABS blends were investigated. Curing characteristics of the NR vulcanizates were characterized using an Oscillating Disk Rheometer. Tensile testing was performed using a Hounsfield Tensometer. Hardness of the samples was measured using a Shore A durometer. Izod impact strength was measured using a Pendulum Impact Tester. Dynamic properties were investigated using a moving die processability tester. Thermal properties of T_d of the samples were investigated using TGA. Morphology of the blends was investigated by SEM.

Chapter VIII provides a summary of the results and conclusions from this study. Recommendations for future work are also provided in this chapter.

CHAPTER II: THEORY AND LITERATURE REVIEW

This chapter provides the theory and literature review relating to this research work. It presents an overview and background of NR and DPNR. An overview for understanding the preparation methods of DPNR latex, modification of NR, and graft copolymerization of vinyl monomers onto NR is provided in this chapter. This chapter includes a review on MA grafting onto NR in the molten and solution states, styrene-assisted grafting of MA onto polyolefins, the differential microemulsion polymerization (DMP) technique, and blending of elastomer with a thermoplastic.

2.1 Natural Rubber (NR)

Natural rubber (NR) of *Hevea brasiliensis* is considered a green polymer as it is obtained from a renewable resource. The NR is widely used in many industrial applications such as transportation, industrial, consumer and medical sectors, mainly due to its outstanding elasticity and good mechanical properties such as high green strength, high tensile strength, low heat build-up, and high damping [3]. The main component of the NR molecule is *cis*-1,4-polyisoprene and the chemical structure is shown in Figure 2.1.

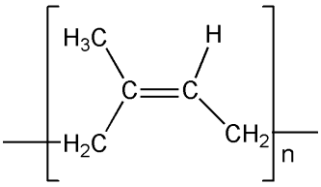

Figure 2.1 Chemical structure of *cis*-1,4-polyisoprene.

Natural rubber latex which is obtained from the rubber tree is known as a field latex or fresh natural rubber latex. A typical composition of fresh NR latex is

presented in Table 2.1. The fresh NR latex contains about 25 – 40% dry rubber content (DRC) with some minor non-rubber components of about 5 – 10% dispersed in water [72]. The non-rubber substances include proteins, sugar, lipid and resin. These compositions differ depending on the clones of rubber, age of the rubber tree, the tapping season, and the tapping technique.

Table 2.1 Typical composition of fresh NR latex [72].

Constituents	Composition (%)
Rubber	36.0
Amino acids and N-bases	0.3
Neutral lipids	1.0
Proteins	1.6
Phospholipids	0.6
Inositols-carbohydrates	1.5
Salts (mainly K, P and Mg)[a]	0.5
Water	58.5

[a] K = Potassium; P = Phosphorus; and Mg = Magnesium

NR can be divided into two main categories of latex concentrates and dry or solid rubber. Concentrates of NR latex are obtained by the process of centrifugation and creaming. Ammonia is added to the latex to prevent coagulation of the rubber. The high-ammonia NR latex contains 0.7% ammonia and the low-ammonia NR latex contains 0.2% ammonia, 0.025% tetramethyl thiuram disulfide/zinc oxide, and 0.05% lauric acid. Meanwhile, the remainder of the latex and field coagulum are processed either into conventional types of rubber (sheet and crepe rubber) or into technically specified rubber (TSR) such as block rubber.

2.2 Deproteinized Natural Rubber (DPNR)

DPNR is purified NR latex which is prepared by removing the proteins using a deproteinization method. The removal of proteins from the NR latex is very important in the area of the medical sector and chemical reaction study relating to the use of NR latex as a raw material. For the medical sector, the NR products obtained from NR latex containing proteins can cause a problem to patients who fall into anaphylactic reactions because of a latex-allergy. Protein in NR causes them to die just after exposing them to latex surgical gloves or condoms [42]. Thus, DPNR is suitable for medical applications as a starting material compared with the raw NR latex. For a chemical reaction study, it has been found that the grafting reaction on the naturally obtained NR latex is not efficient and it may be suppressed by the presence of proteins in the NR latex [14, 18, 20]. The protein can also cause formation of gel or a branched network in NR [42-48]. In addition, it causes reduction of catalyst efficiency in the hydrogenation of NR [12]. Thus the removal of proteins from the NR latex before the grafting operation or hydrogenation of NR is important.

Many researchers have investigated the structure of NR [46, 47]. The rubber molecule is composed of two *trans*-1,4-isoprene units, a long chain of *cis*-1,4-isoprene repeating units, and two terminal groups of ω-terminal and α-terminal. The chain end of the ω-terminal is linked by proteins while the phosphate group at the α-terminal is linked to phospholipids as shown in Figure 2.2.

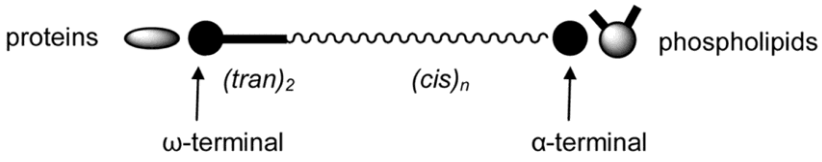

Figure 2.2 Structure for ω-terminal and α-terminal groups of NR [46].

According to the NR structure, it is possible to form a branched network in NR through intermolecular hydrogen bonds of the modified dimethylallyl group at the ω-

terminal with proteins. In addition, the interaction of phospholipids with the phosphate group of α-terminal can be formed as shown in Figure 2.3. A three-dimensional network in the NR latex can also be formed during storage hardening [48]. When water is removed from the rubber by a drying agent (i.e., phosphorus pentoxide), phospholipids can react with each other to form micelles and branched networks are produced by the interactions between the reactive functional groups of the NR chains as shown in Figure 2.4.

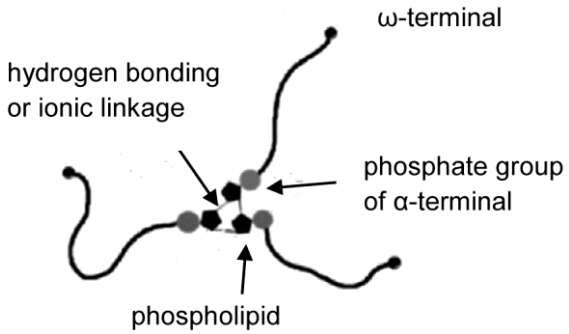

Figure 2.3 Structure of gel in NR originated by α-terminal functional group [47].

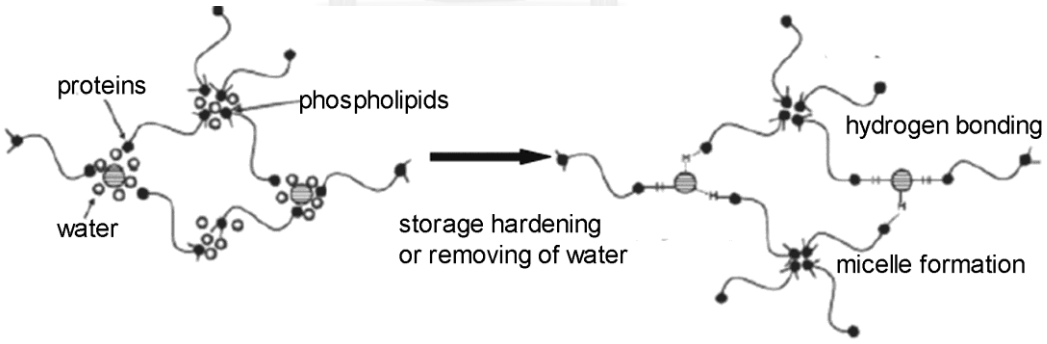

Figure 2.4 Structure of gel in NR after storage hardening [48].

DPNR latex has been successfully obtained by various deproteinization methods, such as urea treatment [42, 43], saponification, surfactant washing [44], and enzymatic treatment [43-45]. The experimental procedure of deproteinization by urea treatment (U-DPNR) and a proteolytic enzyme (E-DPNR) [43] is shown in Figure 2.5.

The NR latex was incubated with 0.1 wt% of urea or 0.04 wt% of proteolytic enzyme in the presence of 1 wt% of sodium dodecyl sulfate as a surfactant at 30 °C. The incubation time for U-DPNR and E-DPNR was 60 min and 720 min, respectively. The latex mixture was later centrifuged and the cream fraction was redispersed. The centrifugation of the redispersed latex was repeated twice. The solid DPNR was then obtained by coagulation.

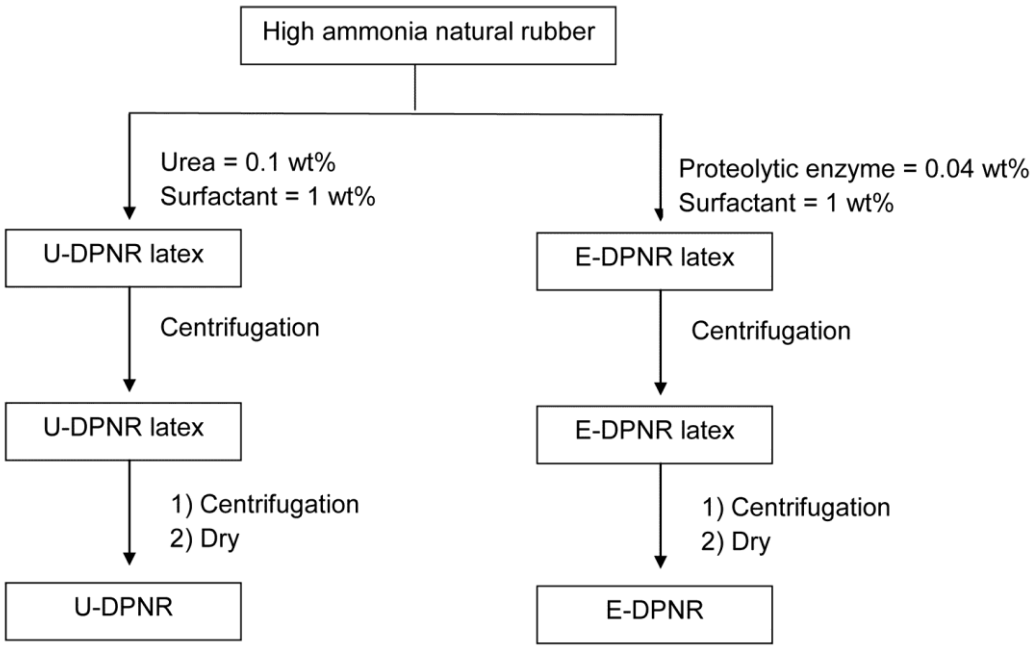

Figure 2.5 Schematic representation of experimental procedure for deprotienizing the NR latex by urea and proteolytic enzyme [43].

Nitrogen content of U-DPNR is markedly reduced after urea treatment as shown in Table 2.2, indicating that proteins in NR latex are attached on the surface of the rubber particles with weak attractive force interactions and they are able to change their conformation by addition of urea. The E-DPNR provided a similar nitrogen content to the U-DPNR which confirmed that proteins were also removed by the proteolytic enzyme. However, the incubation time used for the enzymatic treatment

required a much longer period than that of the urea treatment. Thus urea treatment is a more preferable technique as it can remove proteins from the NR latex rapidly and efficiently.

Table 2.2 Nitrogen content for NR, U-DPNR and E-DPNR [43].

Sample	Incubation time (min)	Nitrogen content (wt%)
HA-NR[a]	0	0.300
U-DPNR[b]	60	0.020
E-DPNR[c]	720	0.017

[a] High ammonia NR latex; [b] Urea treatment; [c] Enzymatic treatment.

Removal of the proteins from fresh NR has been successfully obtained by many deproteinization techniques such as enzymatic treatment, surfactant washing, and saponification of the latex [44]. The nitrogen content of the treated rubber was significantly reduced by all the deproteinization techniques which confirmed the removal of proteins in NR as shown in Table 2.3.

Table 2.3 Nitrogen content and gel content of FNR, DPNR, WSNR and SPNR [44].

Sample	Nitrogen content (wt%)	Gel content (wt%)
FNR[a]	0.65	10.8
DPNR[b]	0.14	2.9
WSNR[c]	0.02	3.6
SPNR[d]	0.12	7.8

[a] Fresh NR; [b] Enzymatic treatment; [c] Surfactant washing; [d] Saponification.

Surfactant washing provided the best results while saponification and enzymatic treatments showed about the same efficiency. A reduction of the gel fraction for the treated rubber was found and thus it was concluded that the gel

content in NR was caused by the proteins in NR. A deproteinization mechanism by enzymatic treatment and surfactant washing is proposed. In the case of enzymatic treatment, proteins were removed by the proteolytic enzyme and some of the low molecular weight proteins fragments and oligopeptides remained in the serum phase of the DPNR latex. For surfactant washing, proteins at the surface of NR particles could be either dislodged and denatured at the same time and then solubilized by the surfactant and entered into the serum phase. However, the mechanism by saponification cannot be identified as yet.

2.3 Chemical Modification of Natural Rubber

Chemical modification of NR has been extensively investigated for several years. Since NR possesses carbon-carbon double bonds (C=C) in every repeating unit of the *cis*-1,4-polyisoprenic structure, chemical reactions of alkenes can be applied to the C=C of the NR backbone. Modification of NR not only uses to improve the undesirable properties of NR but also provides an opportunity to transform NR into new polymeric materials. Various modification techniques have been used to modify the NR structure, such as chlorination [5, 6], epoxidation [7-10], hydrogenation [11, 12], and grafting [13-22]. These techniques are reviewed below.

2.3.1 Chlorination

Chlorination of NR is an addition reaction of the chlorine molecule onto the C=C of NR as shown in Figure 2.6. The chlorinated NR (CNR) can be used as raw material for paint, adhesive, and acid/alkali-proof products, mainly due to its outstanding flame retardant and chemical resistant properties. Chlorination of NR has been carried out in either solution or latex form [5, 6]. Chlorination in solution was carried out by dissolving solid NR in a suitable solvent such as chloroform (CCl_4) followed by chlorination [5]. The advantage of this method is the ease in controlling the reaction and obtaining the CNR with the required chlorine content in a short reaction time. However, the organic solvent used for the reaction medium is very toxic and harmful to the health of workers and the environment. Therefore, the

synthesis of CNR directly from NR latex would be more advantageous. The improved thermal stability of CNR containing 60% chlorine content has been reported [6].

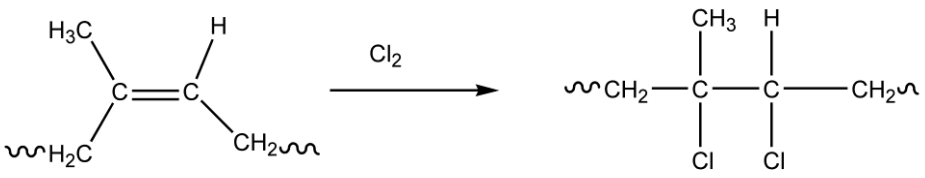

Figure 2.6 Chlorination of NR [5].

2.3.2 Epoxidation

An introduction of the epoxide group (oxirane ring) on the NR backbone by epoxidation, as shown in Figure 2.7, can provide a new polymeric material with improved air permeability, oil and solvent resistance. The expoxidized NR (ENR) is useful for many applications, such as oil seals, tire inner tubes, adhesives, sealants, conveyor belting, shoe soles, floor covering and engine mountings.

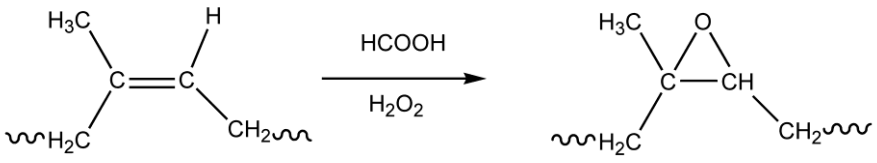

Figure 2.7 Epoxidation of NR [10].

Epoxidation of NR has been carried out in either a solution or latex form [7-10]. In the solution state, it was carried out by dissolving NR in toluene in the presence of hydrogen peroxide and glacial acetic acid. An ENRs containing 10 – 50 mol% of expoxide groups was obtained [8]. The synthesis of ENR in latex form was carried out using formic acid and hydrogen peroxide and ENRs containing 20 – 65

mol% were obtained [7]. The glass transition temperature (T_g) of the ENRs was higher than that of NR. The T_g of NR was -62.4 °C and ENR20, ENR45, ENR65 were -38.2, -27.8, and -19.7 °C, respectively. It was found that the T_g increased with increasing content of epoxide groups. The ENRs showed significantly improved oil resistance compared to NR.

2.3.3 Hydrogenation

Hydrogenation is an attractive technique for reducing the degree of unsaturated carbon-carbon double bonds (C=C) in the NR chains in order to improve the physical, chemical, and thermal properties of NR. Hydrogenated NR (HNR) is more stable against thermal, oxidative, and radiation induced degradation. The hydrogenation of NR is shown in Figure 2.8.

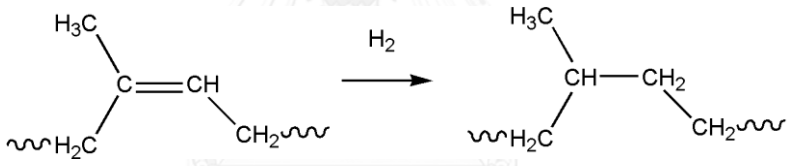

Figure 2.8 Hydrogenation of NR [11].

Catalytic and noncatalytic hydrogenation of NR has been widely investigated [11, 12]. The noncatalytic diimide hydrogenation of NR latex with diimide generated *in situ* by thermolysis of *p*-toluene sulfonylhydrazide (TSH) has been reported [11]. A high rubber hydrogenation of 95% was found at TSH/C=C ratio of 2:1. The improved thermal stability of HNR without affecting its T_g was obtained. Catalytic hydrogenation of NR using $Ru(CH=CH(Ph))Cl(CO)(PCy_3)_2$ (where PCy_3 is tricyclohexylphosphine) in chlorobenzene has also been reported [12]. A high degree of rubber hydrogenation of about 99% was found at a catalyst concentration of 200 μM under a hydrogen pressure of 40.3 bars at 160 °C for 21 h. However, it was found that the impurities or non-rubber components in NR, such as proteins, lipids, and carbohydrates reduced the efficiency of the catalyst. Therefore a small amount of *p*-

toluenesulfonic acid was added to neutralize the poisonous effect during the hydrogenation process and it was found that the reaction time could be reduced to 4 h, while providing a similar percentage of rubber hydrogenation, indicating that the strong acid enhanced the activity of the catalyst.

2.3.4 Grafting

Modification of polymers by grafting with monomer is an attractive method for preparing a new material with improved physical and chemical properties. A graft copolymer composed of a long sequence of one monomer as the backbone polymer with one or more branches as the grafts of long sequences of a second monomer can be prepared. Generally, graft copolymers can be obtained by three main approaches of "grafting onto", "grafting from", and "grafting through" [73]. A schematic illustration for each method is shown in Figure 2.9. The "Grafting onto" approach involves chemical reactions between functional groups (Y) located at the chain end of a polymer with another functional groups (X) randomly distributed on the main chain of the second polymer (Figure 2.9 (a)). The "grafting from" approach involves polymers having functional groups that can initiate polymerization of the added monomer (Figure 2.9 (b)). This approach can be accomplished by treating a polymer substrate with plasma to generate immobilized initiators followed by polymerization. In this case, the polymer substrate contains some thermally cleavable bonds such as azo or peroxide linkages (R); macroradicals are generated at the polymer backbone by heat and then initiate polymerization of the monomer. The "grafting through" approach involves the copolymerization or polymerization of a macromonomer (i.e., vinyl macromonomer) with monomer in the presence of an initiator (Figure 2.9 (c)). The final product of this approach usually contains homopolymer and graft copolymer.

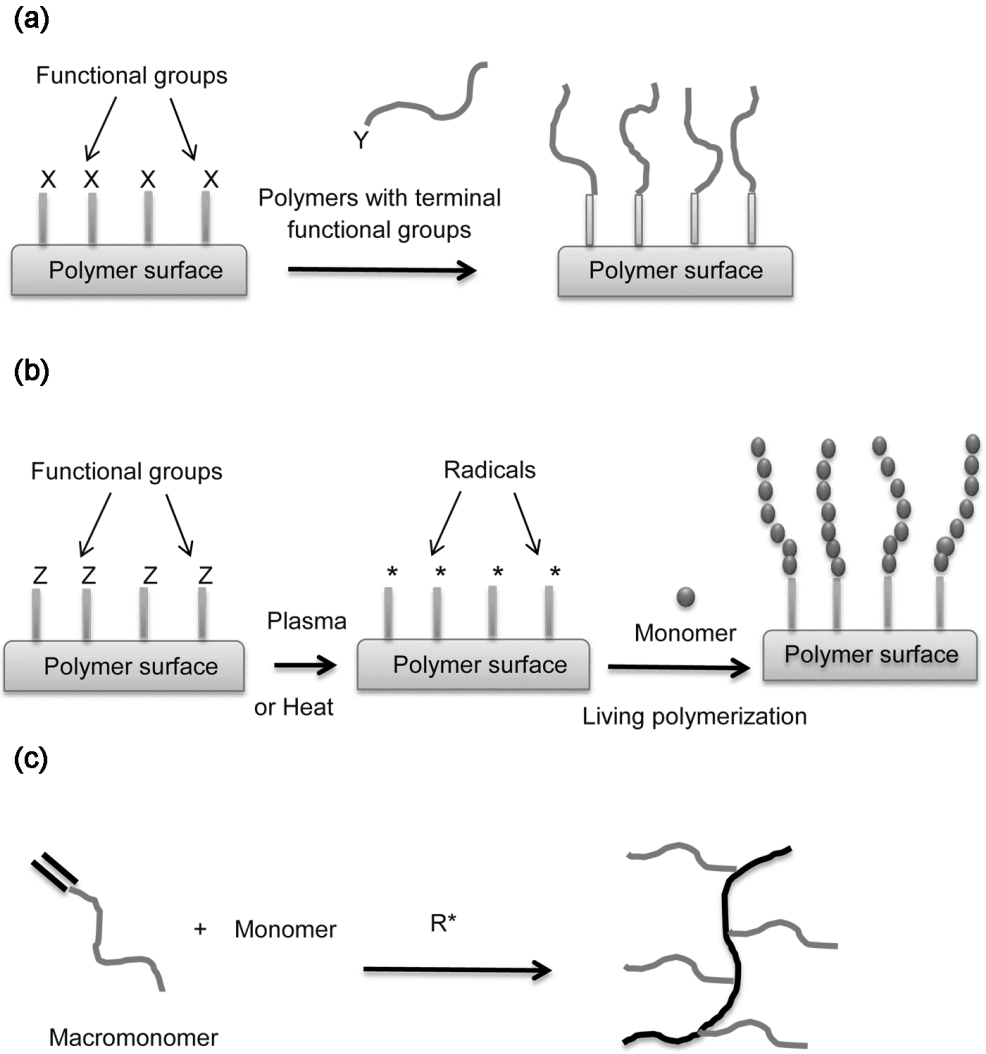

Figure 2.9 Illustration of three methods for synthesizing graft copolymers: (a) "grafting onto"; (b) "grafting from"; and (c) "grafting through" (X and Y = reactive side groups, Z = azo or peroxide group, and R^* = radicals) [74].

Modification of NR by grafting has been investigated for several years. Styrene (ST) [14, 18, 19, 21], methyl methacrylate (MMA) [20, 22], MMA-ST comonomer [13, 15], dimethylaminoethyl acrylate (DMAEA), dimethylaminoethyl methacrylate (DMAEMA) [17], and dimethyl(methacryloyloxymethyl)phosphonate (DMMMP) [16] have been reported for grafting with NR. The grafting of ST onto NR by emulsion polymerization method using cumene hydroperoxide (CHPO) and

tetraethylenepentamine (TEPA) has been investigated [19]. It was found that the graft copolymer was composed of 10.4% free NR, 36.2% free homopolystryrene, and 53.2% grafted NR. The nano-matrix-dispersed polymer based on the grafting of ST onto DPNR has been reported [18]. Various ST concentrations of 0.5, 1.0, 1.5, and 2.0 mol/kg-rubber have been used (i.e., DPNR_ST1, DPNR_ST2, DPNR_ST3, and DPNR_ST4). The highest conversion and G.E of 50% and 93 mol% respectively were found at a ST feed of 1.5 mol/kg-rubber. Rubber particles of about 0.5 μm in diameter were dispersed in the polystyrene-matrix of about 15 nm thicknesses (Figure 2.10).

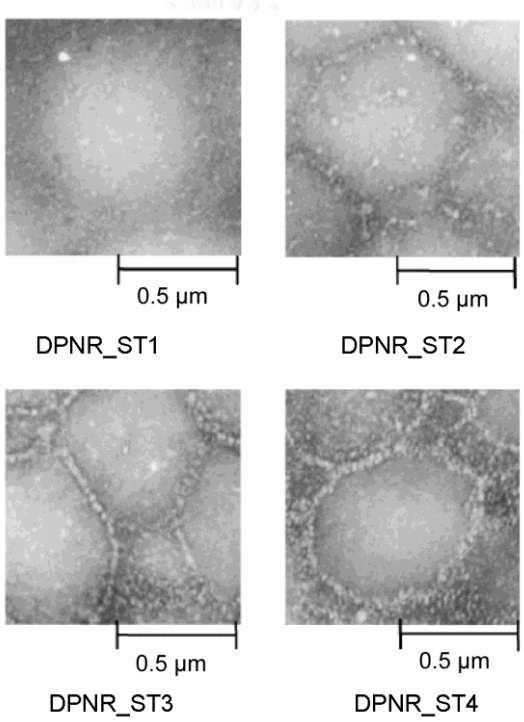

Figure 2.10 TEM micrographs of ST grafting onto DPNR stained with osmium tetroxide (OsO_4) [18].

The grafting of MMA onto NR (NR-*g*-MMA) using potassium persulfate ($K_2S_2O_8$) as an initiator has been reported [22]. The appropriate condition was 100 phr MMA and 0.75 phr $K_2S_2O_8$ at 55 °C for 8 h. The G.E increased with increasing

initiator concentration. The G.E increased with an increasing amount of MMA. The homopolymer (PMMA) was more pronounced at a higher initiator concentration. The morphology of the graft copolymer was of a core-shell type with NR particles as the core and a thin PMMA film as the shell as shown in Figure 2.11.

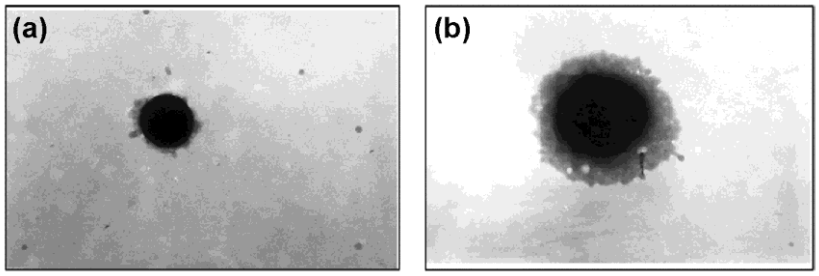

Figure 2.11 TEM micrographs (x24,000) of NR-*g*-MMA stained with 2% OsO_4 at grafting conditions of 100 phr MMA and 0.75 phr $K_2S_2O_8$ at 55 °C for (a) 4 h and (b) 8 h [22].

Graft copolymerization of MMA and ST monomers onto NR using $K_2S_2O_8$ as an initiator has been synthesized [15]. The graft copolymer was composed of 36.8% free NR, 40.7% free copolymer, and 22.5% grafted NR. The effect of redox initiator systems of CHPO/TEPA, *t*-BHP/TEPA, and $K_2S_2O_8/K_2S_2O_5$ for grafting of DMAEA and DMAEMA onto NR has been investigated [17]. CHPO/TEPA provided the highest G.E and the lowest amount of homopolymer. The different characteristics of the graft copolymers were explained by the partitioning ability of CHPO, *t*-BHP, and $K_2S_2O_8$ into NR. TEM micrographs of the NR-*g*-poly(DMAEMA) showed a hairy structure, that is, the surface of the NR particles were covered by poly(DMAEMA) of irregular shapes as shown in Figure 2.12.

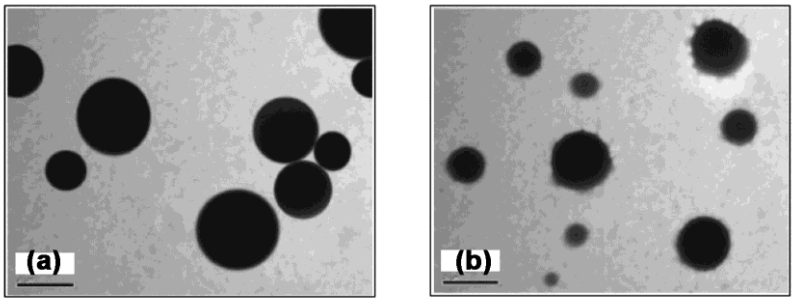

Figure 2.12 TEM micrographs of (a) NR particles and (b) NR-*g*-poly(DMAEMA) particles stained with 2% OsO_4. The scale bar shows 2 mm [17].

2.4 Grafting of Maleic Anhydride (MA) onto Natural Rubber in Molten and Solution State

Grafting of MA onto NR known as maleation results in maleated NR (MNR) has been successfully carried out in either a molten state [23-26, 39] or solution state [32, 40, 41]. The grafting of NR with MA in a molten state using shearing action to generate free radicals has been reported by Kalkornsurapranee et al. [24] and Nakason et al. [26]. The experiment was carried out by mixing 100 phr NR with 6 phr MA in an internal mixer at 145 °C with a rotor speed of 60 rpm for 10 min. The chemical structure of the graft copolymer was confirmed using FTIR and NMR spectroscopy. The signals observed at 1854, 1784, 1736, 1732, and 1710 cm^{-1} were correlated to the C=O stretching of the carbonyl group of grafted MA and the peak at 6.5 ppm was correlated to the proton of MA. Based on ^{1}H NMR calculations, the grafted NR contained 2.9 mol% of MA [24]. The effect of MA concentrations on the grafted MA content has been reported [26]. It was found that the grafted MA increased with an increasing amount of MA, due to a higher possibility for the MA to react with NR via a free radical reaction and/or the Diels-Alder reaction. However, it was observed that the gel content in the grafts increased from 46 to 52 wt% when the MA concentration increased from 4 up to 12 phr. This was caused by the chemical crosslinks between the grafted MA. The grafting mechanism of NR-*g*-MA by free radical mechanism and Diels-Alder reaction is proposed in Figure 2.13.

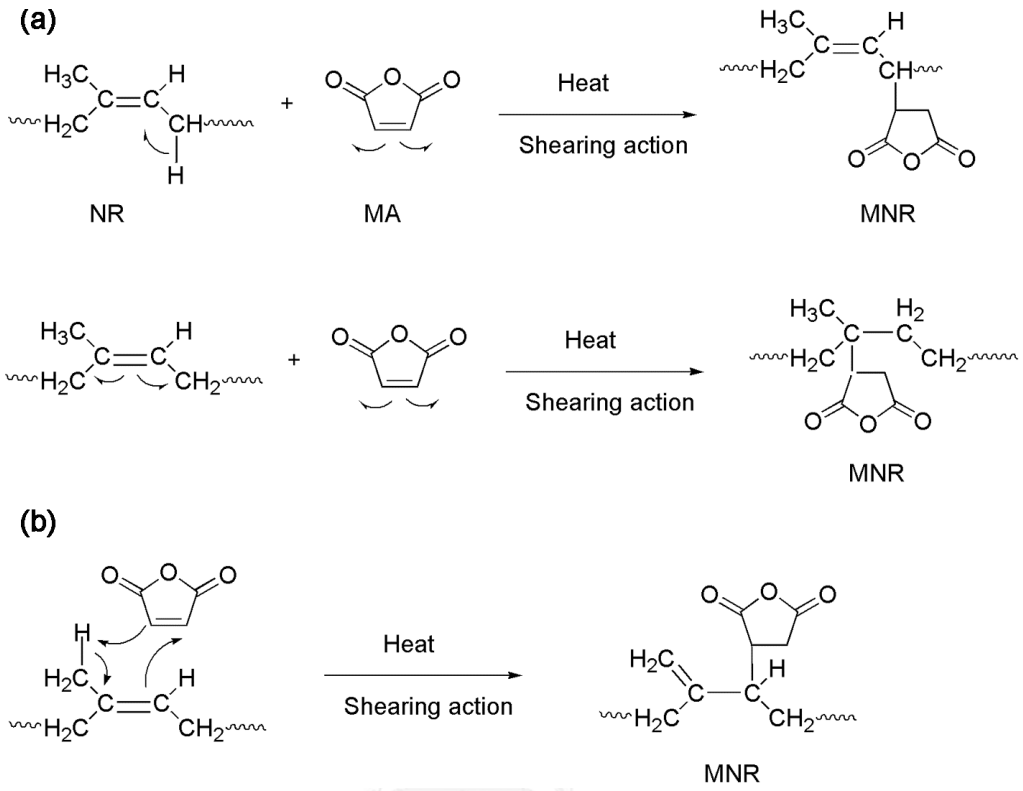

Figure 2.13 Possible grafting mechanism of MA onto NR: (a) Free radical mechanism; and (b) Diels-Alder reaction [26].

The *in situ* compatibilization of polyamide 6/natural rubber (PA6/NR) blends with MA without initiator has been investigated [39]. Compatibilization was carried out by mixing NR with MA in a roll mill at room temperature and it was later used to blend with PA6 at 240 °C. The reaction commenced with the grafting of MA onto NR (NR-*g*-MA) followed by the grafting of PA6 onto the previously grafted NR to obtain the grafted PA6 (NR-*g*-PA6) as shown in Figure 2.14.

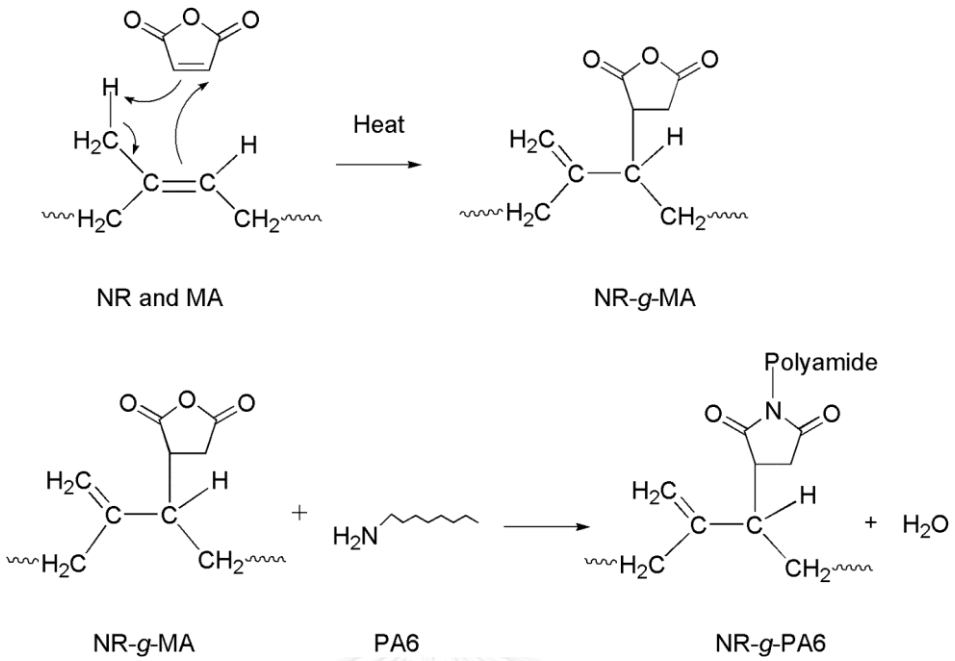

Figure 2.14 Possible reactions of PA6/NR blends with MA [39].

Grafting of MA onto NR in a solution state has also been reported [32, 40]. The experiment has been carried out by dissolving the rubber with a suitable solvent and grafting with MA in the presence of an initiator. Saelao and Phinyocheep [32] have successfully synthesized MNR in a solution state using toluene as the reaction medium. The experiments were carried out using 0.5 – 1.5% by mole of benzoyl peroxide (BPO), 5 – 25% by mole of MA, reaction temperature of 60 – 80 °C, and a reaction time of 0 – 30 h. The highest grafted MA content of about 2.2 wt% was found under grafting conditions of 10% MA and 1.0% BPO in 5% toluene solution at 80 °C for 24 h. However, a high gel fraction in the grafts of about 50% was observed. The gel may be formed by chemical crosslinks of the grafted MA and/or a recombination reaction of rubber macroradicals. The influences of grafting parameters, namely, monomer and initiator concentration, reaction temperature, and reaction time on grafted MA and gel contents in MNR have been investigated by Nakason et al. [40]. The grafted MA content of about 3.3 wt% was obtained at 10 phr MA and 3 phr BPO at 80 °C for 2 h. It was found that the grafted MA content increased with increasing amounts of MA and BPO. An increase in reaction

temperature and time also caused an increase in the level of grafted MA. However, a higher degree of gel formation was more pronounced at a higher initiator concentration (~25 wt% at 3 phr BPO), reaction temperature (~27 wt% at 110 °C), and reaction time (~50 wt% at reaction time of 3 h). The T_g of the graft copolymers increased with increasing MA content.

2.5 Styrene-Assisted Grafting of MA onto Polyolefins

Grafting of MA onto polyolefins in the presence of styrene comonomer has been extensively studied for many years. Styrene (ST) has been used as a comonomer for promoting grafting of MA onto PP [30, 31], NR [32], ethylene-octene copolymer [33], iPB-1 [34], and PE [35]. It has also been reported that ST can improve the grafting degree of GMA onto PE [36], HDPE [37], and PP [38]. These reports are reviewed below.

The styrene-assisted grafting of MA onto PP by reactive processing has been investigated [30, 31]. The addition of ST increased the grafted MA content at a MA/ST ratio of 1:1. The added ST could activate the reactivity of the double bond of the MA molecule by forming a charge transfer complex (CTC), which is later copolymerized with PP to produce the grafted PP as shown in Figure 2.15. Other grafting routes have also been proposed [31]. At a ST/MA ratio of 1:1, ST reacted with MA to produce a ST/MA copolymer (SMA) which was later grafted onto PP. When the amount of MA was higher than ST, part of the MA reacted with ST to produce SMA. At a higher amount of ST, some of the ST reacted with PP macroradicals to produce styryl macroradicals whilst others reacted with MA to form SMA. The effects of styrene and the molecular weight (M_v) of NR on the efficiency of MA grafting onto NR have been reported [32]. The addition of ST improved the grafted MA content (%MA) and the %MA also increased with a decrease in M_v as shown in Figure 2.16. When M_v of the NR is lower, the mobility of the rubber chain is higher, leading to a better chemical reaction of the MA molecules and the rubber macroradical gave a higher %MA incorporation. This indicates that the grafting degree of MA was influenced by styrene and the molecular weight of NR.

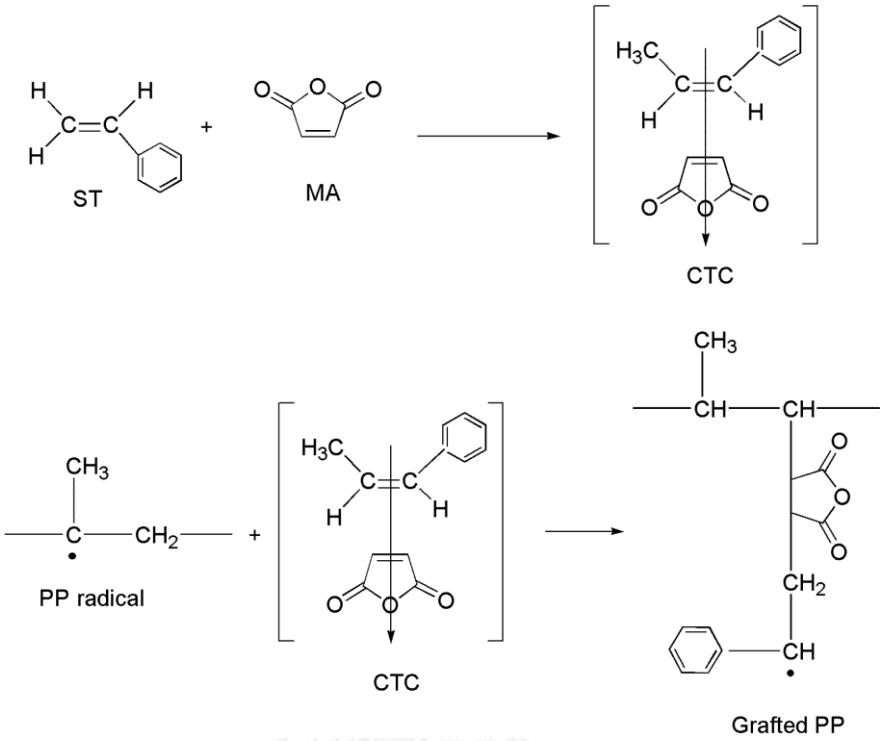

Figure 2.15 Proposed mechanism of styrene-assisted grafting of MA onto PP [30].

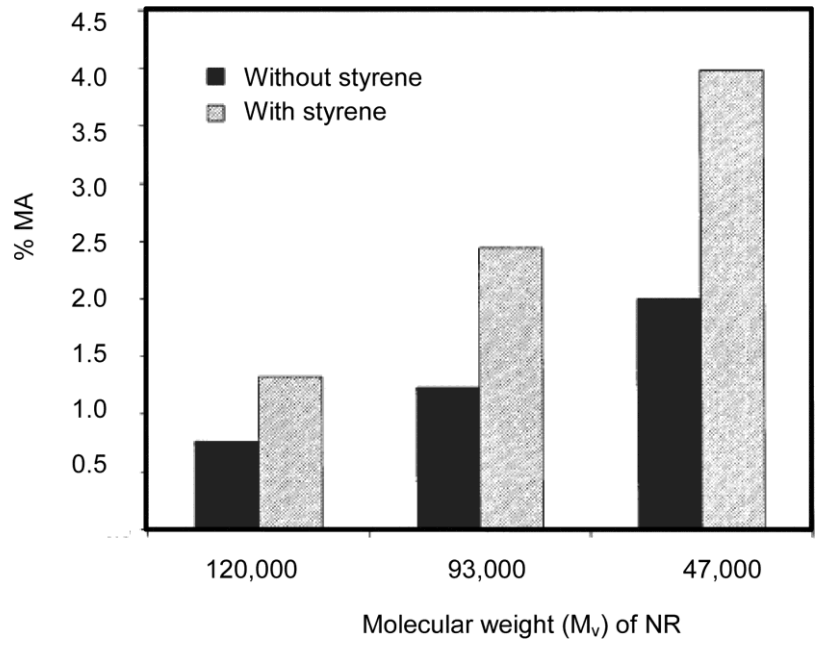

Figure 2.16 Effects of styrene and molecular weight of NR on content of MA grafting onto NR [32].

The melt grafting of MA onto an ethylene-octene copolymer or polyolefin elastomer (POE) in the presence of ST has been investigated [33]. A %MA of about 2.4% and a gel content of approximately 37 wt% were found at 3.0 phr of dicumyl peroxide (DCP). The MFI of the grafted POE decreased with increasing ST or DCP concentrations, indicating that crosslinking was found during the grafting process. The gel content in the grafts increased with an increasing amount of DCP. The degradation temperature of the grafted POE was found to be higher than that of neat POE, indicating that the grafting of MA improved the thermal stability of POE. The use of ST for promoting the grafting of MA onto iPB-1 has also been reported [34] The optimum MA grafting was found at an equimolar ratio of MA and ST with 0.3 phr of DCP at 170 °C. The grafting of GMA onto PE with ST comonomer provided an improvement in the grafting yield [36]. The dominant grafting mechanism was that ST reacted first with secondary macroradicals of PE and the resulting styryl macroradicals later reacted with GMA to form the grafted GMA, as shown in Figure 2.17.

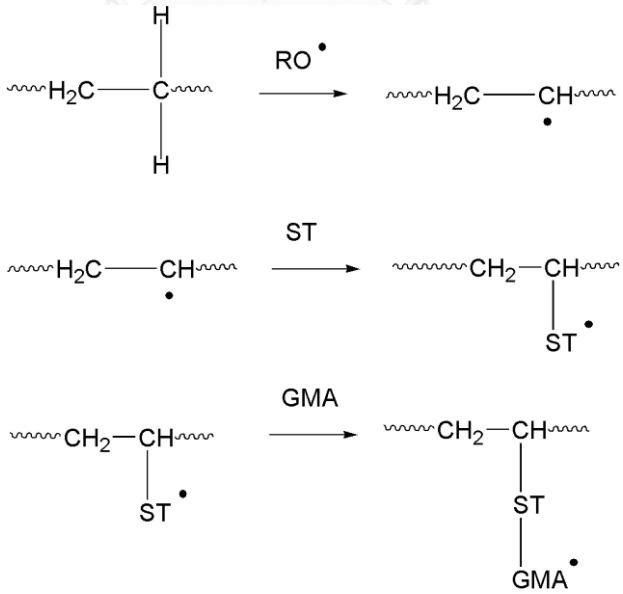

Figure 2.17 Illustration of styrene-assisted free radical grafting of GMA onto PE [36].

2.6 Differential Microemulsion Polymerization (DMP)

Microemulsion polymerization has often been used to prepare polymer nanoparticles. This technique provides ultrafine latex particles with high molecular weight polymers of interesting morphology [75, 76]. However, the use of a high amount of surfactant is the main drawback of this technique as separation of the surfactant from the lattices is a tedious and expensive process. To overcome this problem, many research groups investigating microemulsion polymerizations attempted to provide monomer to the reaction locus from an external reservoir rather than from the interior of the nanodroplets. Different terms such as differential microemulsion [49-54], modified microemulsion [77, 78], and semibatch/semicontinuous microemulsion polymerization [79-82] have been used for this technique. The formation of the polymer nanoparticles required a lower amount of surfactant compared to conventional microemulsion polymerization.

Differential microemulsion polymerization (DMP) is considered as one of the interesting techniques for synthesizing polymer nanoparticles since it requires a lower amount of surfactant than conventional microemulsion polymerization [49-54]. A DMP technique composed of water, surfactant, monomer, and initiator. Monomer feeding is provided as very small drops and the time interval between drops is very short. The smaller monomer-swollen micelles can be formed. The continuous feeding of monomer causes the monomer amount in the reaction system to be much lower; therefore, there are no monomer droplets during polymerization because the added monomer is quickly used by the growing chains in the polymer particle. Under this condition, there usually exist monomer droplets that act like a monomer reservoir. The free radical in the micelles can propagate with enough monomer transferred quickly from the monomer reservoir. However, the DMP process requires a certain temperature to initiate polymerization and suitable agitation to form stable emulsion droplets. It takes place in three steps: (i) an initial period in which a mixture of initiator and surfactant is heated in the reactor; (ii) a suitable addition period in which the total monomer is introduced to the reactor; and (iii) an aging period to allow for a complete polymerization of unreacted monomer. The DMP can provide a new technique for synthesizing polymer nanoparticles.

The DMP technique has been employed for synthesizing poly(methyl methacrylate) (PMMA) using ammonium persulfate (APS) as water-soluble initiator [50, 51]. The PMMA particles with a size of 13 – 16 nm (Figure 2.18) and a solid content of about 14 wt% were obtained at SDS/MMA and SDS/H_2O weight ratios of 1:18 and 1:120, respectively. The required surfactant amount was lower and the obtained polymer particles were smaller compared to those resulting from conventional microemulsion polymerization.

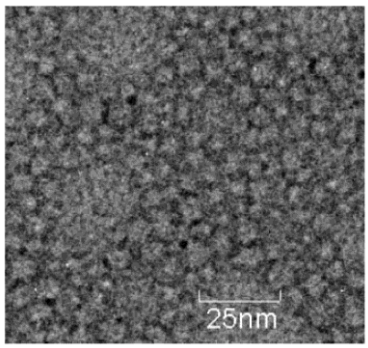

Figure 2.18 TEM images of PMMA nanoparticles [50].

The concept of homogeneous nucleation and heterogeneous nucleation for MMA polymerization is proposed in Figure 2.19. Homogeneous nucleation occurs in the water phase in which free radicals from initiator react with monomers dissolved in the water phase to form oligomeric radicals. These radicals continue to propagate until they reach a certain length and precipitate to produce polymer particles. However, the radical termination by combination or disproportion of active or dead polymer particles also occurred in the water phase. On the other hand, heterogeneous nucleation does not occur in water phase in which generated oligomeric radicals in the water phase enter into monomer-swollen micelles to form polymer radicals. Some of these radicals can continue to grow and form polymer particles by chain transfer to monomer, and others can terminate by another radical. The monomeric radicals formed by chain transfer in the particle can continue to initiate polymerization or move out into the aqueous phase.

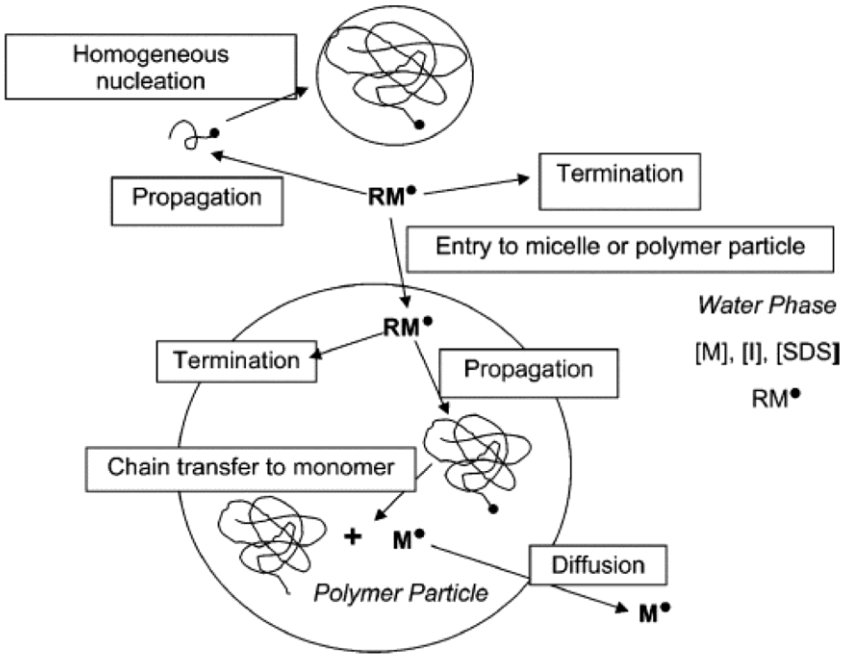

Figure 2.19 Proposed mechanism of nanosized PMMA synthesis by DMP [50].

The synthesis of PMMA/polystyrene core-shell nanoparticles via the DMP method using a small amount of PMMA as the seeds and APS as a water-soluble initiator has been reported [49]. Particle sizes smaller than 20 nm in diameter were obtained at a SDS/(ST+MMA) weight ratio of 0.043. The PMMA nanoparticles with a particle size of about 20 nm were successfully synthesized by adding the MMA monomer via a differential manner using 2,2'-azoisobutyronitrile (AIBN) as an oil-soluble initiator [52]. The PMMA having a molecular weight of about 10^6 g/mol was obtained at a very low SDS/MMA and SDS/H_2O weight ratios of 1:130 and 1:600, respectively. The effect of various initiator types of BPO, APS, and AIBN for synthesizing the PMMA nanoparticles using the DMP method has been investigated [54]. PMMA particles in the range of 2 – 5 nm (Figure 2.20) and a high solid content of more than 13 wt% were obtained at SDS/MMA and SDS/H_2O weight ratios of 1:16 and 1:100, respectively. The BPO micellar nucleation was more favorable for synthesizing smaller PMMA nanoparticles than APS homogeneous nucleation and AIBN partially heterogeneous nucleation. The proposed micellar nucleation is shown

in Figure 2.21. The primary radicals produced by the decomposition of BPO occupy the micelles to form nanoreactors. These generated radicals later react with monomers in the micelles to form oligomeric radicals and then propagate to form polymer nanoparticles.

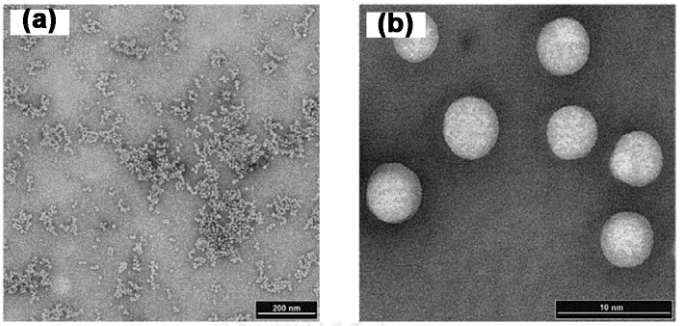

Figure 2.20 TEM images of PMMA nanoparticles negatively stained with 2% uranyl acetate: (a) and (b) particle size below 5 nm under two different magnitudes [54].

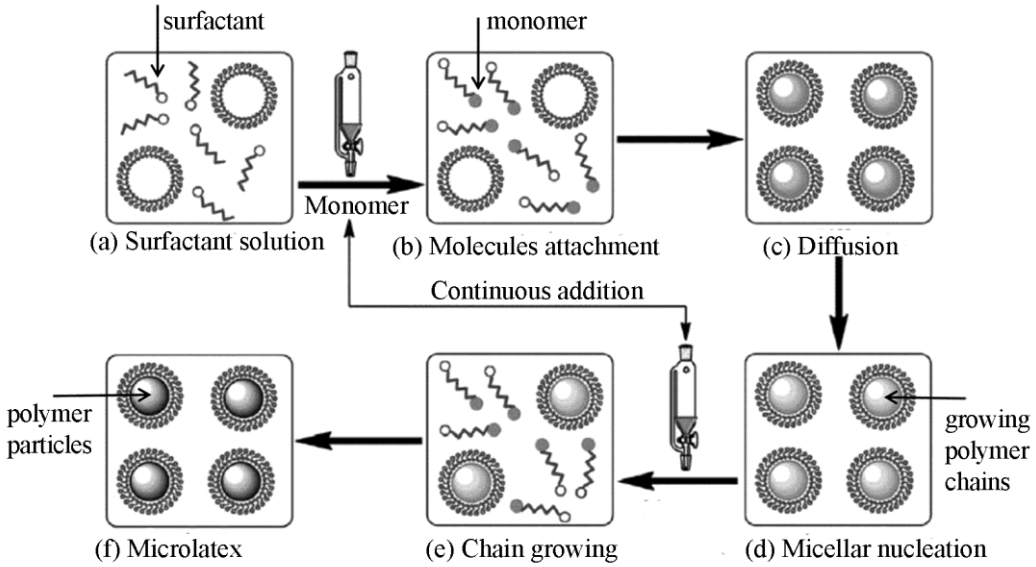

Figure 2.21 Illustration of micellar nucleation process of the BPO initiation DMP system for synthesizing the PMMA nanoparticles [54].

Recently, the DMP method has been employed to synthesize the nanoparticles of poly((butyl acrylate)-*co*-(methyl methacrylate)-*co*-(methacrylic acid)) [53]. The effects of various initiator types such as BPO, APS, and AIBN on particle size and molecular weight of polymer were investigated. The nanoparticles of the terpolymers with a particle size in the range of about 5 – 20 nm were obtained. The results showed that the initiator type could significantly affect the particle size and the molecular weight of the terpolymers. The AIBN initiator provided the smallest particle size and stable latex.

Based on the literature review, polymer nanoparticles have been successfully synthesized by the DMP method. The required surfactant amount was lower and the obtained polymer particles were smaller compared to conventional microemulsion polymerization.

2.7 Blending of Thermoplastic Polymer with Elastomeric Polymer

Elastomer/thermoplastic blends have been prepared using either a simple blend [27, 55-57] or dynamic vulcanization [58-70]. Thermoplastic polyolefins (TPOs) are produced via a simple blend by blending an elastomer with a polyolefin under a high shear condition without a curing agent. The morphology of the TPO has dual continuous phases of rubber and thermoplastic having a co-continuous morphology. Thermoplastic vulcanizates (TPVs) are produced by dynamic vulcanization, in which the curing agent is added and the rubber phase is vulcanized during mixing at high temperature. The morphology of the TPV consists of small crosslinked elastomeric domains dispersed in a thermoplastic matrix, resulting in an improvement of the properties of the blends. The change in morphology of the blends during dynamic vulcanization is shown in Figure 2.22. During the dynamic vulcanization process, a co-continuous morphology of the blends can be changed to a matrix and dispersed-phase morphology as shown in Figure 2.22 (a). In addition, the cross-linked rubber phase may become finely and uniformly dispersed in the plastic matrix as shown in Figure 2.22 (b). During the dynamic crosslinking, the viscosity of the rubber phase increases and the rubber domains can no longer be sufficiently deformed by local shear stress and are eventually broken down into small droplets.

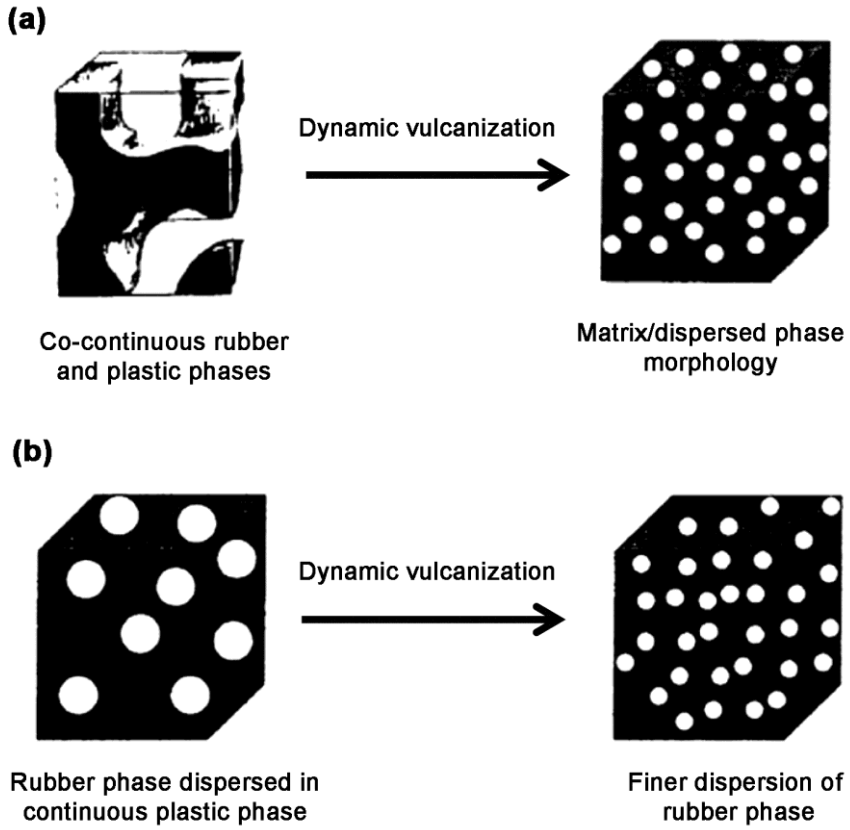

Figure 2.22 Schematic illustration of the dynamic vulcanization: (a) co-continuous morphology changes to matrix/dispersed phase morphology; and (b) finer dispersion of dispersed rubber domains [59].

The TPVs based on NBR/ABS blends by dynamic vulcanization using a styrene-butadiene-styrene block copolymer (SBS) as a compatibilizer has been investigated [70]. The addition of the SBS compatibilizer to the blends provided an improvement in the mechanical properties of TPVs and the tensile strength and elongation at break reached a maximum at a compatibilizer content of 1 phr. Morphology of the blends showed that the vulcanized NBR particles were dispersed evenly in the TPVs and the dimensions of the NBR particles were decreased remarkably with the introduction of the compatibilizer. Vulcanized NR/ethylene-

vinylacetate copolymer (EVA) blends using NR-*g*-PDMMMP as the compatibilizer have been investigated [16]. The elastic modulus and complex viscosity increased with increasing content of the compatibilizer. The highest tensile strength and elongation at break with the lowest tension set were found at a loading of 9 wt% NR-*g*-PDMMMP. Under this condition, the smallest vulcanized rubber particles dispersed in the EVA matrix with the lowest tan δ were also obtained. This is attributed to the high chemical interaction between the two phases caused by a compatibilizing effect. SEM micrographs of the blends are shown in Figure 2.23.

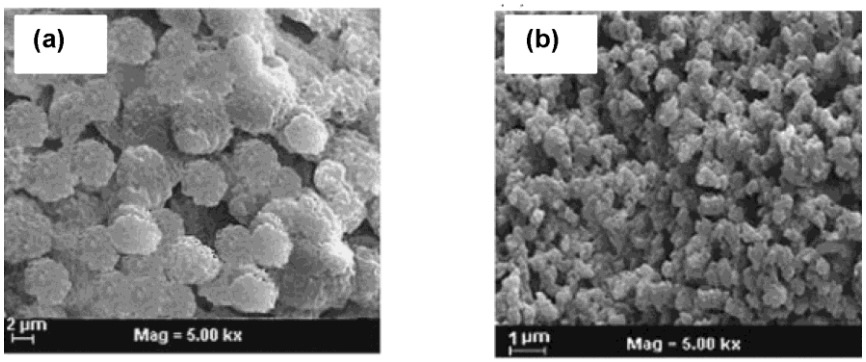

Figure 2.23 SEM micrographs of dynamically cured 40/60 NR/EVA blends with and without compatibilizer [16].

Since the hydrophilicity of NR is improved by grafting with polar monomers, the modified NR or grafted NR can be widely used in the area of reactive blending as a blend compatibilizer or blend composition with other polymers. Blending of NR-*g*-(ST-*co*-MMA)) with modified acrylic sheet has been reported [15]. The improved mechanical properties of the blends were observed when a graft copolymer of 0.5 – 4 parts to the acrylic sheets was added. The tensile strength, elongation at break and Charpy impact strength of the blends increased with increasing content of the graft copolymer. This is attributed to the compatibility between the graft copolymer and the modified acrylic sheet. SEM micrographs confirmed the better compatibility that

caused the higher impact strength of the modified acrylic sheet. MNR has been used for blending composition or blending compatibilizer for MNR/cassava starch blends [23]. The Mooney viscosity, apparent shear stress, and shear viscosity of the MNR blended were highest at a given concentration of cassava starch. The blends with MNR as a compatibilizer at a given level of cassava starch exhibited a rheological behavior between the blends of neat NR and MNR, indicating that the chemical interaction between the polar groups in the MNR backbone and cassava molecules was responsible for the dynamic characteristics of the blends. Influences of three types of modified NR (i.e., MNR, ENR, and NR-*g*-PMMA) as the compatibilizers for NR/TPU blends have been reported [24]. The blends with modified NR exhibited superior stiffness, entropy effect and damping factor compared to other blends with unmodified NR. The mechanical properties and rubber elasticity of the blends were ranked as follows: MNR/TPU > ENR/TPU > NR-*g*-PMMA/TPU and unmodified NR/TPU blends, respectively. This is attributed to the chemical interaction of the functional groups of modified NR molecules with polar functional groups of the TPU molecules which enhanced the interfacial adhesion of the two phases. Recently, NR, PS-*g*-NR, and hydrogenated PS-*g*-NR or H(PS-*g*-NR) have been used as a modifier in ABS [71]. The introduction of H(PS-*g*-NR) of 10 wt % to ABS increased the tensile and impact strengths and the thermal resistance of the blends, and to a greater extent than that provided by blending with NR or PS-*g*-NR. Morphology of the blends with 10 wt% H(PS-*g*-NR) showed a homogeneous fracture surface. This contributed to H(PS-*g*-NR) acting as an interfacial agent to impart compatibility with ABS and thus improved the mechanical properties of the blends.

2.8 Summary

NR latex contains rubber with some minor non-rubber components such as proteins and lipid. Based on the NR structure, a branched network in NR or gel can be formed through intermolecular hydrogen bonds of the modified dimethylallyl group at the ω-terminal with proteins and the interaction of phospholipids with the phosphate group of α-terminal.

DPNR is purified NR latex which is prepared by removing the proteins using deproteinization methods, such as enzymatic treatment, surfactant washing, and saponification, and urea treatment. Among these techniques, urea treatment is a more preferable technique as it can remove proteins from the NR latex rapidly and efficiently. The gel content of DPNR was reduced, indicating that the gel in NR might be caused by the proteins.

Various modification methods, such as chlorination, epoxidation, hydrogenation, and grafting, have been used to modify the NR structure for improving physical and chemical properties of NR. Grafting is one of the most attractive techniques. The MMA, ST, and MMA-ST comonomer are the commonly used monomers for grafting onto NR. Recently, MA has become an interesting monomer for grafting with NR to improve the hydrophilicity of the NR backbone. The grafted product can be widely used as blend component and blend compatibilizer.

Graft copolymer of MA onto NR has been obtained by either a molten state or solution state. However, a small content of grafted MA with high gel fraction in the grafts was found. The main drawback of grafting in solution is that a large amount of toxic solvent is needed for the reaction medium which has a negative impact on the production cost and environment. Grafting reaction in the latex form is a more feasible technique as NR is naturally available in a latex phase. Unfortunately, side reactions due to the presence of proteins in NR latex were found. Moreover, protein also causes formation of gel in NR. Therefore, it would be better to remove proteins from the NR latex before the grafting reaction.

It is very difficult to achieve a favorable grafting efficiency of MA onto polyolefins due to the fact that MA is not reactive towards the polymer macroradicals

because of their structural symmetry and deficiency of electron density around the double bond, resulting to a low grafting efficiency. Styrene comonomer has been employed for promoting the activity of MA. An introduction of styrene can improve the efficiency of MA grafting.

Differential microemulsion polymerization (DMP) is a unique technique that requires a lower amount of surfactant than conventional microemulsion polymerization. The surfactant is not only expensive but also causes water sensitivity of the final product. The main difference between the DMP and conventional microemulsion method is the monomer feeding operation. The former involves a slow addition of monomer with continuous dropping into the reaction system whilst the latter is incorporated via a single addition.

Rubber/thermoplastic blends have been successfully prepared using either a simple blend or dynamic vulcanization. Thermoplastic vulcanizates (TPVs) obtained by dynamic vulcanization showed better mechanical and thermal properties of the blends compared to the simple blend. This is attributed to fine and uniform crosslinked rubber particles dispersed in the thermoplastic matrix.

Although it is possible to combine the properties of two polymers by blending, many of the blends are incompatible. These immiscible blends showed a low interfacial adhesion between the different phases and exhibited poor mechanical properties. Compatibilizer can enhance the interfacial adhesion between the two phases and improve the properties of the blends.

CHAPTER III: DEPROTEINIZATION OF NATURAL RUBBER LATEX BY UREA TREATMENT

This chapter focuses on the preparation of a DPNR latex by urea treatment. The effect of the amount of urea on efficiency of removing the proteins from NR latex was investigated. The nitrogen and protein contents in the NR and DPNR were determined using the Kjeldahl procedure. The gel content of rubber before and after deproteinization was determined. Removing the proteins from the NR latex was confirmed using FTIR analysis. The DPNR latex obtained was later used as a preferred substrate for MA grafting.

3.1 Materials

High ammonia stabilized NR latex containing about 60% of dried rubber content (DRC) was provided by Thai Rubber Latex Co., Ltd., Rayong, Thailand. The overall composition of the NR latex is summarized in Appendix A (Table A-1). Sodium dodecyl sulfate ($CH_3(CH_2)_{11}OSO_3Na$; SDS; 99%) as a surfactant was purchased from Sigma-Aldrich (USA). Urea ($CO(NH_2)_2$; 99.5%) as a deproteinizing agent was purchased from Loba Chemie (India). Chloroform ($CHCl_3$; 99.5%) and formic acid (HCOOH; 98%) were manufactured by EMD Chemicals Inc. (USA). Toluene ($C_6H_5CH_3$; reagent grade) was purchased from Caledon Laboratories Ltd. (Canada). Deionized water (DI) was used throughout this research work.

3.2 Preparation of Deproteinized Natural Rubber (DPNR)

Deproteinized natural rubber (DPNR) was prepared by urea treatment according to the work of Kawahara and co-workers [42]. The preparation of DPNR latex was conducted according to the following steps. The NR latex was incubated with 0.1 – 0.3 wt% urea and 1.0 wt% SDS. The incubation temperature and time were 30 °C and 60 min, respectively. The latex was later centrifuged at 13,000 rpm for 40

min using a Sorvall RC 6 plus centrifuge. The cream fraction was redispersed with 1.0 wt% SDS followed by centrifugation and this step was repeated twice. The final cream fraction was redispersed with 0.1 wt% SDS to make latex with about 30 wt% dry rubber content. The solid DPNR was isolated from hot formic acid (40% v/v) and later washed with deionized water and dried to constant weight in a vacuum oven at 50 °C. Nitrogen content in rubber was later determined by the Kjeldahl procedure. The experimental procedure is shown in Figure 3.1.

3.3 Characterization

3.3.1 Determination of Nitrogen and Protein Contents in Rubber

The nitrogen content of rubber (NR) and deproteinization (DPNR) was measured by the Kjeldahl procedure according to the Rubber Research Institute of Malaysia Test Method B7 [83]. The sample was introduced into a digestion tube and mixed with a $K_2SO_4/CuSO_4/Se$ composite catalyst at a ratio of 15:2:1. Then concentrated H_2SO_4 was added and the sample was digested until the solution became clear. The reaction system was cooled down to room temperature and the digestion mixture was later distilled. The distillates were titrated with 0.01 N H_2SO_4 using methyl red and methylene blue mixture as an indicator. The nitrogen content was calculated as follows:

$$\text{Nitrogen content (wt\%)} = \left(\frac{(V_1 - V_2)N \text{ x } 0.014}{W} \right) \text{x } 100 \qquad (3.1)$$

where V_1 (ml) and V_2 (ml) are the volumes of the H_2SO_4 used in the sample and blank test, respectively. N is the normality concentration of the H_2SO_4 and W (g) is the weight of the sample. The nitrogen content is related to the protein content and a factor of 6.25 is multiplied to determine the amount of protein from the nitrogen content [84].

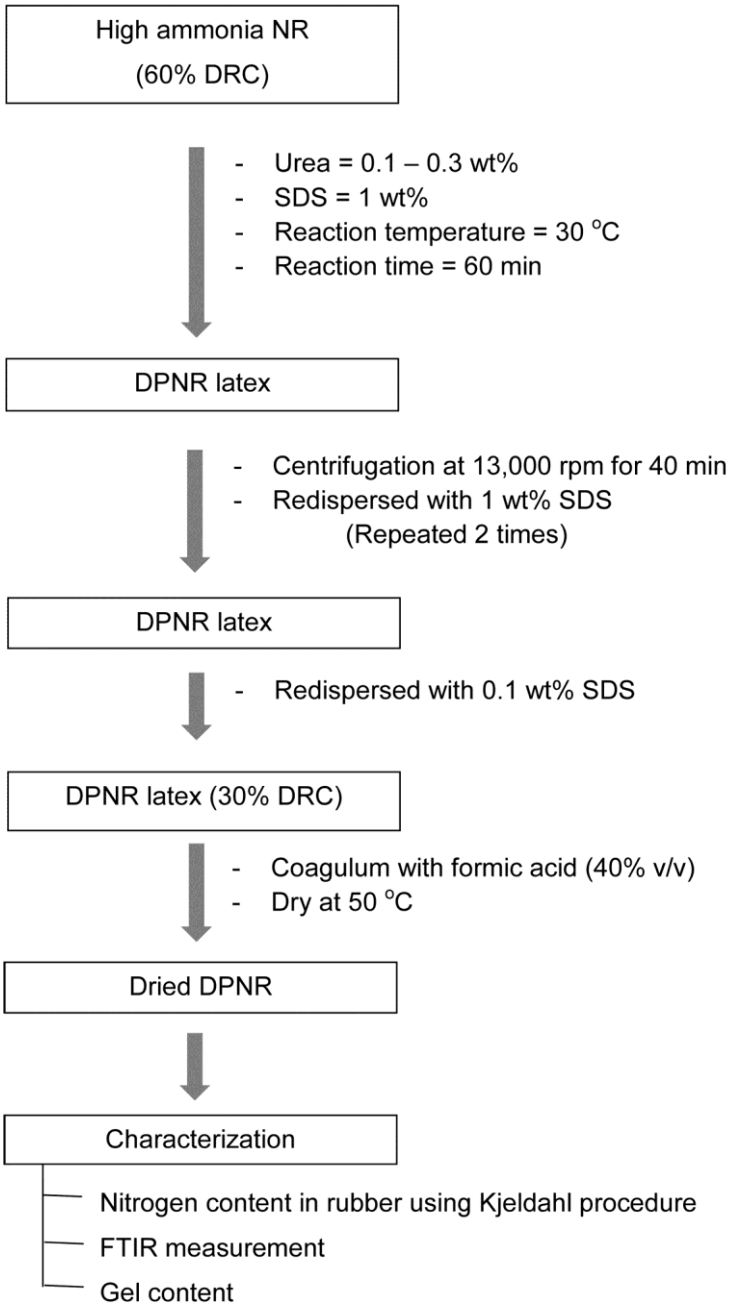

Figure 3.1 The experimental procedure of deproteinization of NR latex by urea and characterization of DPNR.

3.3.2 Fourier Transform Infrared Spectroscopy

Fourier transform infrared (FTIR) spectroscopy was used to confirm the removal of proteins from NR. FTIR spectra of NR and DPNR were recorded on a Nicolet 6700 spectrometer with a resolution of 4.0 cm^{-1} and 100 scans on the samples which were prepared by casting 1 wt% $CHCl_3$ solutions onto a NaCl disk.

3.3.3 Determination of Gel Content in Rubber

The gel content of the rubber was determined by extracting the dry sample using toluene at its boiling temperature for 24 h. The extracted sample was dried to constant weight in a vacuum oven at 50 °C. Weights of the initial sample and the extracted sample were measured. The gel content of NR and DPNR were calculated as follows:

$$\text{Gel content (\%)} = \frac{W}{W_o} \text{ x } 100 \qquad (3.2)$$

where W and W_o are weights of the dried gel fraction and the initial sample, respectively.

3.4 Results and Discussion

3.4.1 Nitrogen and Protein Contents in Rubber

DPNR latex was carried out by incubation of the NR latex with urea in the presence of surfactant at 30 °C for 60 min. The protein content in rubber was determined based on the nitrogen content measured by the Kjeldahl procedure. The nitrogen and protein content in NR and DPNR prepared using various amounts of urea are shown in Table 3.1. It was found that the nitrogen content and protein content significantly decreased after incubation of the NR latex with urea which confirmed that the proteins in NR latex had been removed. The effect of the amount of urea over the range of 0.1 – 0.3 wt% on nitrogen content and protein content in DPNR was also

investigated. It can be seen that the nitrogen and protein contents decreased with increasing urea content and it went through a minimum at an amount of urea of 0.2 wt% and thereafter increased. It was found that the nitrogen content of rubber significantly decreased from 0.2075 wt% (NR) to 0.0126 wt% (DPNR) after the incubation of the latex with 0.2 wt% of urea at 30 °C for 60 min. Under the same condition, the protein content also decreased from 1.2971 wt% (NR) to 0.0787 wt% (DPNR). However, when using 0.3 wt% urea, the nitrogen content of DPNR increased again. This may be due to the residue of urea in the reaction mixture. It can be seen that under the best condition, the protein content in the DPNR was approximately 94% less than the protein content of untreated NR. Therefore, the appropriate conditions for preparing the DPNR were 0.2 wt% of urea, 1.0 wt% of SDS, incubation temperature of 30 °C, and incubation time of 60 min.

Table 3.1 Effect of urea concentration on nitrogen and protein contents in rubber.

Sample[a]	Urea Amount (wt%)	Nitrogen content (wt%)	Protein content (wt%)
NR	0	0.2075 ± 0.0021	1.2971 ± 0.0129
DPNR	0.1	0.0255 ± 0.0005	0.1591 ± 0.0035
DPNR	0.2	0.0126 ± 0.0006	0.0787 ± 0.0038
DPNR	0.3	0.0272 ± 0.0022	0.1703 ± 0.0136

[a] Deproteinizing conditions: 0 – 0.3 wt% urea and 1 wt% SDS at 30 °C for 60 min.

The efficiency of urea in the presence of surfactant for removing the proteins from the NR latex could be explained as follows. The protein content of NR can significantly be decreased because most proteins in the NR latex are attached on the surface of the rubber particles with weak attractive force interactions and they can be disturbed or changed in their conformation by urea [42, 43]. Furthermore, a decrease in nitrogen content and protein content is attributed to the denaturation of protein by washing the NR latex with surfactant. The deproteinization mechanism by urea

treatment in the presence of surfactant is proposed in Figure 3.2. For deproteinizing the NR latex by urea, the protein was removed since urea and the surfactant can dislodge, denature, or change the conformation of the protein and then they are solubilized by surfactant and enter into the serum phase.

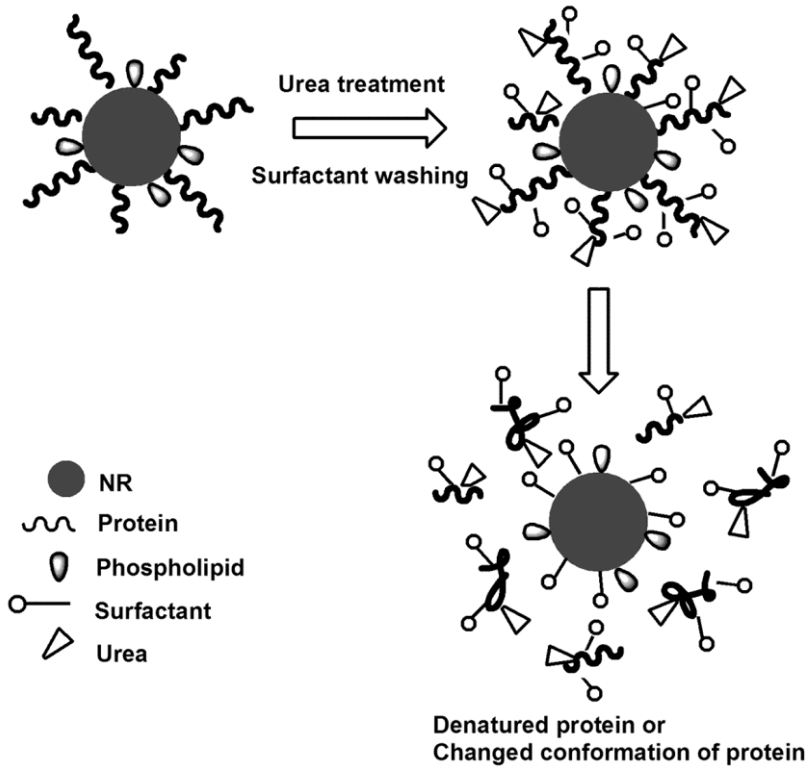

Figure 3.2 Schematic illustration of the proposed deproteinization mechanism of NR latex using urea treatment in the presence of surfactant.

Generally, gel content is used to determine the branched network or presence of cross-linking in the rubber. The gel content of NR was found to be 16 wt% and after the proteins of NR had been removed, no gel content was found in the DPNR. That is, a branched network or gel in NR is attributed to the association of the proteins at the surface of the rubber particles [42-48]. At the ω-terminal chain end of NR, two *trans*-1,4-isoprene units and a modified dimethylallyl unit are linked with functional

groups, which is associated with proteins to form crosslinks via hydrogen bonding. In addition, the cross-linked network in NR can also be formed by the interaction of phospholipids with the phosphate group of the α-terminal chain end. The results thus obtained allow us to conclude that the non-rubber constituents present in the NR latex, such as proteins, are presumed to be the origin of gel formation or a branched network in NR.

3.4.2 Confirmation of Removing Proteins from Rubber

FTIR measurements were used to confirm the removal of proteins from the natural rubber. FTIR spectra for NR and DPNR are shown in Figure 3.3. The important characteristic signals of NR and DPNR are shown at 3035 cm^{-1} (olefinic C–H stretching), 2961 cm^{-1} (C–H stretching of CH_3), 2916 cm^{-1} (C–H stretching of CH_2), and 2854 cm^{-1} (C–H stretching of CH_2 and CH_3), 1664 cm^{-1} (C=C stretching), 1448 cm^{-1} (C–H bending of CH_2), and 1375 cm^{-1} (C–H bending of CH_3), and 836 cm^{-1} (=C–H deformation) [85]. The signal at 1738 cm^{-1} is attributed to the carbonyl group of phospholipids attached to the NR particle. It can be seen that no clear difference in FTIR spectra between NR and DPNR was observed. This indicated that the NR and DPNR have similar chemical functionalities.

However, the characteristic peaks of the protein were found at 3440 – 3537 cm^{-1}. Therefore, a plot of absorbance versus wavenumber over the range of 3200 – 3400 cm^{-1} for NR and DPNR was conducted as shown in Figure 3.4. The absorbance *A* was normalized in comparison with the absorbance of the reference peak at 1664 cm^{-1} (A_o) which is attributed to a C=C stretching vibration. The spectrum of NR shows a signal at 3280 cm^{-1} which is attributed to the stretching vibration of proteins or peptides and the absorbance peak at 3320 cm^{-1} could be attributed to mono- or di-peptides [42, 43]. A decrease in the intensity of the 3280 cm^{-1} absorbance for DPNR indicated that some of the proteins from the NR latex were removed. However, the signal at 3320 cm^{-1} still appears after the deproteinization indicating that the source of residual nitrogen in DPNR could be due to the presence of mono- or di-peptides. The

results obtained from the FTIR analysis provide firm evidence that proteins were removed from the NR latex by urea-deproteinization.

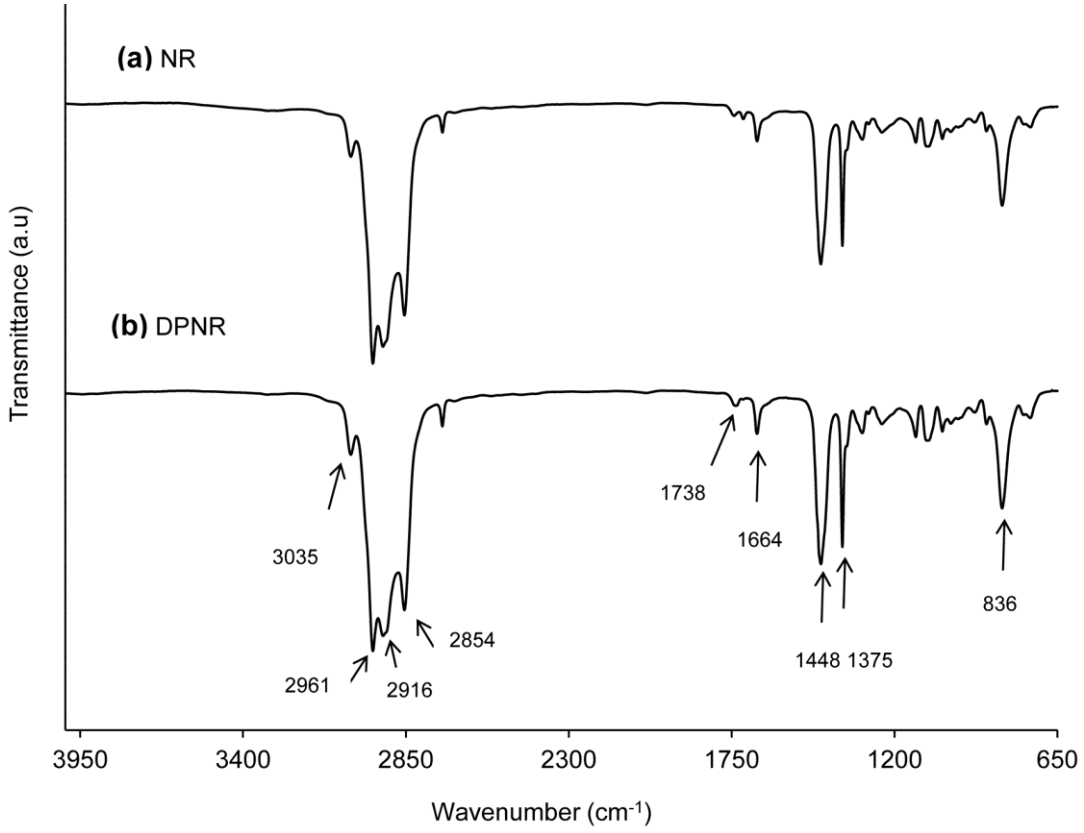

Figure 3.3 FTIR spectra of (a) NR and (b) DPNR. (Deproteinization conditions: 0.2 wt% urea and 1 wt% SDS at 30 °C for 60 min)

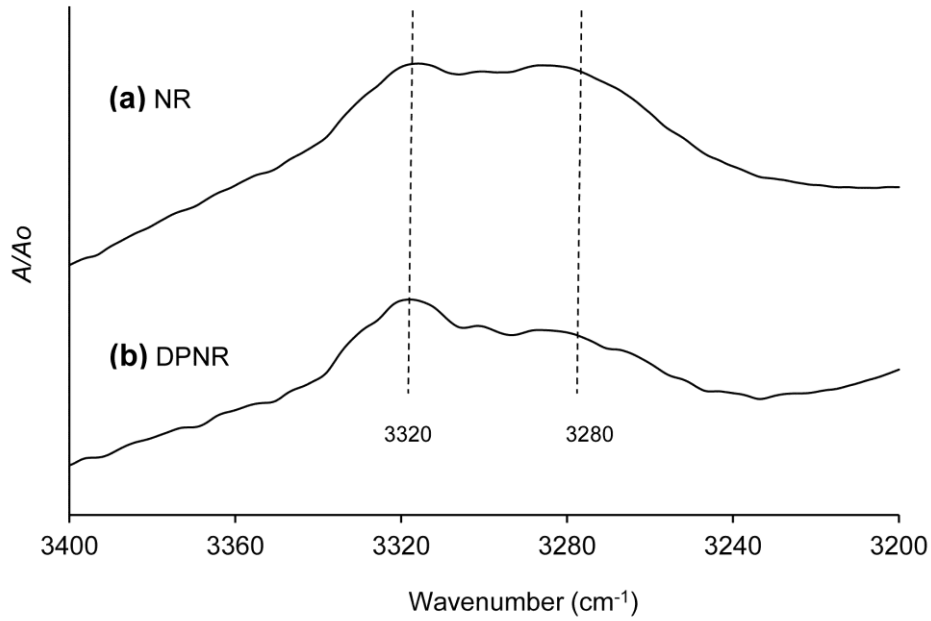

Figure 3.4 Selected regions FTIR spectra of (a) NR and (b) DPNR. (Deproteinization conditions: 0.2 wt% urea and 1 wt% SDS at 30 °C for 60 min)

3.5 Conclusions

Deproteinization of NR latex was successfully carried out by urea treatment in the presence of a surfactant. An extremely low protein containing NR (0.0787 wt%) was obtained under the conditions of 0.2 wt% urea and 1.0 wt% SDS at 30 °C for 60 min. The protein content in the DPNR was approximately 94% less than the protein content of untreated NR. The results showed that the nitrogen and protein contents significantly decreased after urea treatment. This indicates that most proteins in NR latex are attached on the surface of the rubber particles with weak attractive force interactions, which are able to disturb or change their conformation by urea. It was found that no gel content was found in the DPNR after removing the proteins, indicating that the branched network in NR is attributed to non-rubber components present in the NR latex such as proteins. It is seen that urea treatment can produce DPNR with low protein content. This demonstrates that urea-deproteinization is a very effective method to remove proteins from the natural rubber latex.

CHAPTER IV: GRAFTING OF MALEIC ANHYDRIDE ONTO DEPROTEINIZED NATURAL RUBBER

This chapter concentrates on the grafting of MA onto DPNR via a differential microemulsion polymerization (DMP) technique. The effects of monomer and initiator amount, reaction temperature, reaction time, and monomer addition rate on G.E and gel content in the grafts were investigated. FTIR, NMR, and XPS analyses were used to confirm the chemical structures of the graft copolymer. The diameters of the rubber and graft copolymer latex particles by DLS, morphology by TEM and AFM, thermal properties by DSC and TGA were investigated and the results obtained were also discussed. This chapter also provides a plausible grafting mechanism for MA grafting onto DPNR. The effect of proteins in the NR latex on the graft copolymerization is discussed. The effectiveness of the DMP method for MA grafting onto DPNR in latex form is also elucidated in this chapter.

4.1 Materials

High ammonia stabilized NR latex containing about 60% dried rubber content (DRC) was provided by Thai Rubber Latex Co., Ltd., Rayong, Thailand. Sodium dodecyl sulfate ($CH_3(CH_2)_{11}OSO_3Na$; SDS; 99%) as an emulsifier and benzoyl peroxide (($(C_6H_5CO)_2O_2$; BPO; 75%) as an initiator were purchased from Sigma-Aldrich (USA). Maleic anhydride ($C_2H_2(CO)_2O$; MA; 99%) as a monomer was purchased from Fluka (Switzerland). Chloroform ($CHCl_3$; 99.5%), formic acid (HCOOH; 98%), sodium carbonate anhydrous (Na_2CO_3; 99.5%), and sodium bicarbonate ($NaHCO_3$; 99.7%) were manufactured by EMD Chemicals Inc. (USA). Potassium hydroxide (KOH; 85%) was manufactured by ACP company (Canada). Isopropanol (($(CH_3)_2CHOH$; 99.7%), acetone ($(CH_3)_2CO$; reagent grade) and toluene ($C_6H_5CH_3$; reagent grade) were purchased from Caledon Laboratories Ltd. (Canada). Deionized water (DI) was used throughout the work.

4.2 Preparation of Grafting of MA onto DPNR

The graft copolymerization of MA onto DPNR latex (DPNR-*g*-MA) was carried out using a DMP technique. The recipes and variable factors for the graft copolymerization are presented in Table 4.1.

Table 4.1 Typical recipe used for grafting of MA onto DPNR.

Ingredients	Quantities
DPNR	15[a] g
Deionized water	25 g
KOH	0.1 g
Isopropanol	1.5 g
SDS	0.2 g
$Na_2CO_3/NaHCO_3$ (pH ~10)	10 ml
BPO	1, 3, 5, 7 wt%[b]
MA	1, 3, 5, 9, 13 wt%[b]

[a] Weight of the dried rubber content in DPNR latex.

[b] Percent by weight of the dried rubber content.

The weights of MA and BPO (wt%) are based on dried rubber content (DRC) of the latex. The preparation of the graft copolymer was conducted according to the following steps. The DPNR latex was first introduced into a 500 cm^3 glass reactor equipped with a reflux condenser, magnetic stirrer, thermometer and peristaltic pump. Potassium hydroxide (KOH) and the $Na_2CO_3/NaHCO_3$ buffer were added to maintain the pH of the system at about 10. Then isopropanol as a stabilizer and sodium dodecyl sulfate (SDS) as an emulsifier were introduced. The reaction mixture was stirred under a nitrogen atmosphere for 30 min to remove the dissolved oxygen in the latex. Afterwards the reaction mixture was heated up to a desired temperature (i.e., 60 – 90 °C), and then benzoyl peroxide (BPO) as an initiator was added, followed by a differential addition of MA monomer using a peristaltic pump at a fixed feeding rate

of 0.2 ml/min. After the feeding of MA was completed, the reaction system was kept at the same temperature (i.e., 60 – 90 °C), for another hour (i.e., 4 – 10 h) to increase the monomer conversion. The schematic illustration of experimental procedure for MA grafting onto DPNR is shown in Figure 4.1. The grafting of MA onto NR by the DMP method was carried out as the same procedure of MA grafting onto DPNR. For the case of MA grafting onto DPNR using the conventional microemulsion polymerization technique, the grafting condition was the same as explained earlier, however MA was introduced into the system in one portion.

4.3 Characterization

4.3.1 Determination of Grafting Efficiency

A Soxhlet extraction procedure was carried out to assess the amounts of free NR and graft copolymer in the final product. Free NR was removed by extracting with light petroleum ether at its boiling point of around 35 – 60 °C for 24 h and later washed several times with acetone to remove the ungrafted MA [13, 33]. The extracted sample was dried to constant weight in a vacuum oven at 50 °C. After solvent extraction, the purified DPNR-*g*-MA was obtained. Weights of both the initial sample and the extracted sample were measured for determination of the grafting efficiency (G.E) as follows:

$$\text{G.E}\,(\text{wt}\%) = \left(\frac{\text{Weight of graft copolymer}}{\text{Weight of dried coagulum product}} \right) \text{x}\,100 \qquad (4.1)$$

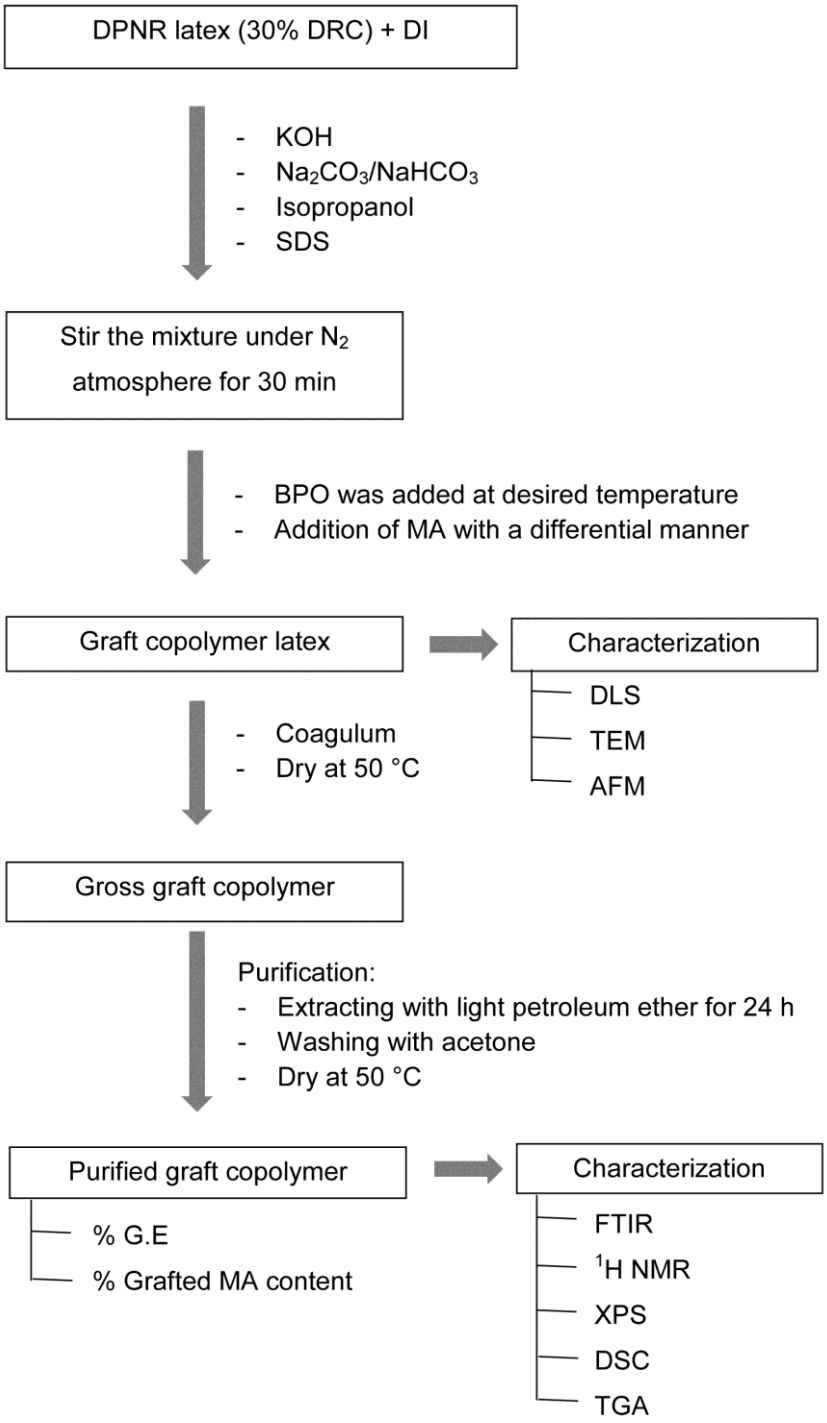

Figure 4.1 The experimental procedure of MA grafting onto DPNR and characterization of graft copolymer.

4.3.2 Determination of Grafted MA Content

The quantity of grafted MA was determined by a titration method according to the work of Nakason and co-workers [40]. 1.0 g of the purified graft copolymer was dissolved in 100 ml of toluene at its boiling temperature. Then 0.2 ml of distilled water was added to hydrolyze the anhydride into the carboxylic acid group. Afterwards, the solution was refluxed for 2 h to complete the hydrolysis. The hot solution was immediately titrated with 0.025 N KOH using phenolphthalein as an indicator. A blank test for NR was carried out in the same way. The quantity of the grafted MA was calculated as follows:

$$\mathrm{MA(wt\%)} = \frac{(V_1 - V_o)N}{2W} \mathrm{x}\, 98 \,\mathrm{x}\, 100 \qquad (4.2)$$

where V_o (l) and V_1 (l) are the volumes of the KOH used in the blank and sample test, respectively. N is the concentration of KOH (mol/l), and W is the weight (g) of the purified graft copolymer. The molecular weight of MA is 98 g/mol.

4.3.3 FTIR and NMR Spectroscopies

FTIR spectra of DPNR and DPNR-*g*-MA were recorded on a Nicolet 6700 spectrometer with a resolution of 4.0 cm^{-1} and 100 scans on the samples which were prepared by casting 1 wt% $CHCl_3$ solutions onto a NaCl disk. The level of the grafted MA was estimated using the absorbance ratio of the IR peaks at 1720 cm^{-1} to 836 cm^{-1} (A_{1720}/A_{836}). These peaks are assigned to the C=O stretching of grafted MA and =C–H deformation of NR, respectively. Proton NMR (^{1}H NMR) spectra were recorded on a Bruker 300 MHz spectrometer using the samples which were swollen with $CDCl_3$. The number of scans for ^{1}H NMR was 64.

4.3.4 X-ray Photoelectron Spectroscopy

The chemical composition at the surface of the DPNR and DPNR-*g*-MA was investigated by X-ray photoelectron spectroscopy (XPS). The experiment was carried out on a VG Scientific ESCALAB 250 with an Al Kα X-ray source (1486.6 eV). A flood gun for the charge compensation was used and the emission current was 0.15 mA. Survey scans were taken over the range 0 – 1200 eV. Atomic concentration calculations and curve fitting were analyzed by using CasaXPS software.

4.3.5 Particle Size and Morphology

The particle size of the rubber and graft copolymer latex was measured by dynamic light scattering (DLS) using a Nanotrac instrument analyzer. The morphology was investigated by transmission electron microscopy (TEM) using a Philips CM10 transmission electron microscope at 100 kV. The latex was diluted by about 400 times of its original concentration with distilled water and then the sample was vapor deposited on a grid and stained with osmium tetroxide overnight for TEM measurement. The surface roughness of DPNR and DPNR-*g*-MA was determined by atomic force microscopy (AFM) measurements. The samples were prepared by casting the latex as a thin film. The experiment was performed in a tapping mode on a DI Nanoman IV instrument. The average roughness of the samples was calculated directly from the AFM image.

4.3.6 Determination of Gel Content

The gel content of graft copolymer was determined by extracting the dry sample with toluene at its boiling temperature for 24 h. The extracted samples were dried to constant weight in a vacuum oven at 50 °C. The gel content of the graft copolymer was calculated as follows:

$$\text{Gel content (\%)} = \frac{W}{W_O} \text{ x } 100 \qquad (4.3)$$

where W and W_o are weights of the dried gel fraction and the initial sample, respectively.

4.3.7 Thermal Analysis

Thermal properties of DPNR and DPNR-*g*-MA were studied by differential scanning calorimetry (DSC) and thermal gravimetric analysis (TGA). The glass transition temperatures (T_g) of DPNR and grafted DPNR were investigated by DSC on a TA Instrument DSC 2920 analyzer using a heating rate of 10 °C/min. A sample of about 10 mg was weighed and put into an aluminum pan and covered with an aluminum lid. The sample was cooled down to -90 °C, heated up to 160 °C, cooled down again to -90 °C, and then heated up again to 160 °C to remove the heat history and the heating scan was later recorded. The T_g was determined from the midpoint of the baseline shift of the DSC thermogram. The decomposition temperature (T_d) was investigated by TGA on a TA Instruments SDT Q600 analyzer. The mass of the sample was about 10 mg and the carrier gas was nitrogen with a flow rate of 60 ml/min. The temperature was scanned from 30 to 800 °C with a constant rate of 10 °C/min. The decomposition temperature was obtained from the peak maxima of the derivative of the TG curves.

4.4 Results and Discussion

4.4.1 Confirmation of the Graft Copolymer

FTIR spectra of the DPNR and DPNR-*g*-MA are shown in Figure 4.2. From the spectrum of the graft copolymer, new signals at 1780 (very weak) and 1720 cm^{-1} (very strong and sharp) are attributed to the C=O stretching of the grafted succinic anhydride rings and succinic acid, respectively. The strong signal at 1720 cm^{-1} indicated that most of grafted MA is in the form of an open ring. The signal at 3455 cm^{-1} is assigned to the OH stretching of carboxylic groups by partial hydrolysis of the succinyl groups and the signal at 712 cm^{-1} is attributed to the C=C of the grafted anhydride rings [32, 40, 86].

Confirmation of the chemical structure of the graft copolymer was further obtained from NMR spectroscopy. The ^{1}H NMR spectra of DPNR and DPNR-*g*-MA are presented in Figures 4.3 and 4.4. The characteristic signals of *cis*-1,4-isoprene units appear at 1.67, 2.03, and 5.12 ppm, which could be attributed to the methyl, methylene, and unsaturated methine protons, respectively [87]. On the other hand, the spectrum of the DPNR-*g*-MA shows additional peaks at 2.69 and 2.91 ppm, which could be assigned to the two methylene protons of the grafted MA [88]. These observations are similar to those observed for the grafting of the MA onto ethylene-diene copolymers [86], HDPE [89], and PP [90] based polymers. A broad peak at 3.85 ppm could be assigned to the methine proton of the succinic anhydride ring [91, 92]. The result seems to suggest that the graft reaction may occur at the allylic hydrogen atom of DPNR because of the absence of the chemical shift at 3.3 ppm indicating the succinyl group is attached at the tertiary carbon site. The methine proton of the anhydride ring could be in the deshielding region of the carbon-carbon double bond and therefore it appears at a lower field (3.85 ppm). This is consistent with the structure of DPNR-*g*-MA (1). The peak at 7.40 ppm could be assigned to the unsaturated methine proton of the grafted anhydride ring which is consistent with structure of DPNR-*g*-MA (2). The signal at 9.85 ppm could be attributed to the proton of the carboxylic acid by ring opening of the anhydride ring. Homopolymer of MA and residual MA were not found because of the absence of their characteristic signals at 4.5 and 6.9 ppm, respectively.

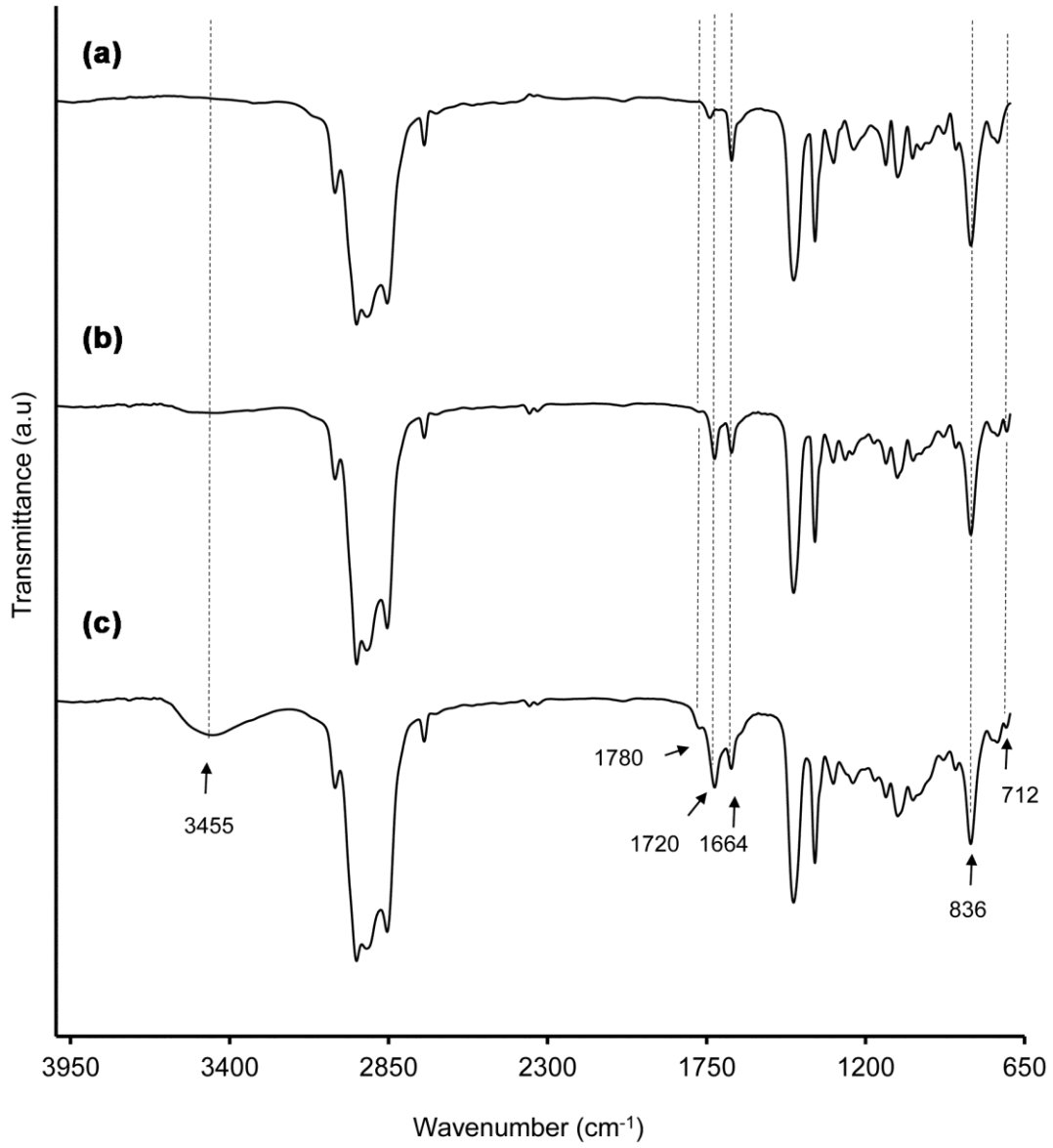

Figure 4.2 FTIR spectra of (a) DPNR, (b) and (c) DPNR-*g*-MA. (Grafting conditions: 7 wt% BPO and 9 wt% MA at (b) 80 °C and (c) 60 °C for 8 h; feeding rate of MA of 0.2 ml/min)

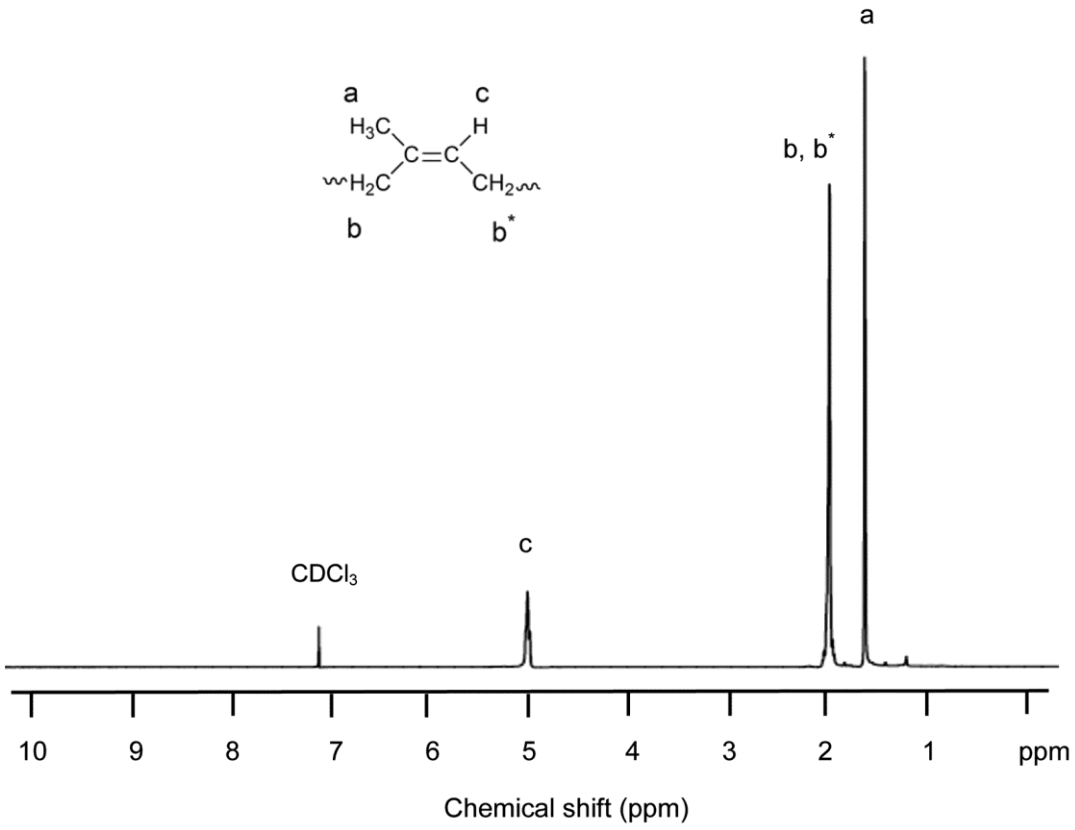

Figure 4.3 ^{1}H NMR spectra of DPNR. (Deproteinization conditions: 0.2 wt% urea and 1 wt% SDS at 30 °C for 60 min)

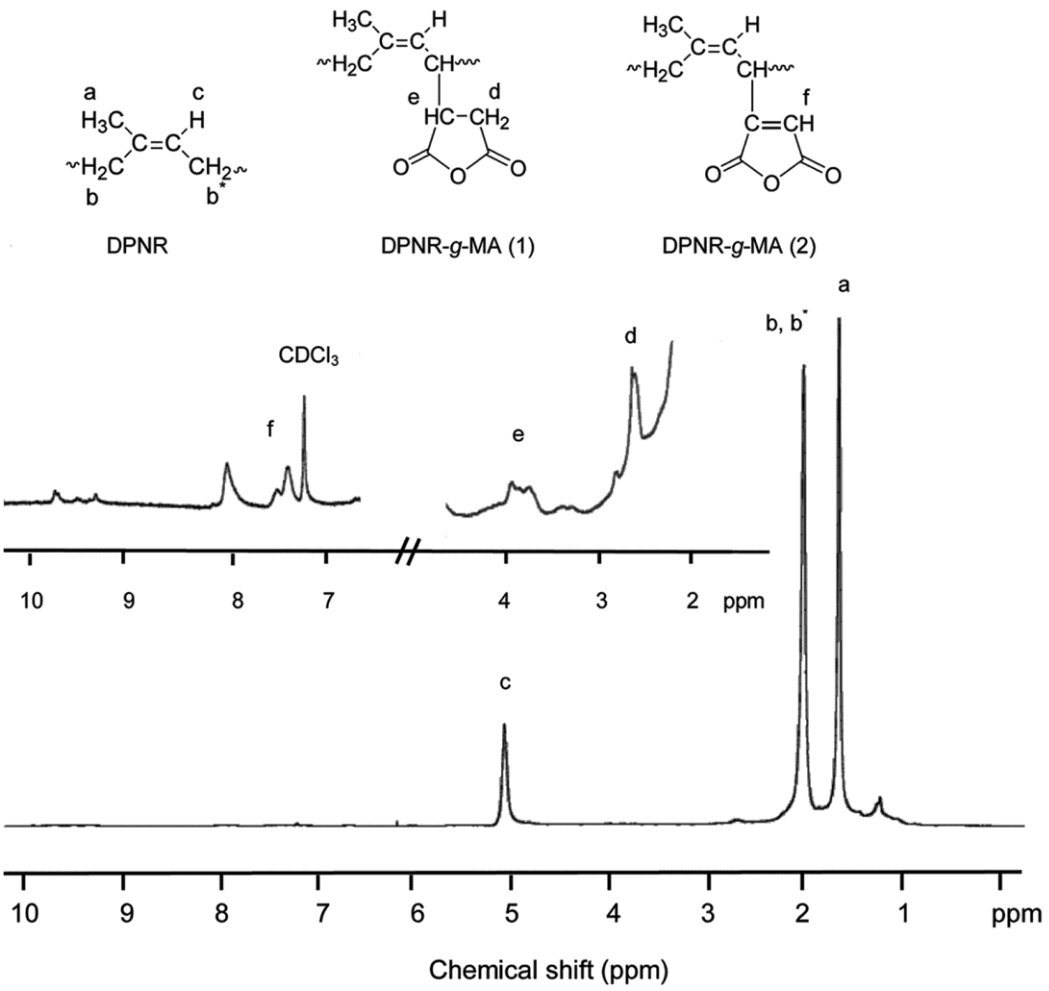

Figure 4.4 ^{1}H NMR spectra of DPNR-*g*-MA. (Grafting conditions: 7 wt% BPO and 9 wt% MA at 80 °C for 8 h; feeding rate of MA of 0.2 ml/min)

The XPS method is also used to determine the fixation of MA onto DPNR because it is an accurate technique to measure the elements and the elemental composition at the surface of a material. This technique is more sensitive to measure the elements at the surface (top 1 – 10 nm usually) than the bulk of the sample. Therefore, the detected signals are mainly from the surface unlike the bulk analysis provided by FTIR for functional group determination. The chemical composition at the surface of the graft copolymer using an XPS method is shown in Figure 4.5.

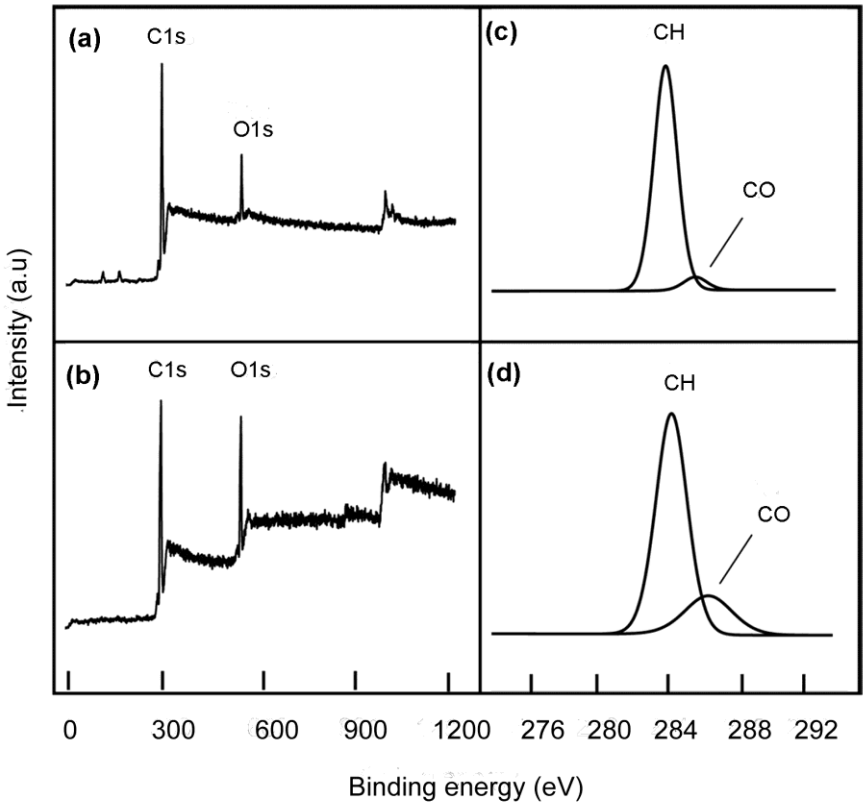

Figure 4.5 XPS spectra of DPNR and DPNR-*g*-MA: (a) wide scan spectrum of DPNR; (b) wide scan spectrum of DPNR-*g*-MA; (c) C1s core-level spectrum of DPNR; (d) C1s core-level spectrum of DPNR-*g*-MA. (Grafting conditions: 7 wt% BPO and 9 wt% MA at 80 °C for 8 h; feeding rate of MA of 0.2 ml/min)

The C1s and O1s core-level signals were observed at binding energies of 284.1 and 531.5eV, respectively. The C1s core-level spectrum is curve-fitted with two peak components. The binding energy at 284.1 eV could be assigned to the C–H species of both the rubber substrate and the grafted MA and the minor peak at 286.2 eV could be assigned to the C–O species of the grafted MA [93]. The surface elemental composition is presented in Table 4.2. It can be seen that most of the chemical composition of the neat rubber surface is due to the carbon atoms and the presence of a small amount of oxygen content may correspond to impurities in the rubber latex. An increase in the O/C atomic ratio of the graft copolymer indicates that MA had been grafted onto the rubber backbone. Furthermore, the grafting composition (% CO) of the graft copolymer of about 21% was obtained, indicating that a 21% yield of MA was fixed onto the rubber backbone. According to the FTIR, NMR, and XPS analyses, firm evidence that the MA was grafted onto the DPNR backbone is provided.

Table 4.2 Surface elemental compositions of DPNR and DPNR-*g*-MA.

Material	Composition (%)		O/C	Composition (%)[a]	
	C	O		C–H	C–O
DPNR[b]	97.7	2.3	0.02	94.7	5.3
DPNR-*g*-MA[c]	84.9	15.1	0.18	78.9	21.1

[a] Deproteinization conditions: 0.2 wt% urea and 1 wt% SDS at 30 °C for 60 min.

[b] Carbon species by curve fitting of C1s core-level.

[c] Grafting conditions: 7 wt% BPO and 9 wt% MA at 80 °C for 8 h; feeding rate of MA of 0.2 ml/min.

4.4.2 Grafting Mechanism of the Graft Copolymer

The grafting mechanism of MA onto polyolefins has been proposed by a number of researchers [29, 89]. In the present study, the reaction mechanism of MA grafting onto DPNR via a free radical reaction was proposed as shown in Figure 4.6. The primary radical species ($R^{\bullet}$) decomposed by BPO could generate the rubber macroradicals ($DPNR^{\bullet}$) in two different ways i.e., via the abstraction of the allylic hydrogen atom (reaction route *a*) and the addition of the radical to the double bond of DPNR (reaction route *b*). It should be noted that, the natural rubber has a highly *cis*-1,4-polyisoprenic structure and it contains labile allylic protons in every repeating unit. These protons are prone to hydrogen abstraction by radical active species generated from the BPO initiator. The $DPNR^{\bullet}$ can later react with MA to produce succinyl radicals (DPNR-*g*-$MA^{\bullet}$) as shown in reaction routes *c* and *d*. However, due to the difficulty of homopolymerization, only one MA unit could be attached on each active site along the rubber chains [28, 29]. The side chain graft copolymer of MA grafting onto DPNR (DPNR-*g*-MA) structures 1 and 3 were obtained by the termination of succinyl radicals with another rubber chain through a chain transfer reaction or hydrogen abstraction (reaction routes *e* and *g*). The disproportionation reactions also can be involved to produce the DPNR-*g*-MA graft copolymer structures 2 and 4 (reaction routes *f* and *h*). According to NMR analysis, it is suggested that the substitution of MA onto the DPNR backbone should occur at the allylic hydrogen atom of DPNR; hence, the DPNR-*g*-MA graft copolymer structures 1 and 2 should be the main products.

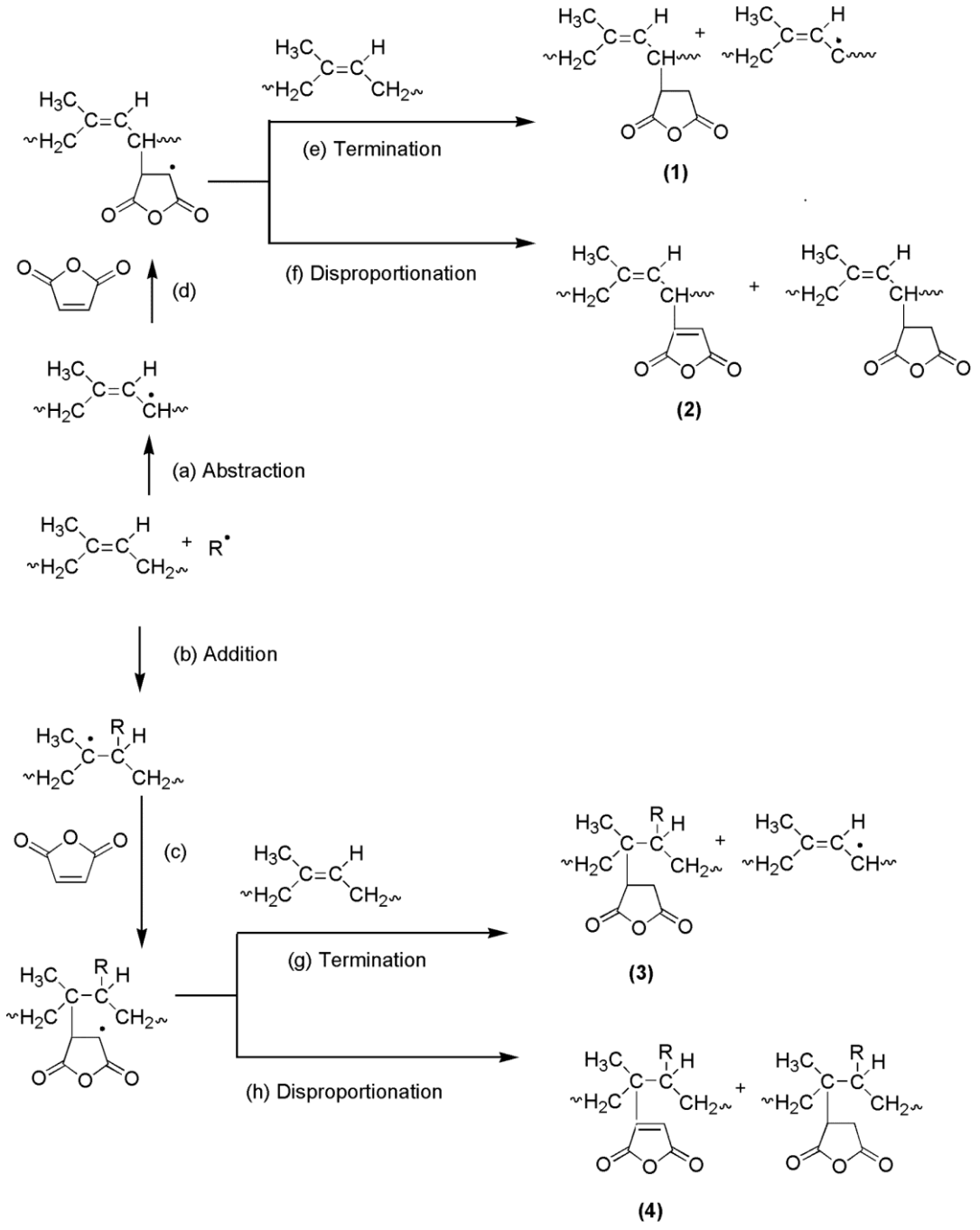

Figure 4.6 Schematic representation of the proposed free radical mechanism of MA grafting onto DPNR.

4.4.3 Parameters Affecting Grafting Efficiency and Gel Content

The reaction parameters affecting the grafting efficiency (G.E) and gel content for MA grafting onto DPNR, namely, initiator and monomer concentration, reaction temperature, and reaction time were investigated as follows.

4.4.3.1 Initiator Amount

The effect of initiator over the range of 1 – 7% wt% BPO was investigated using 9 wt% MA at 80 °C for 8 h. The results are shown in Figure 4.7.

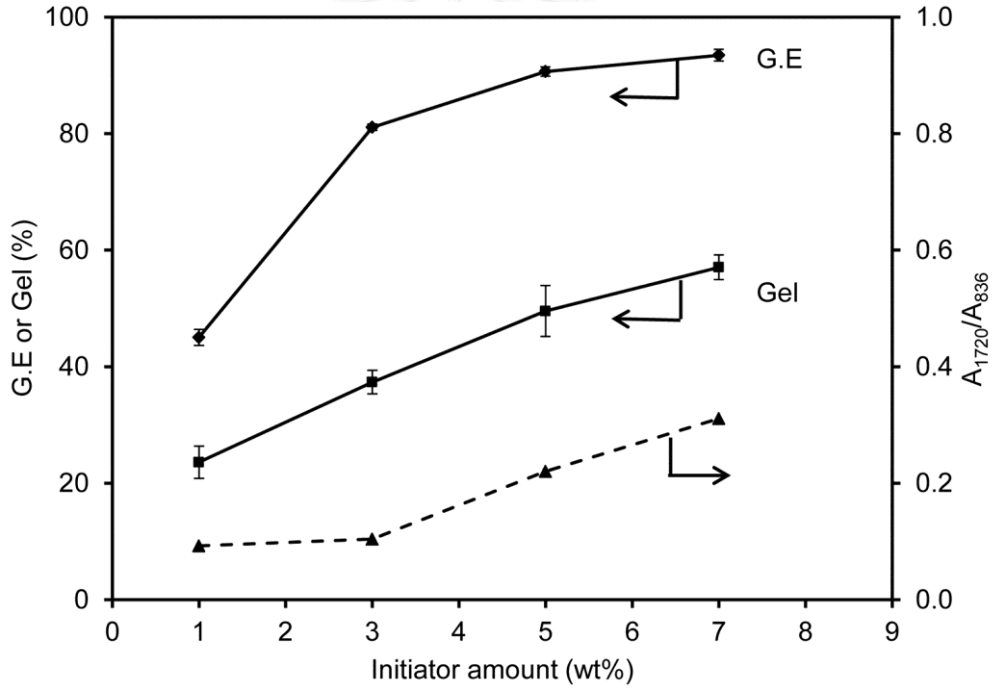

Figure 4.7 Effect of initiator amount on grafting efficiency (G.E), gel content, and absorbance ratio (A_{1720}/A_{836}) of graft copolymers. (Grafting conditions: 9 wt% MA at 80 °C for 8 h; feeding rate of MA of 0.2 ml/min)

It was found that the grafting efficiency (G.E) increases with an increase in the ratio of the initiator over DPNR, which is consistent with the general understanding that a higher initiator ratio generates more active sites on the DPNR backbone for grafting. It can be seen that the grafting efficiency and the estimated grafted MA content using the absorbance ratio (A_{1720}/A_{836}) showed the same trend. However, a high gel fraction was found when using a high amount of BPO initiator. As mentioned earlier, the increase in the initiator ratio resulted in more free radicals to produce active sites, hence, the chance of the interaction of rubber macroradicals with each other to form gel or a branched network increases. The chemical structure of cross-linked polymer by recombination of rubber macroradicals [32] is shown in Figure 4.8 (a). However, to obtain a high grafting efficiency, a BPO amount larger than 3 wt% is required for the given conditions.

4.4.3.2 Monomer Amount

The effect of MA monomer over a range of 1 – 13% by weight of dried rubber was investigated. The experiments were carried out using 7 wt% BPO at 80 °C for 8 h and the results are shown in Figure 4.9. It can be seen that both the G.E and A_{1720}/A_{836} increase with increasing content of MA up to 3 wt% of MA, after which a further increase in the MA ratio, the G.E and absorbance ratio would not change except for an increase in the gel content. Due to a steric effect, only one MA molecule was grafted onto one isoprene unit. This suggested that because of the immiscibility between MA and DPNR, that graft copolymerization may occur only on the surface of the latex particles. Thus, for the DPNR used in this work, the particle size of the latex was fixed, for which only 3 wt% MA is sufficient and a further increase in MA would not help in increasing the grafting efficiency but would promote gel formation. As previously discussed, high gel content was more pronounced at a high concentration of MA. This means that a high number of succinyl macroradicals were generated, leading to a high possibility of interaction between the rubber macroradicals and succinyl macroradicals to form gel as presented in Figure 4.8 (b). Therefore, the presence of the gel fraction in the grafts was found and it increases with an increasing

amount of MA. This result is supported by the Mooney test for the graft copolymer of MA synthesized in the molten state based on the literature [26]. It was found that the Mooney viscosity increased with an increasing amount of gel. The chemical interactions to form gel or cross-linking caused a resistance to the flow of the molten material.

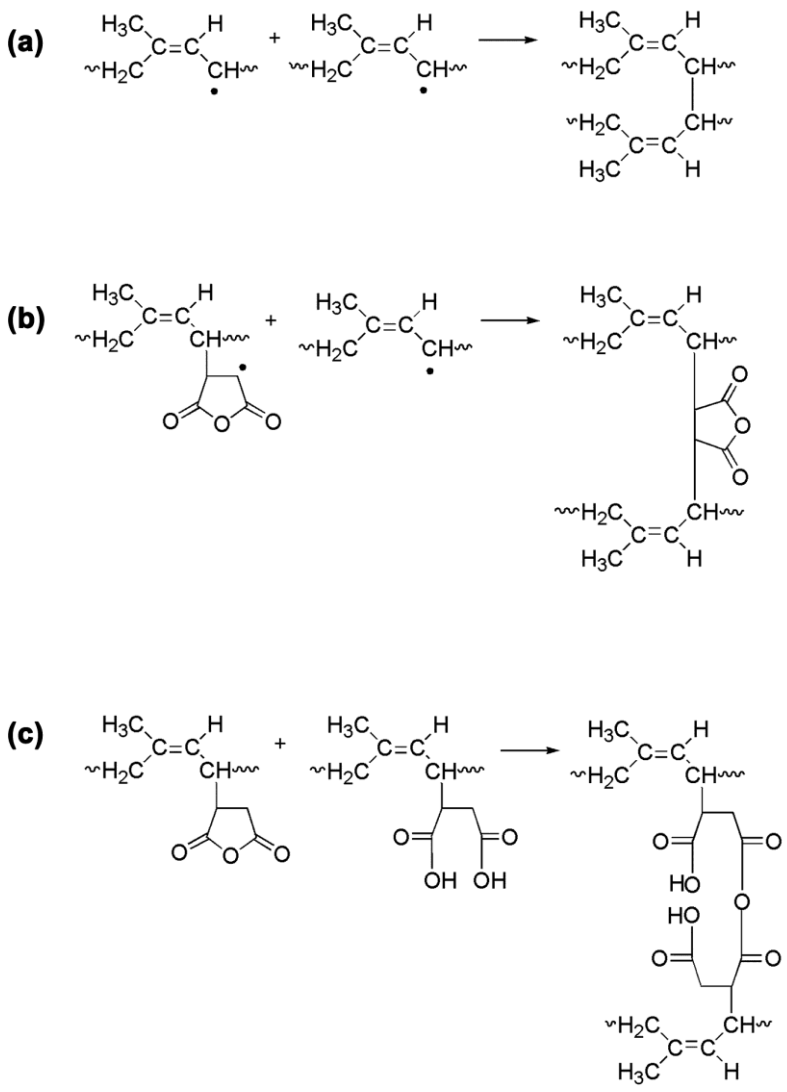

Figure 4.8 Schematic representation of the proposed crosslinking mechanism during grafting reaction of MA onto NR [26, 32].

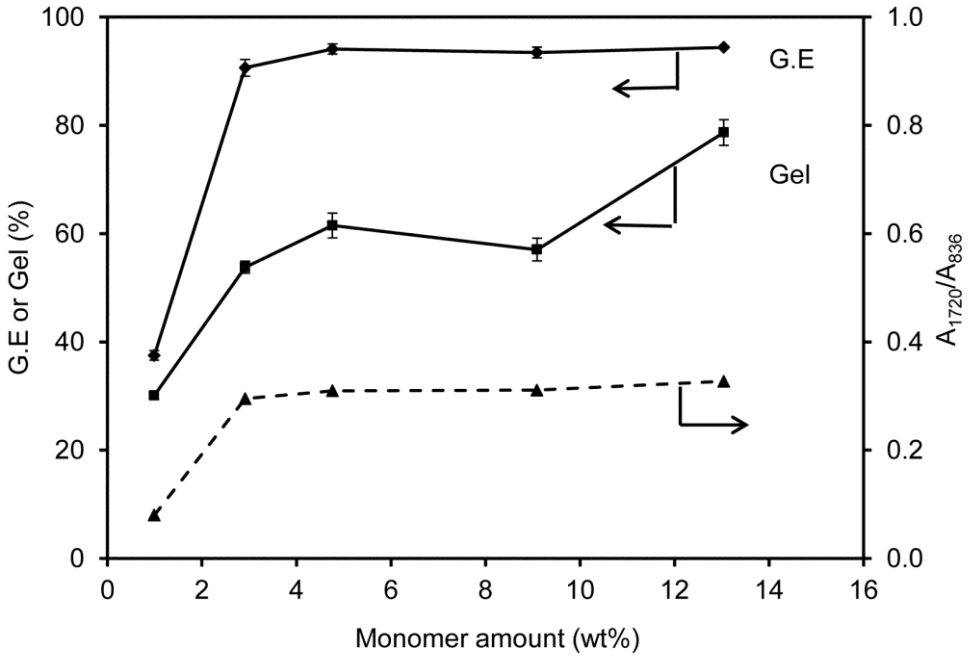

Figure 4.9 Effect of monomer amount on grafting efficiency (G.E), gel content, and absorbance ratio (A_{1720}/A_{836}) of graft copolymers. (Grafting conditions: 7 wt% BPO at 80 °C for 8 h; feeding rate of MA of 0.2 ml/min)

4.4.3.3 Reaction Temperature

The effect of reaction temperature on grafting efficiency and gel content was carried out over the range of 60 – 90 °C for 8 h with a fixed 7 wt% BPO, 9 wt% MA, and the results are shown in Figure 4.10. It was found that a high grafting efficiency was observed at a high reaction temperature. At higher temperatures, the decomposition of the BPO initiator is faster, leading to an increase in the free radical concentration to initiate more active sites on the natural rubber chains. Thus the rate of graft copolymerization increased. However, the grafting efficiency went through a maximum at a reaction temperature of 80 °C and thereafter decreased. The phenomena may be also associated with the surface reaction. That is, at a certain reaction time and temperature, the surface reaction was completed so a further increase in the reaction temperature would not help with the MA grafting but may increase the cross-linking reaction.

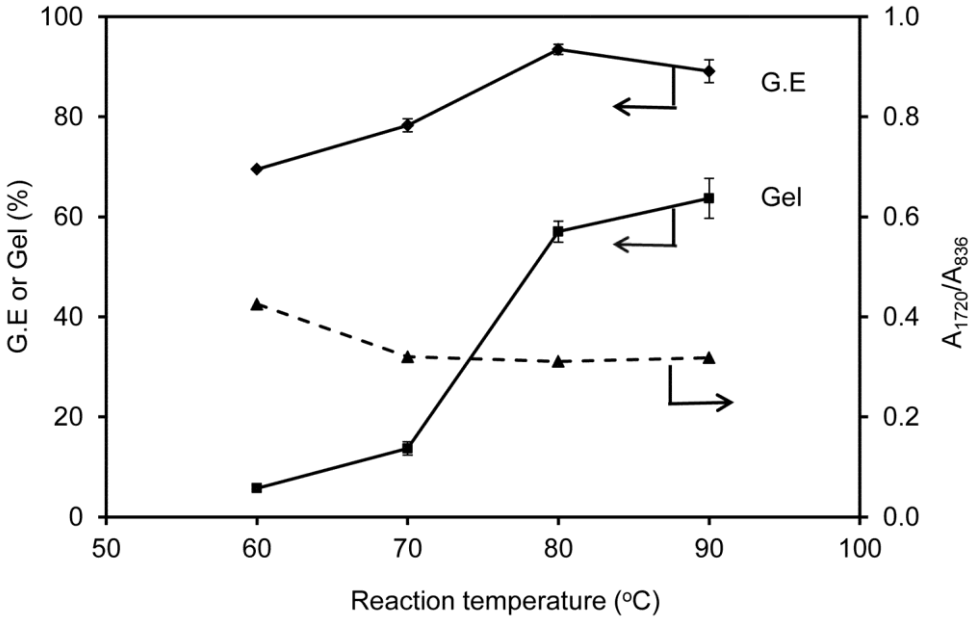

Figure 4.10 Effect of reaction temperature on grafting efficiency (G.E), gel content, and absorbance ratio (A_{1720}/A_{836}) of graft copolymers. (Grafting conditions: 7 wt% BPO, 9 wt% MA, and reaction time for 8 h; feeding rate of MA of 0.2 ml/min)

At high grafting temperatures, the carboxylic acid by ring opening of the anhydride ring of the graft copolymer can interact with the reactive polar functional groups of the graft copolymer to form gel as shown in Figure 4.8 (c). Therefore, the presence of gel content in the graft copolymer was found and it increases with increasing reaction temperatures. It is interesting to note that a high absorbance ratio (i.e., grafted MA) with a low gel fraction was found at a low reaction temperature of 60 and 70 °C, which implies that less chemical interactions of macroradicals occurs to form gel at a lower reaction temperature. Under these conditions, a low gel content of about 6 –13 wt% was found, which was lower than that of the graft copolymer of MA synthesized in the molten state at the high grafting temperatures and in the solution state using toluene as the solvent (~50 wt%) [26, 32]. In order to minimize gel content in the grafts to be less than 50 wt%, the grafting temperature should be lower than 80 °C. The obtained graft copolymer with low gel content of about 6 wt% which was synthesized at reaction temperature of 60 °C, dissolved well in toluene and thus the

quantity of grafted MA could be determined by a titration method. The percentage of MA grafted onto DPNR molecules was about 2.59 wt%, which indicated that about 29% yield of MA was fixed onto the DPNR backbone when 9% by weight of MA was used.

4.4.3.4 Reaction Time

The effect of reaction time was studied over the range of 4 – 10 h at 80 °C with a fixed 7 wt% BPO, 9 wt% MA, and the results are shown in Figure 4.11.

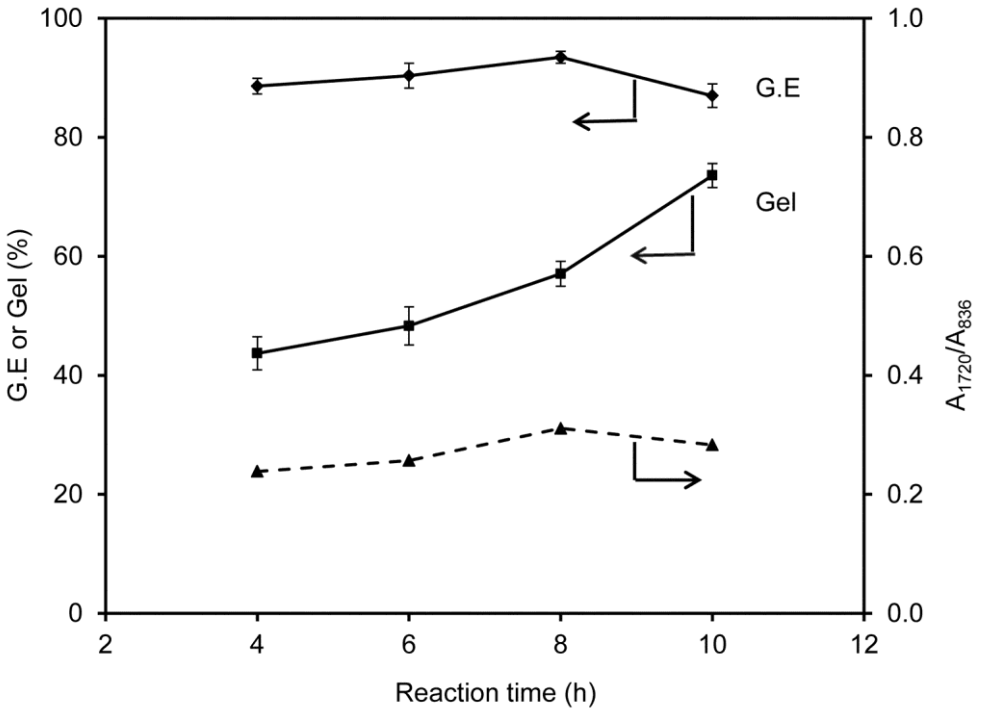

Figure 4.11 Effect of reaction time on grafting efficiency (G.E), gel content, and absorbance ratio (A_{1720}/A_{836}) of graft copolymers. (Grafting conditions: 7 wt% BPO, 9 wt% MA, and reaction temperature of 80 °C; feeding rate of MA of 0.2 ml/min)

The G.E increases with increasing reaction time and it went through a maximum at a reaction time of 8 h and thereafter decreased. The estimated grafted MA using the absorbance ratio also shows the same trend. The reason is that for a long reaction time, there is a greater possibility of more collisions between the excited MA and the rubber macroradicals to complete the graft copolymerization. It should be noted that a reaction time of 8 h is sufficient for the surface grafting reaction and so a further increase in the grafting time does not give any improvement in grafting but increases the cross-linking reaction. Therefore, the optimal grafting time should be about 8 h.

4.4.4 Effect of the Proteins in the Latex on Graft Copolymerization

The grafting of MA onto NR (NR-*g*-MA) was carried out to investigate the effect of the proteins in the NR latex. The grafting conditions of 7 wt% BPO and 9 wt% MA at 80 °C for 8 h were used. The obtained results are compared with grafting of MA onto DPNR (DPNR-*g*-MA). The effects of NR and DPNR substrates on the graft copolymerization are shown in Table 4.3.

Table 4.3 Effects of NR and DPNR latex and synthesis methods on graft copolymerization.

Graft copolymer	Synthesis method	A_{1720}/A_{836}	G.E (%)	Gel (wt%)
NR-*g*-MA[a]	DMP	0.104	50.3 ± 1.3	35.7 ± 1.6
DPNR-*g*-MA[a]	DMP	0.430	71.0 ± 0.2	5.9 ± 0.3
DPNR-*g*-MA[b]	Conventional	0.220	55.4 ± 2.1	19.5 ± 1.7

[a] Using the differential microemulsion polymerization (DMP) technique at grafting conditions of 7 wt% BPO and 9 wt% MA at 60 °C for 8 h; feeding rate of MA of 0.2 ml/min.

[b] Using the conventional microemulsion polymerization technique at grafting conditions of 7 wt% BPO and 9 wt% MA at 60 °C for 8 h; MA was introduced into the system in one portion of the total amount.

It is clearly seen that the higher absorbance ratio (A_{1720}/A_{836}) (i.e., grafted MA content) with a lower gel fraction was observed for grafting on the DPNR latex. Based on the A_{1720}/A_{836} of NR-*g*-MA and DPNR-*g*-MA, the grafted MA content was improved by a factor of four. The different characteristics of the grafting behavior were caused by the removal of the proteins in the natural rubber latex. The grafting reaction can be suppressed by side reactions with the presence of proteins in the NR latex. In addition, protein can act as a free-radical scavenger and terminate the free-radical species. Therefore, they provide a less efficient graft copolymerization on NR latex and result in a lower level of grafted MA. These observations are similar to those observed for the graft copolymerization of styrene (ST) [14, 18] and methyl methacrylate (MMA) [20] onto DPNR. It has previously been reported that the grafting efficiency for DPNR was found to be higher than that of NR latex, and thus it was concluded that the difference between the grafting reactions was attributed to the presence of proteins in the NR latex. It should be noted that another main drawback of the NR substrate for grafting is a high gel content in the grafts. This is attributed to the association of the inherent components from the natural rubber latex such as phospholipids and proteins which are able to form gel during the grafting reaction [42, 45]. Thus the importance of removal of proteins from natural rubber latex before grafting is clearly evident, and hence the pretreatment of deproteinization of NR is essential for efficient grafting copolymerization with maleic anhydride.

4.4.5 Effectiveness of the DMP Method for Graft Copolymerization

To investigate the effectiveness of the differential microemulsion polymerization (DMP) technique for grafting of MA onto DPNR latex, a conventional microemulsion polymerization method was also applied. The grafting efficiency, gel content, and absorbance ratio obtained from these two techniques are also presented in Table 4.3. The DMP technique clearly gives much better results for the grafting efficiency and the grafted MA content (i.e., A_{1720}/A_{836}). The level of grafted MA was increased by a factor of two. On the other hand, the graft copolymer synthesized using the conventional microemulsion polymerization method not only produces a lower

content of grafted MA but also results in a higher gel fraction in the grafts. The different characteristics of these grafting reactions were caused by the difference in the MA monomer feeding procedure into the reaction system. The feeding of MA monomer for the DMP technique is provided as a slow addition with continuous dropping into the reaction system whereas in the conventional microemulsion polymerization method, the MA monomer is introduced in one portion of the total amount.

In particular, graft copolymers could be obtained by either "grafting to" or "grafting from" methods. The proposed mechanism of MA grafted DPNR suggests a free radical reaction as depicted earlier in Figure 4.6, in which the macroradicals act as active sites for grafting along the rubber chains. Then the MA monomer can interact with these radicals to produce the graft copolymer, which is related to the "grafting from" method. The schematic illustration of the MA grafting onto DPNR via the "Grafting from" method using the DPM technique is shown in Figure 4.12.

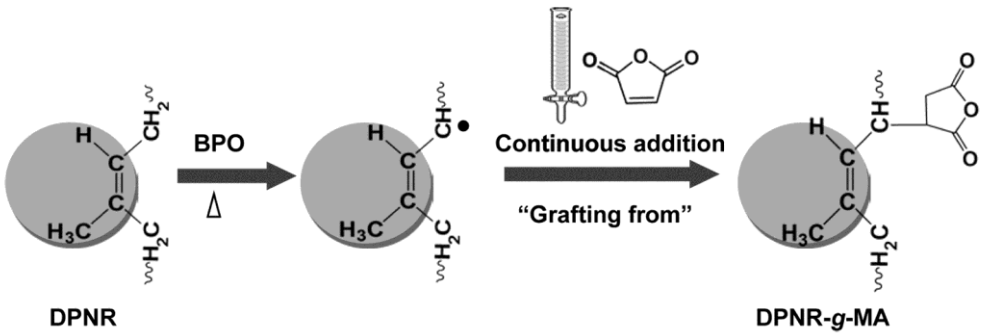

Figure 4.12 Schematic illustration of the grafting of MA onto DPNR via "Grafting from" method using DMP technique.

Obviously, a differential addition of MA could offer advantages over the conventional microemulsion polymerization method in terms of a better control of

monomer droplets into the reaction system. In bulk grafting via the conventional microemulsion polymerization method, a high concentration of carboxylic acid due to the ring opening of MA resulting in a rapid drop in the pH of the system which causes the DPNR latex to coagulate. In this system, the competition of side reactions is unavoidable and therefore provides a low level of grafted MA (i.e., A_{1720}/A_{836}) with a high gel content as shown in Table 4.3. On the other hand, for each time interval of monomer dropping in the differential method, only one MA molecule is expected to graft onto one isoprene unit before the next drop of fresh monomer is introduced resulting in a more efficient graft copolymerization via the "grafting from" method.

Generally, the gel content of the graft copolymer synthesized by bulk grafting is expected to be higher than that of grafting using the differential method. In the present work, the gel fraction obtained by bulk grafting on the DPNR exhibited a lower gel content compared to grafting on the NR latex using the differential method. This result confirmed the necessity of the pretreatment of deproteinization of NR before grafting. The results obtained in this work demonstrate that the DMP technique is not only useful for synthesizing nanosized polymers [49-54] but also it is an effective method to synthesize graft copolymers of natural rubber. In addition, this technique is more favorable because it could directly graft MA in the latex phase without using any organic solvents.

4.4.6 Particle Size and Morphology

The DLS plots of the DPNR and DPNR-*g*-MA latex are shown in Figure 4.13. It can be seen that the DLS plots show a bimodal distribution which indicated that the latex was composed of both small and large rubber particles. For DPNR latex, the first population was found at 210 nm and the second one was detected at 700 nm. The particle sizes of the DPNR-*g*-MA graft copolymer also showed two different populations with diameters of 270 nm and 880 nm. On comparison with the DPNR particles, a larger diameter of the graft copolymer was observed. The larger diameter size was caused by MA molecules being grafted at the surface of the rubber particles.

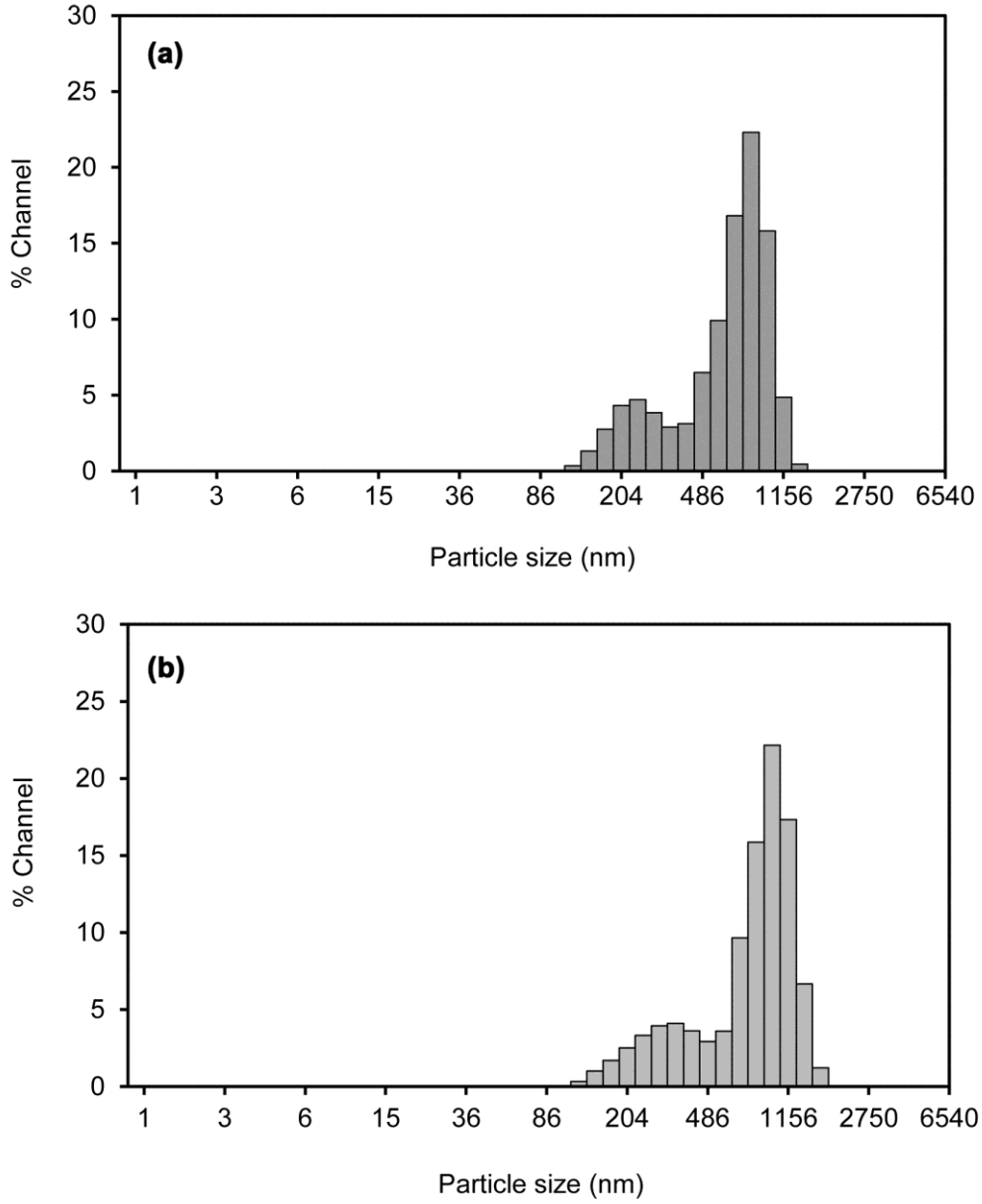

Figure 4.13 DLS plots of (a) DPNR and (b) DPNR-*g*-MA. (Grafting conditions: 7 wt% BPO and 9 wt% MA at 80 °C for 8 h; feeding rate of MA of 0.2 ml/min)

Morphology of the DPNR and DPNR-*g*-MA was investigated by transmission electron microscopy (TEM) and the results are shown in Figure 4.14. It was observed that the morphology of the DPNR rubber particles was spherical in shape with a smooth surface. On the other hand, the morphology of the DPNR-*g*-MA graft copolymer contained a darker core area of rubber encompassed by a lighter shell area of the grafted maleic anhydride. Therefore, it could be concluded that the graft copolymer of MA grafting onto DPNR is a core-shell type.

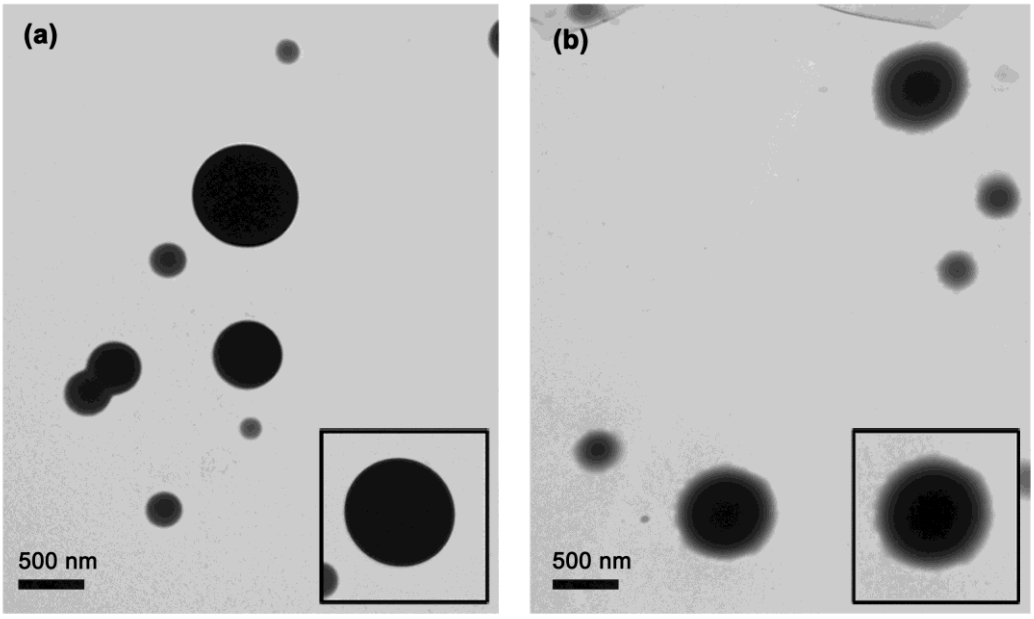

Figure 4.14 Transmission electron micrographs of (a) DPNR and (b) DPNR-*g*-MA; the inset figure is a magnified particle. (Grafting conditions: 7 wt% BPO and 9 wt% MA at 80 °C for 8 h; feeding rate of MA of 0.2 ml/min)

Surface morphologies of the DPNR and DPNR-*g*-MA were also investigated by atomic force microscopy (AFM) and the results are shown in Figure 4.15. The mean roughness (R_a) over a 20 x 20 μm surface region for the unmodified NR was about 10 nm. After the surface graft copolymerization with MA, the surface morphology changed substantially. The surface becomes rougher with a R_a value

increasing up to 18 nm which is due to the MA molecules being grafted at the surface of the rubber particles. It can be seen that the DLS, TEM, and AFM analyses strongly support that MA was grafted onto the DPNR backbone.

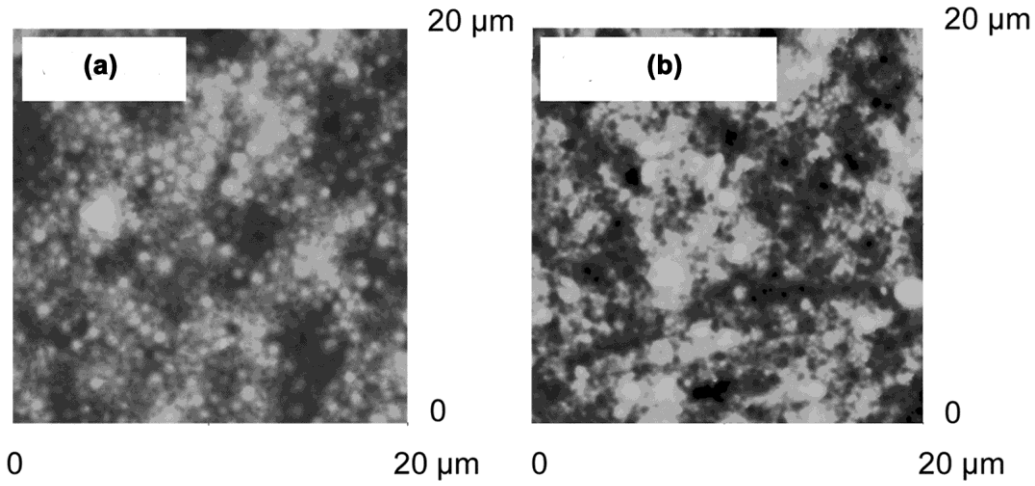

Figure 4.15 Two-dimensional AFM images of (a) DPNR and (b) DPNR-*g*-MA. (Grafting conditions: 7 wt% BPO and 9 wt% MA at 80 °C for 8 h; feeding rate of MA of 0.2 ml/min)

4.4.7 Thermal Analysis

Thermal properties of the DPNR and DPNR-*g*-MA were investigated by DSC and TGA. DSC curves of the DPNR and DPNR-*g*-MA are displayed in Figure 4.16. The glass transition temperature (T_g) of the DPNR was -63.5 °C while the glass transition temperature of the DPNR-*g*-MA graft copolymer was -61.5 °C. There was a slight shift in glass transition temperature of the natural rubber and the graft copolymer which is caused by stiffening or an increased interchain interaction between polar functional groups of the graft copolymer. Figure 4.17 shows TGA curves of the DPNR and DPNR-*g*-MA; (a) weight lost versus temperature; and (b) derivative weight loss versus temperature.

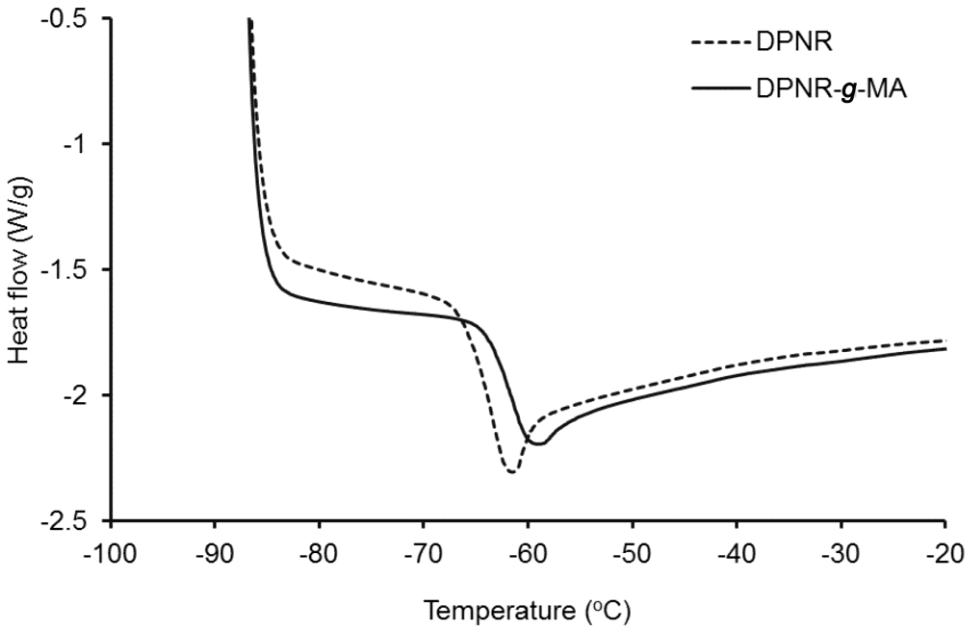

Figure 4.16 DSC curves of DPNR and DPNR-*g*-MA. (Grafting conditions: 7 wt% BPO and 9 wt% MA at 80 °C for 8 h; feeding rate of MA of 0.2 ml/min)

It can be seen that a single decomposition temperature (T_d) of DPNR was observed at 392.3 °C. On the other hand, the DPNR-*g*-MA graft copolymer showed a first decomposition temperature at 392.3 °C and a second decomposition step was found at 440.1 °C. The higher decomposition temperature relates to the degradation temperature caused by the graft copolymer. This indicates that the MA grafting improved the thermal stability of the DPNR. This observation is in agreement with the thermal degradation of maleic anhydride grafting onto polyethylene (PE-*g*-MA) [94]. It can be seen that no char residue at 500 °C of DPNR was found whilst it was about 3 wt% for the DPNR-*g*-MA graft copolymer. This result demonstrates the ability of MA grafting to improve the thermal stability of DPNR.

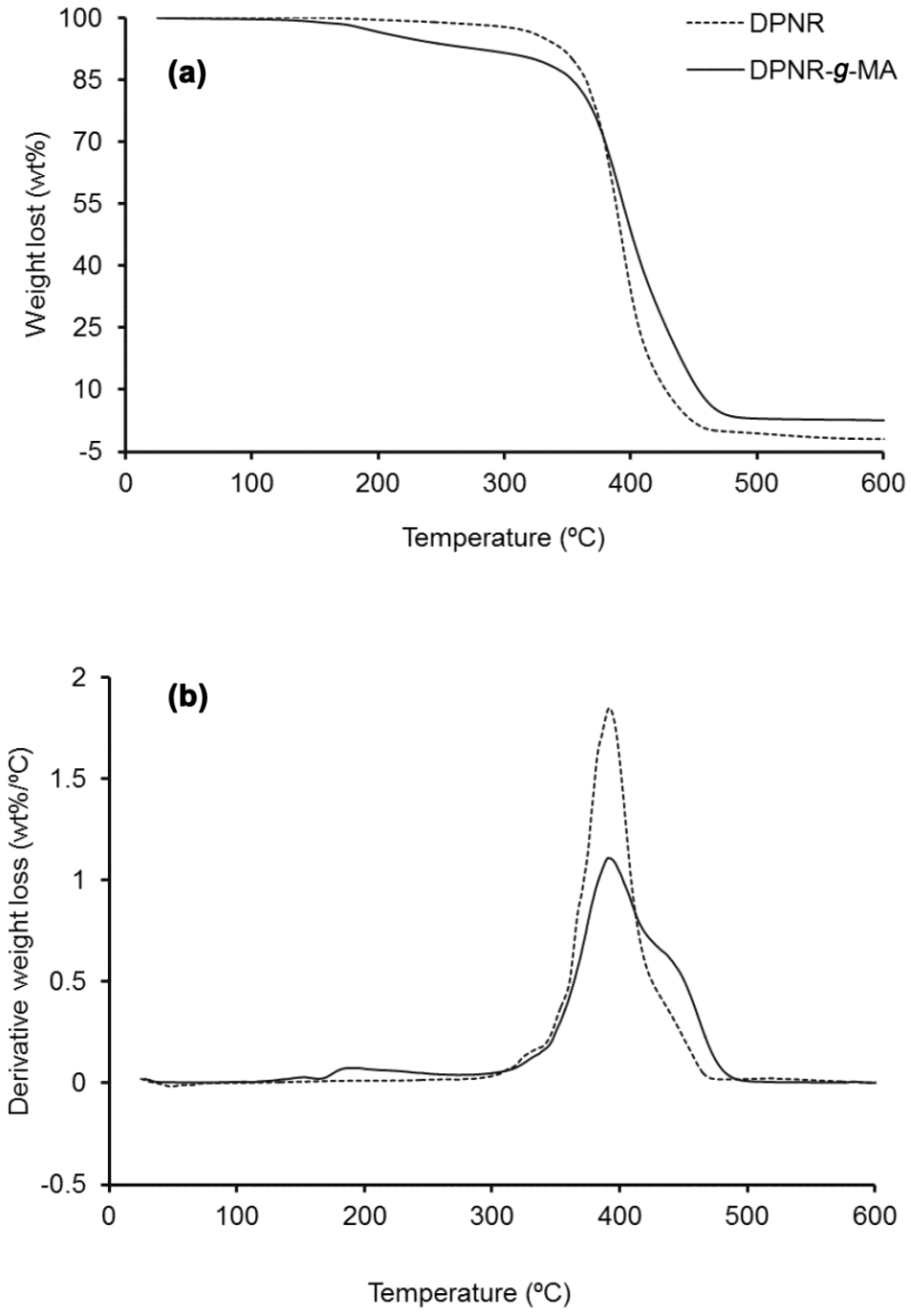

Figure 4.17 TGA curves of DPNR and DPNR-*g*-MA: (a) weight lost versus temperature; and (b) derivative weight loss versus temperature. (Grafting conditions: 7 wt% BPO and 9 wt% MA at 80 °C for 8 h; feeding rate of MA of 0.2 ml/min)

4.5 Conclusions

The grafting of MA onto DPNR was successfully carried out in the latex phase via the DMP technique. A high G.E of more than 90% was found at appropriate grafting conditions of 7 wt% BPO, 9 wt% MA, and feeding rate of MA of 0.2 ml/min at 80 °C for 8 h. The G.E and gel content were influenced by initiator and monomer concentration, reaction temperature, and reaction time. A high G.E was found at a high initiator concentration and/or a high grafting temperature. A low gel fraction in the grafts of 6 wt% was found at a low grafting temperature of 60 °C. A larger diameter size and a higher mean roughness of the graft copolymer than that of neat rubber was caused by MA molecules being grafted at the surface of the rubber particles as a core-shell type. The increase in thermal decomposition temperature of the graft copolymer indicated that the MA grafting increased the thermal stability of the DPNR. The removal of proteins showed the different characteristics of the grafting behavior of MA onto NR and DPNR substrates. Due to the lower gel content and higher G.E so obtained, DPNR is thus a preferred substrate for grafting with MA. On a comparison of two techniques of conventional and differential methods, it was found that the differential method gives much better results with respect to grafting efficiency and the grafted MA content. This demonstrates that the DMP technique is an effective method to synthesize graft copolymers of natural rubber.

CHAPTER V: STYRENE-ASSISTED GRAFTING OF MALEIC ANHYDRIDE ONTO DEPROTEINIZED NATURAL RUBBER

In the previous chapter, graft copolymers obtained by the DMP method provided higher grafting efficiency than those obtained from the conventional emulsion polymerization method (i.e., bulk grafting). Unfortunately, a small amount of gel (~6 wt%) was still observed under these conditions. The presence of gel may be caused by the addition rate of monomer into the reaction system. That is, when the dropping rate of monomer is very slow (0.2 ml/min), the gel formation by the recombination reaction of the rubber macroradicals may occur due to monomer starvation in the reaction system for grafting during intermittent monomer addition. Therefore, determining the proper addition rate of the monomer is important. However, the effects of the monomer addition rate using DMP method on grafting efficiency and gel content in the grafts have not been investigated yet.

This chapter investigates the styrene-assisted grafting of MA onto DPNR. The effect of the MA addition rate on grafting efficiency was investigated and the optimum addition rate so obtained was therefore used as a constant parameter for the investigation of other grafting parameters, namely, monomer and initiator amount, reaction temperature, and reaction time. The effects of copolymerizing styrene with various ST/MA ratios on grafting efficiency and gel content were investigated. The chemical structures of the graft copolymers were characterized by FTIR, NMR, and XPS techniques. The diameters of the graft copolymer latex particles by DLS, morphology by TEM and thermal analysis by DSC and TGA were investigated and the results obtained were later discussed in detail. A plausible grafting mechanism for the styrene-assisted grafting of MA onto DPNR is provided in this chapter. The performance of styrene comonomer for promoting the grafting of MA onto DPNR is discussed.

5.1 Materials

High ammonia stabilized NR latex containing about 60% dried rubber content (DRC) was provided by Thai Rubber Latex Co., Ltd., Rayong, Thailand. Sodium dodecyl sulfate ($CH_3(CH_2)_{11}OSO_3Na$; SDS; 99%) as an emulsifier, benzoyl peroxide (($C_6H_5CO)_2O_2$; BPO; 75%) as an initiator, and styrene ($C_6H_5CH=CH_2$; ST; 99%) as a comonomer were purchased from Sigma-Aldrich (USA). Maleic anhydride ($C_2H_2(CO)_2O$; MA; 99%) as a monomer was purchased from Fluka (Switzerland). Chloroform ($CHCl_3$; 99.5%), formic acid (HCOOH; 98%), sodium carbonate anhydrous (Na_2CO_3; 99.5%), and sodium bicarbonate ($NaHCO_3$; 99.7%) were manufactured by EMD Chemicals Inc. (USA). Potassium hydroxide (KOH; 85%) was manufactured by ACP company (Canada). Isopropanol (($CH_3)_2CHOH$; 99.7%) and reagent grade of acetone ($(CH_3)_2CO$) and toluene ($C_6H_5CH_3$) were purchased from Caledon Laboratories Ltd. (Canada). 2-butanone ($CH_3C(O)CH_2CH_3$; AR grade) was purchased from Qrec Chemicals Ltd. (New Zealand). Hydroquinone ($C_6H_4(OH)_2$; 99%) was purchased from Sigma-Aldrich (Japan). Deionized water (DI) was used throughout the work.

Styrene monomer was purified, to remove inhibitor added for storage purposes, by washing several times with an aqueous solution of 10% sodium hydroxide (NaOH) and followed by reduced pressure distillation. The purified styrene was stored in the refrigerator. The other chemicals mentioned above were used as received unless specifically stated.

5.2 Preparation of Grafting of MA onto DPNR in Presence of Styrene

The recipes and variable factors for the grafting of MA onto DPNR in the presence of the styrene comonomer are presented in Table 5.1. The ST/MA mole ratio was calculated accordingly from the weight of ST and MA. It should be noted that the weight ratio of ST/MA is close to the mole ratio due to their very similar molecular weight. The experimental procedure was conducted as follows. When the appropriate condition for MA grafting onto DPNR latex was found, this condition was later applied for the grafting with inclusion of ST to obtain the DPNR-*g*-(MA-*co*-ST). The

DPNR was first swollen with a specific amount of ST for 30 min at the reaction temperature. The subsequent procedure was the same as that for the DPNR-*g*-MA preparation. A schematic illustration of the experimental procedure for MA grafting in the presence of styrene is shown in Figure 5.1.

Table 5.1 Typical recipe used for the grafting of MA onto DPNR in the presence of styrene comonomer.

Ingredients	Quantities
DPNR	15[a] g
Deionized water	25 g
KOH	0.1 g
Isopropanol	1.5 g
SDS	0.2 g
Na_2CO_3/$NaHCO_3$ (pH ~10)	10 ml
BPO	1, 3, 5, 7, 9 wt%[b]
MA	3, 5, 9, 13 wt%[b]
ST/MA[c]	1:1, 2:1, 3:1, 4:1 (mole ratio)

[a] Weight of the dried rubber content in DPNR latex.

[b] Percent by weight of the dried rubber content.

[c] Fixed amount of MA.

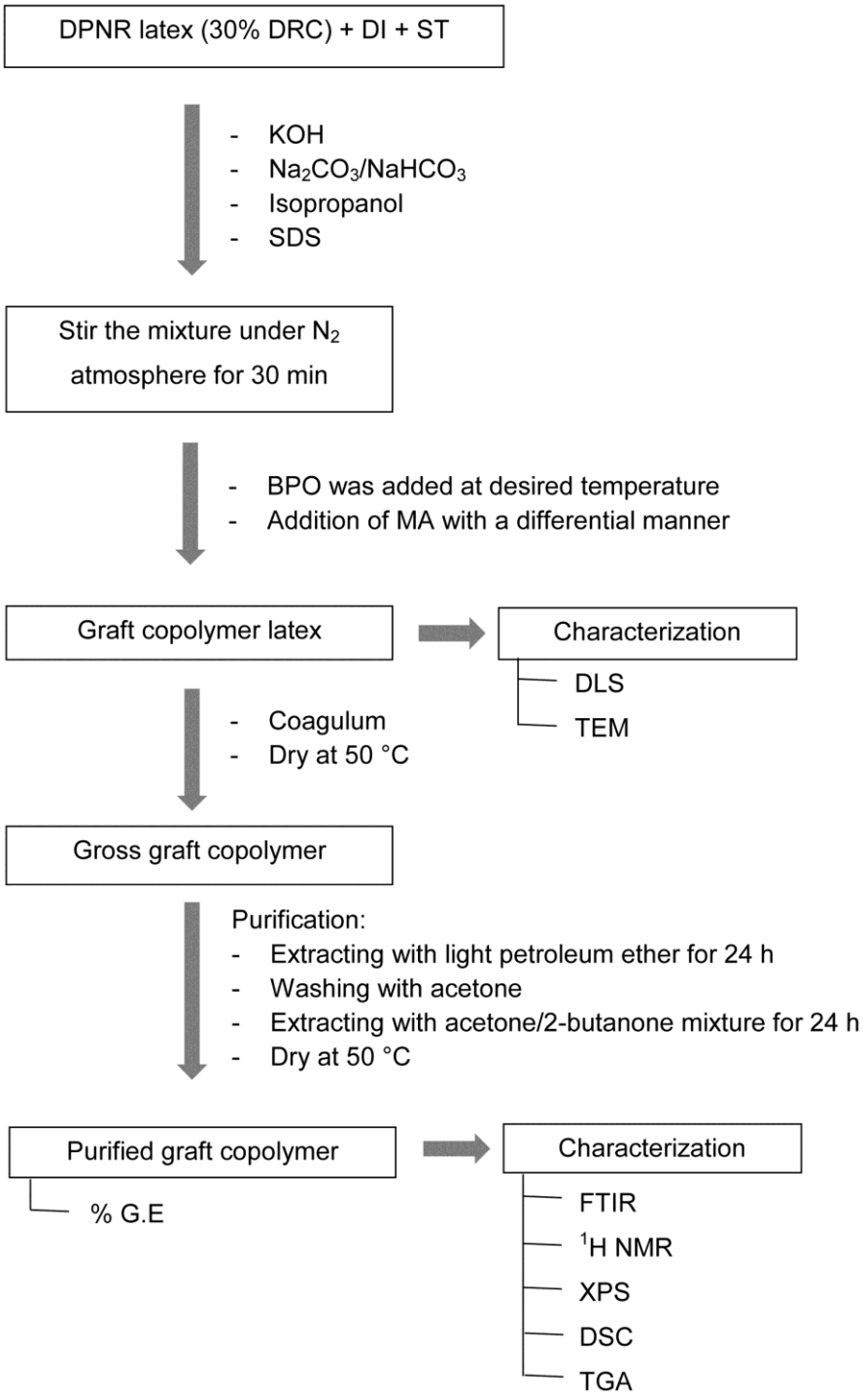

Figure 5.1 The experimental procedure of MA grafting onto DPNR in the presence of styrene comonomer and characterization of graft copolymer.

5.3 Determination of Grafting Efficiency

The solid product of DPNR-*g*-(MA-*co*-ST) was isolated from hot formic acid (40% v/v) and then dried to a constant weight in a vacuum oven at 50 °C. There are many components in the gross polymer products of ungrafted NR and MA, polystyrene, poly(ST-*co*-MA), DPNR-*g*-MA, DPNR-*g*-ST, and DPNR-*g*-(MA-*co*-ST). Soxhlet extraction procedures were used to purify the graft copolymer. The ungrafted NR (free NR) was removed by extracting with light petroleum ether at its boiling point around 35 – 60 °C for 24 h; and the ungrafted MA, polystyrene, and poly(ST-*co*-MA) were later extracted using a mixture of acetone and 2-butanone (50/50 v/v) at its boiling point around 50 – 60 °C for 24 h [13, 33]. After Soxhlet extraction, the purified graft copolymers containing DPNR-*g*-MA, DPNR-*g*-ST, and DPNR-*g*-(MA-*co*-ST) were obtained. This purified graft copolymer is named DPNR-*g*-(MA-*co*-ST) in the following content. Weights of the initial sample and the extracted sample were measured for determination of the grafting efficiency (G.E) as follows:

$$\text{G.E (wt\%)} = \left(\frac{\text{Weight of graft copolymer}}{\text{Weight of dried coagulum product}} \right) \text{x } 100 \qquad (5.1)$$

5.4 Characterization

The chemical structures of the graft copolymers containing DPNR-*g*-MA, DPNR-*g*-ST, and DPNR-*g*-(MA-*co*-ST) were characterized by FTIR, ^{1}H NMR, and XPS methods. The grafting content of graft copolymers by XPS was calculated as follows:

Grafting content (%) = % composition of CO + % composition of COO (5.2)

The diameters of the graft copolymer latex particles were measured by DLS. The morphology was investigated by TEM. Thermal properties of T_g and T_d of graft copolymers were investigated by DSC and TGA. The experimental procedure for each method was the same as explained earlier.

5.5 Results and Discussion

5.5.1 Confirmation of the Graft Copolymers

FTIR spectra of the DPNR, DPNR-*g*-MA, and DPNR-*g*-(MA-*co*-ST) are compared in Figure 5.2. The assignments of the characteristic signals for DPNR-*g*-(MA-*co*-ST) are presented in Table 5.2. The important characteristic signals for grafted MA were observed at 1780 and 1720 cm^{-1} which are attributed to the C=O stretching of the grafted succinic anhydride and succinic acid, respectively [32, 40, 86]. The strong signal at 1720 cm^{-1} indicated that most of the grafted MA is in the form of an open ring. In the case of MA grafting with ST, three forms of graft copolymers can be produced such as DPNR-*g*-MA, DPNR-*g*-ST and DPNR-*g*-(MA-*co*-ST). As seen in Figure 5.2 (c), the characteristic signals for the grafted styrene were observed at 759 and 702 cm^{-1} which are attributed to the C–H out of plane of polystyrene or monosubstituted benzene [14, 18, 19]. This confirms that both MA and ST monomers were grafted onto DPNR.

^{1}H NMR spectra of the DPNR-*g*-(MA-*co*-ST) are shown in Figures 5.3 and the assignments of the important signals are presented in Table 5.3 The characteristic signals of grafted MA found at 2.69 and 2.91 ppm are attributed to the two methylene protons of the grafted MA and a broad peak at 3.85 ppm is correlated to the methine proton of the succinic anhydride ring [88, 92]. A new signal at 7.40 ppm is correlated with the unsaturated methine proton of the grafted anhydride ring. The observed signal at 9.85 ppm is assigned to the proton of the carboxylic acid by ring opening of the anhydride ring. The characteristic signals of grafted ST were observed in the range of 6.2 – 7.3 ppm, which are assigned to the aryl protons of the aromatic group of the grafted styrene [14, 18, 19]. As described earlier, the graft reaction should occur at the allylic hydrogen atom of DPNR, therefore, the graft copolymer structures of DPNR-*g*-(MA-*co*-ST) (1) and DPNR-*g*-(MA-*co*-ST) (2) were obtained.

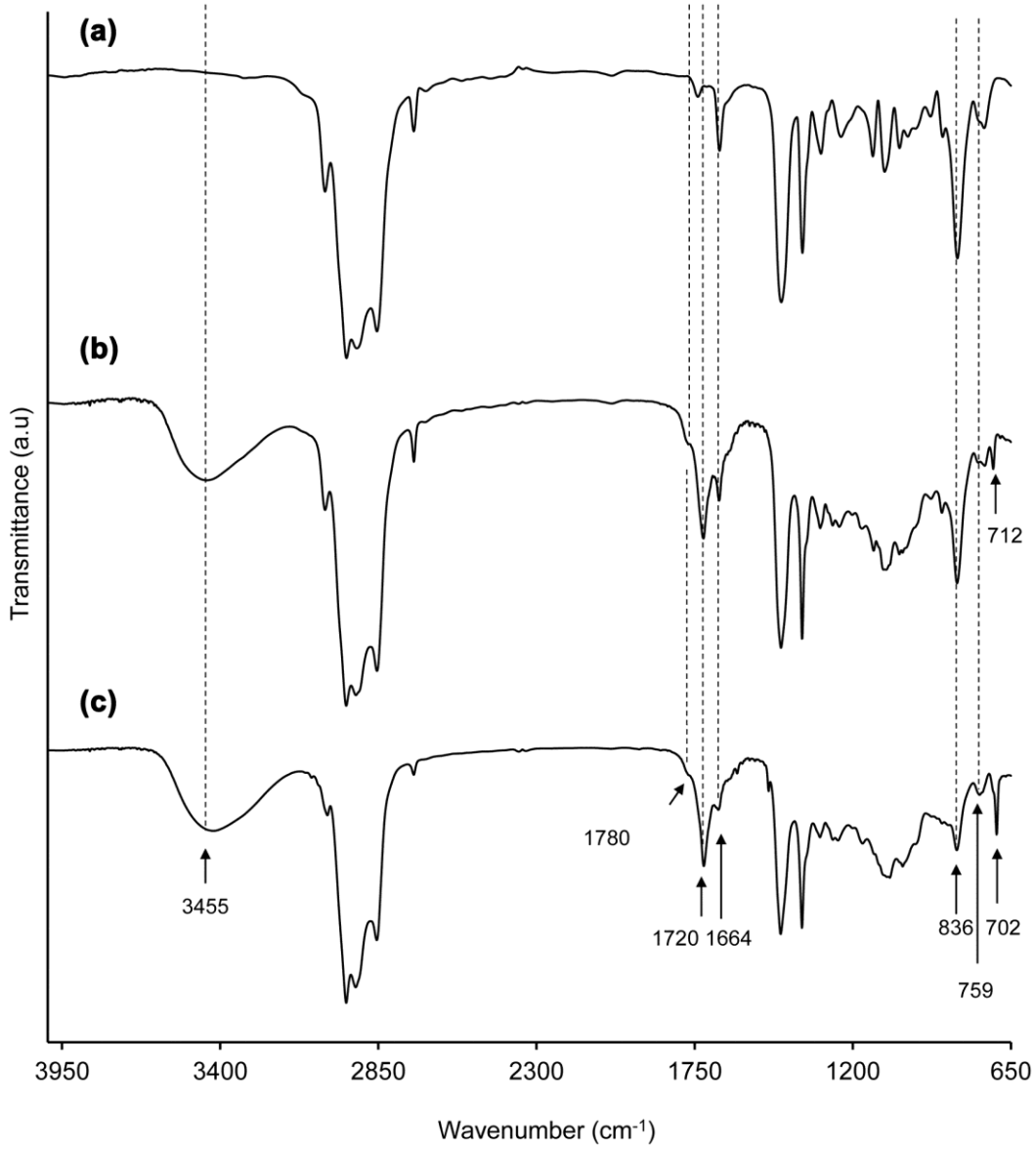

Figure 5.2 FTIR spectra of (a) DPNR, (b) DPNR-*g*-MA, and (c) DPNR-*g*-(MA-*co*-ST. (Grafting conditions: DPNR-*g*-MA: 7 wt% BPO, 9 wt% MA, and feeding rate of MA of 0.6 ml/min at 60 °C for 4 h; DPNR-*g*-(MA-*co*-ST): 7 wt% BPO, 9 wt% MA, ST/MA mole ratio of 4:1, and feeding rate of MA of 0.6 ml/min at 60 °C for 4 h)

Table 5.2 Assignments of the characteristic signals for the DPNR-*g*-(MA-*co*-ST) obtained from FTIR.

Samples	Wave number (cm^{-1})	Assignments	Ref.
DPNR	3035	olefinic C–H stretching	[85]
	2854, 2961, 2916	aliphatic C–H stretching	
	1664	C=C stretching	
	1448, 1375	C–H bending	
	836	=C–H deformation	
DPNR-*g*-(MA-*co*-ST)	1780	C=O stretching of succinic anhydride ring	[18, 19] [14, 40]
	1720	C=O stretching of succinic acid	[86]
	712	C=C of the anhydride ring	
	759, 702	C–H out of plane of polystyrene or monosubstituted benzene	

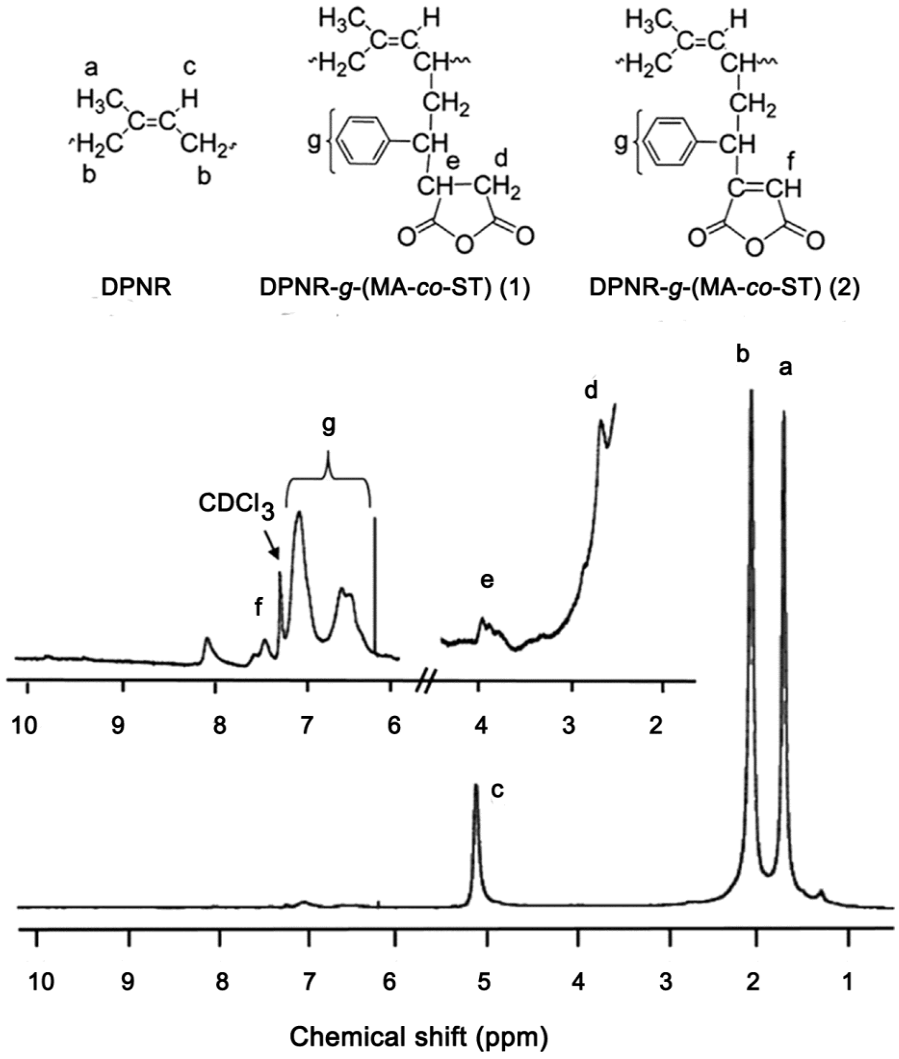

Figure 5.3 ^{1}H NMR spectra of DPNR-*g*-(MA-*co*-ST). (Grafting conditions: 7 wt% BPO, 9 wt% MA, ST/MA mole ratio of 4:1, and feeding rate of MA of 0.6 ml/min at 60 °C for 4 h)

Table 5.3 Assignments of the characteristic signals for DPNR-*g*-(MA-*co*-ST) obtained from ^{1}H NMR.

Samples	Chemical shift (ppm)	Assignments	Ref.
DPNR	1.67	Methyl proton	[87]
	2.03	Methylene proton	
	5.12	Unsaturated methine proton	
DPNR-*g*-(MA-*co*-ST)	2.69, 2.91	Methylene proton of grafted MA	[18, 19]
	3.85	Methine proton of grafted MA	[14, 88]
	6.2 – 7.3	Aryl protons of the aromatic rings	[92]
	7.40	Unsaturated methine proton of grafted MA	
	9.85	Proton of carboxylic acid	

The chemical composition at the surface of DPNR, DPNR-*g*-MA, and DPNR-*g*-(MA-*co*-ST) using an XPS method is compared in Figure 5.4. The C1s and O1s core-level signals were observed at binding energies of 284.1 and 531.5 eV, respectively. The C1s core-level spectrum is curve-fitted with three peak components. The major peak at 284.1 eV is attributed to the CH species of both the rubber and the grafted MA and the minor peaks at 285.4 and 288.2 eV are attributed respectively to the CO and COO species of the grafted MA [93]. The surface elemental composition is presented in Table 5.4. A comparison of an atomic concentration of the DPNR, DPNR-*g*-MA and DPNR-*g*-(MA-*co*-ST) show that a decrease in carbon (C) and an increase in oxygen (O) were obtained for the DPNR-*g*-MA and DPNR-*g*-(MA-*co*-ST) copolymers. Furthermore, an increase in the O/C atomic ratio of the DPNR-*g*-MA and DPNR-*g*-(MA-*co*-ST) indicates the fixation of MA onto the DPNR backbone. According to FTIR, ^{1}H NMR, and XPS analyses, strong evidence that the MA and ST were grafted onto DPNR is provided.

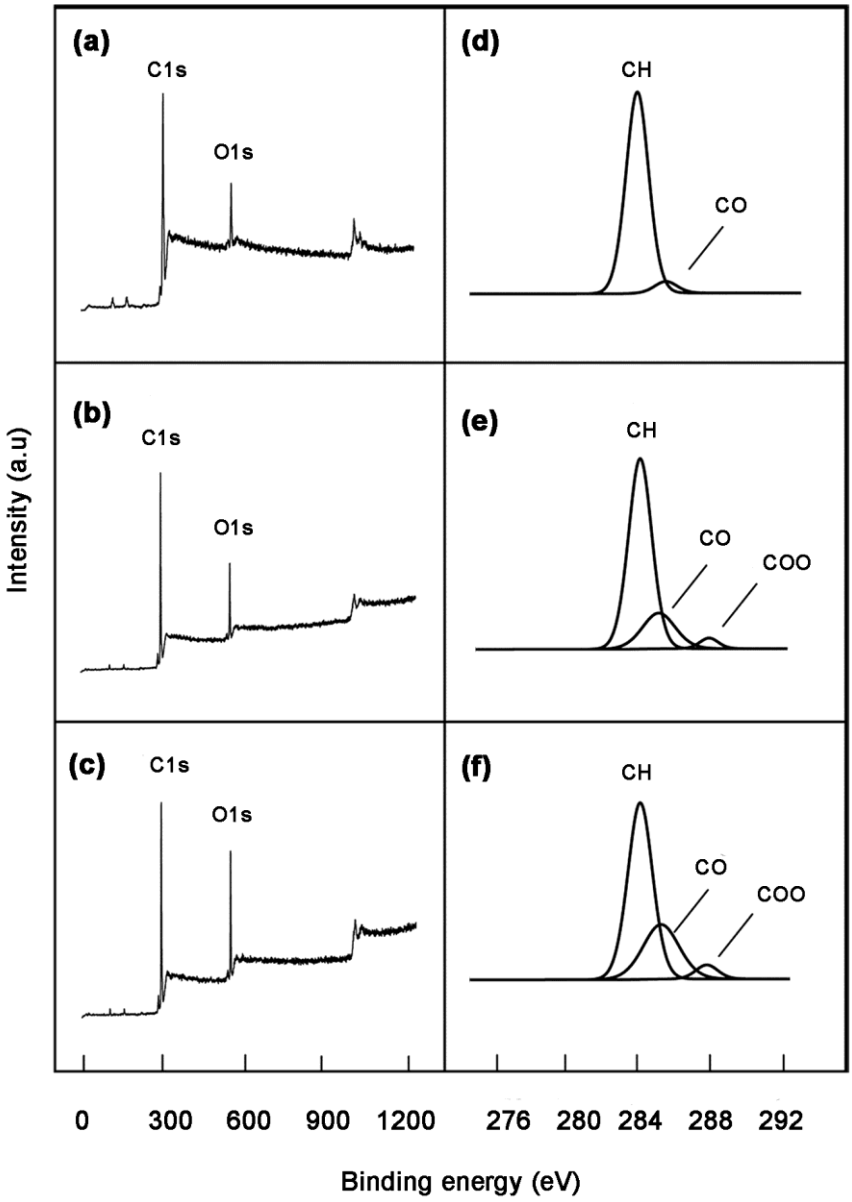

Figure 5.4 XPS spectra of DPNR, DPNR-*g*-MA, and DPNR-*g*-(MA-*co*-ST): (a) – (c) are wide scan spectrum of DPNR, DPNR-*g*-MA, and DPNR-*g*-(MA-*co*-ST), respectively; (d) – (f) are C1s core-level spectrum of DPNR, DPNR-*g*-MA, and DPNR-*g*-(MA-*co*-ST), respectively. (Grafting conditions: DPNR-*g*-MA: 7 wt% BPO, 9 wt% MA, and feeding rate of MA of 0.6 ml/min at 60 °C for 4 h; DPNR-*g*-(MA-*co*-ST): 7 wt% BPO, 9 wt% MA, ST/MA mole ratio of 4:1, and feeding rate of MA of 0.6 ml/min at 60 °C for 4 h)

Table 5.4 Surface elemental compositions of DPNR, DPNR-*g*-MA, and DPNR-*g*-(MA-*co*-ST).

Material	Composition (%)		O/C	Composition (%)[a]		
	C	O		CH	CO	COO
DPNR[b]	97.7	2.3	0.02	94.7	5.3	-
DPNR-*g*-MA[c]	87.5	12.5	0.14	76.5	20.2	3.3
DPNR-*g*-(MA-*co*-ST)[d]	84.6	15.4	0.18	65.8	29.6	4.6

[a] Carbon species by curve fitting of C1s core-level.

[b] Deproteinization conditions: 0.2 wt% urea and 1 wt% SDS at 30 °C for 60 min.

[c] Grafting conditions: 9 wt% MA and 7 wt% BPO at 60 °C for 4 h; feeding rate of MA of 0.6 ml/min.

[d] Grafting conditions: 9 wt% MA, 7 wt% BPO, and ST/MA mole ratio of 4:1 at 60 °C for 4 h; feeding rate of MA of 0.6 ml/min.

5.5.2 Parameters Affecting Grafting Efficiency and Gel Content

The parameters affecting the grafting efficiency (G.E), absorbance ratio (A_{1720}/A_{836}), and gel content for the graft copolymerization of MA onto DPNR latex, namely, monomer addition rate, initiator and monomer concentration, reaction temperature, and reaction time were investigated as follows.

5.5.2.1 Monomer Addition Rate

In the previous chapter, we reported that the addition of the MA monomer in a differential manner provided a higher G.E and lower gel content than those obtained from the conventional method. However, a gel content in the grafts of about 6 wt% was observed under the appropriate grafting conditions of 7 wt% BPO and 9 wt% MA at 60 °C for 8 h using a fixed feeding rate of MA at 0.2 ml/min. The presence of gel may correspond to the monomer addition rate when the dropping rate of MA monomer is very slow; the gel content from the recombination reaction of the rubber macroradicals may occur due to MA starvation in the reaction system for graft copolymerization. Therefore, the proper addition rate of monomer should be revisited.

In this section, the effect of the monomer addition rate over the range of 0.2 – 1.5 ml/min was reinvestigated with 7 wt% BPO and 9 wt% MA at 60 °C for 4 h and the results are shown in Figure 5.5. It is seen that the maximum G.E and A_{1720}/A_{836} were found at an addition rate of MA of 0.6 ml/min. It tended to decrease when the feeding rate of MA monomer was greater than 0.6 ml/min. In addition, a high gel content was obtained at a high addition rate of MA. That is, the graft copolymerization system changes from a differential microemulsion system to a conventional emulsion system when the rate of monomer addition greatly increases. Therefore an optimum monomer addition rate of 0.6 ml/min was used as a constant parameter for the investigation of other reaction parameters.

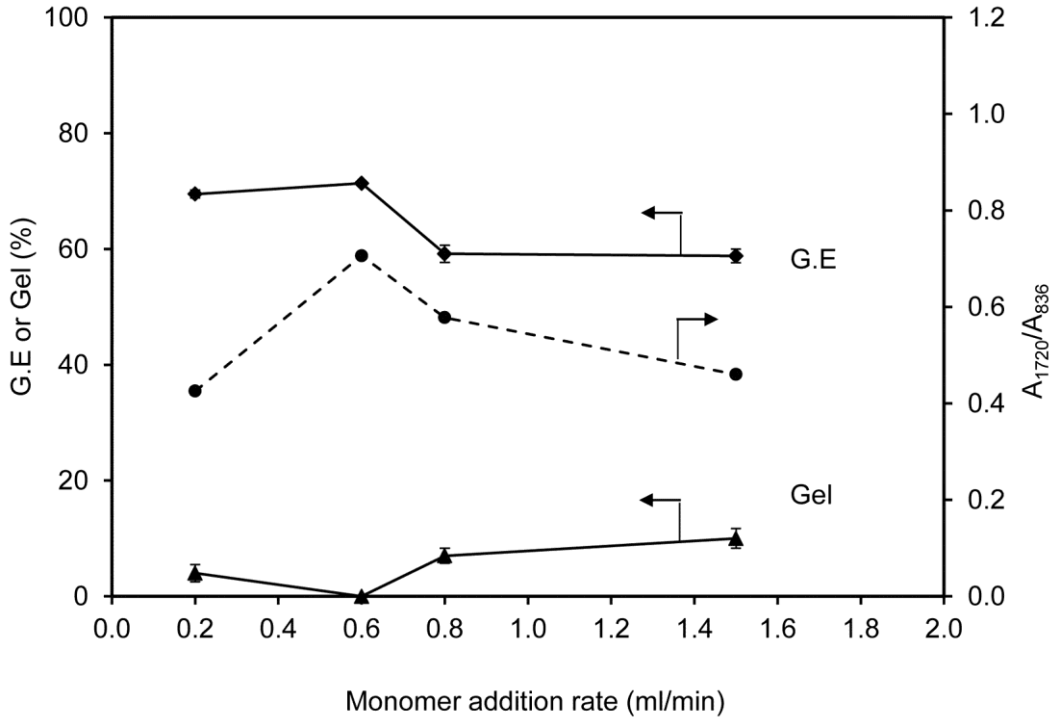

Figure 5.5 Effect of addition rate of MA on grafting efficiency (G.E), gel content, and absorbance ratio (A_{1720}/A_{836}) of graft copolymers. (Grafting conditions: 7 wt% BPO and 9 wt% MA at 60 °C for 4 h)

5.5.2.2 Monomer Amount

The effect of monomer amount over the range of 3 – 13 wt% MA was investigated with 7 wt% BPO at 60 °C for 4 h. An addition rate of MA of 0.6 ml/min was used and the results are shown in Figure 5.6. It was found that both the G.E and the A_{1720}/A_{836} increased with an increasing amount of MA and reached a maximum at 9 wt% and thereafter decreased. Due to the fact that MA and DPNR are mutually immiscible, the grafting reaction occurs largely on the surface of the rubber particles and therefore the G.E depends on the diffusion rate of MA into the DPNR phase. At a higher amount of MA, more MA molecules can diffuse onto the rubber phase for grafting and therefore provide a higher level of grafted MA.

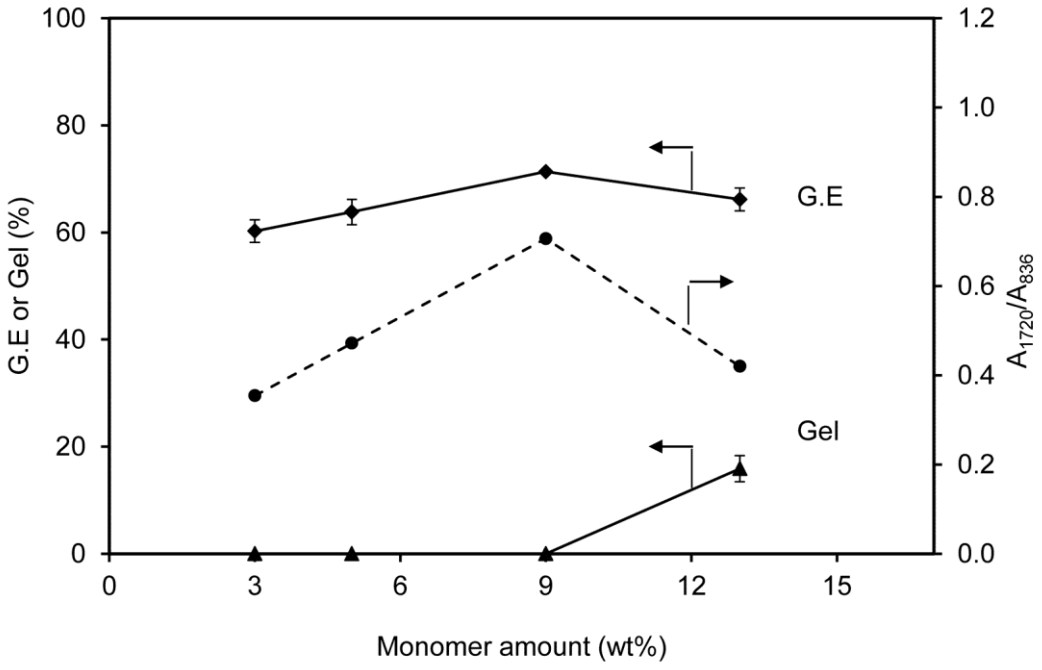

Figure 5.6 Effect of monomer amount on grafting efficiency (G.E), gel content, and absorbance ratio (A_{1720}/A_{836}) of graft copolymers. (Grafting conditions: 7 wt% BPO at 60 °C for 4 h; feeding rate of MA of 0.6/min)

However, a further increase in the MA ratio beyond 9 wt% would not help increase the grafting efficiency but would unfortunately rather promote gel formation caused by phase separation between MA and DPNR. Another reason is probably that an increase in MA amount decreases the amount of excited MA molecules as the excited MA is quenched by the MA in the ground state and hence less excited MA molecules are available for the grafting reaction resulting in a lower grafting efficiency. A similar result was observed for the grafting of MA onto ethylene-propylene diene terpolymer rubber (EPDM) [95] and high-density polyethylene (HDPE) [96] based polymers. In addition, side reactions such as chain transfer to monomer can be involved at the higher amount of MA monomer. As a result, 9 wt% MA seems optimal for an effective surface grafting on the natural rubber particles.

5.5.2.3 Initiator Amount

The effect of initiator amount over the range of 1 – 9 wt% BPO was investigated. The experiments were carried out using 9 wt% MA at 60 °C for 4 h and the MA addition rate of 0.6 ml/min was used. The results are shown in Figure 5.7. It can be seen that the G.E increased on increasing the amount of the initiator, which is consistent with the general understanding that a higher initiator amount generated more active sites on the DPNR backbone for graft copolymerization. It was found that the estimated grafted MA content (i.e., A_{1720}/A_{836} ratio) increases with increasing amounts of initiator over the range of 1 – 7 wt% BPO. However, a gel fraction was observed when using a high amount of initiator (i.e., higher than 7 wt% BPO). That is, an increase in initiator amount leads to an increasing number of free radicals to generate the active sites along the polymer chains, and therefore the possibility of the interaction of rubber macroradicals with each other to produce gel increases. Similar behavior has been observed for the MA grafting onto NR in a solution state [32, 40] and the grafting of MA onto EPDM [95] and HDPE [96] in a molten state at a high reaction temperature (i.e., 160 – 185 °C). However, on comparison to those literatures, it should be noted that gel formation was not observed in the present work within the range of 1 – 7 wt% BPO which may be due to the fact that the grafting reaction was conducted under milder conditions and hence there is less chance of an

intermolecular reaction of the generated radicals to form a crosslinked polymer of gel. Thus, to obtain a high G.E with no gel content in the grafts, 7 wt% BPO was used as a constant parameter for the investigation of the other reaction parameters.

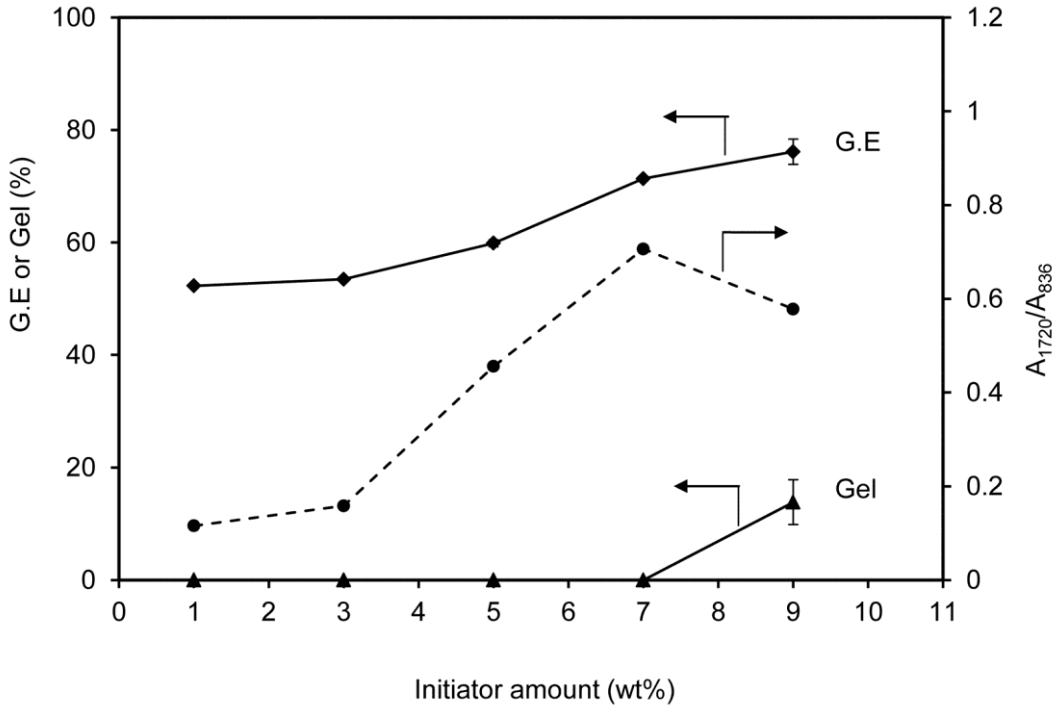

Figure 5.7 Effect of initiator amount on grafting efficiency (G.E), gel content, and absorbance ratio (A_{1720}/A_{836}) of graft copolymers. (Grafting conditions: 9 wt% MA at 60 °C for 4 h; feeding rate of MA of 0.6/min)

5.5.2.4 Reaction Temperature

The effect of reaction temperature was carried out over the range of 50 – 90 °C with 7 wt% BPO, 9 wt% MA, reaction time of 4 h, and MA addition rate of 0.6 ml/min. The results are shown in Figure 5.8. The G.E increased with increasing reaction temperature. Since the decomposition of the BPO is faster at higher temperature, an increase in the free radical concentration to initiate more active sites on the rubber chains occurred and thus the rate of graft copolymerization increased.

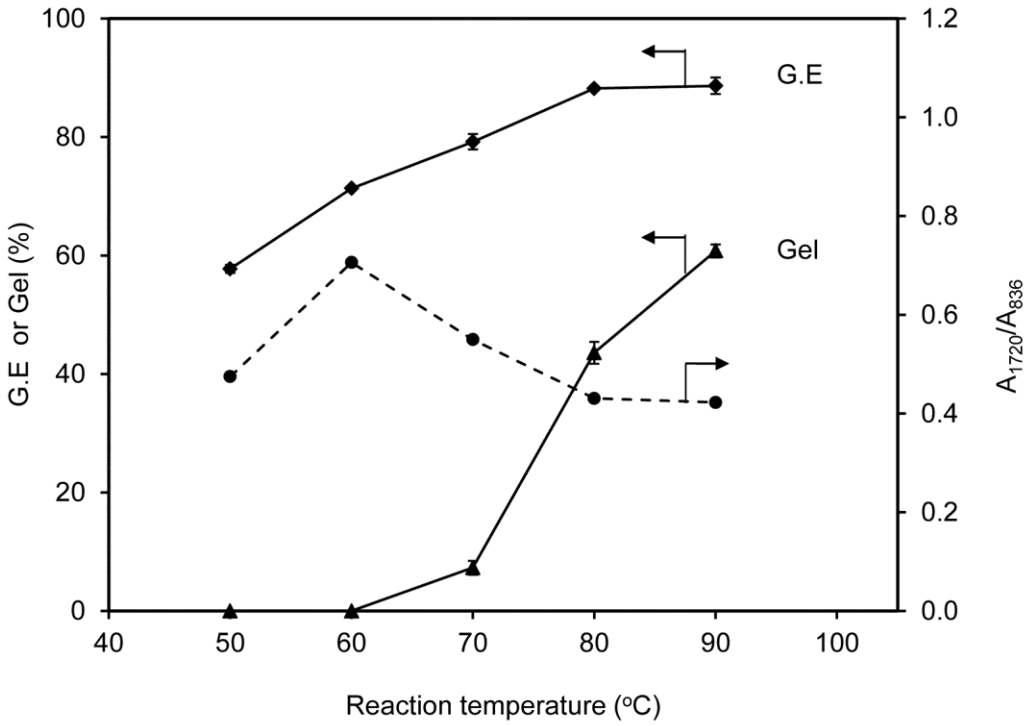

Figure 5.8 Effect of reaction temperature on grafting efficiency (G.E), gel content, and absorbance ratio (A_{1720}/A_{836}) of graft copolymers. (Grafting conditions: 7 wt% BPO, 9 wt% MA, and grafting time for 4 h; feeding rate of MA of 0.6 ml/min)

However, the G.E went through a maximum at 80 ºC and thereafter decreased. These results are associated with the surface reaction. That is, at a certain reaction time and reaction temperature, the surface reaction probably was completed so a further increase in the reaction temperature would not help the MA grafting but would rather promote a crosslinking reaction. It can be seen that the G.E leveled off after 80 °C. In this part, due to the high gel content (up to around 60 wt%) at high reaction temperature, G.E values does not indicate a real grafting efficiency because the crosslinked structure is obstructed the extraction of free polymers. It can be seen that the A_{1720}/A_{836} ratio decreased after 60 °C indicating less grafted MA. The gel content increased with increasing reaction temperature. The results showed that the graft copolymers synthesized at grafting temperatures over the range of 50 – 70 °C provide a low gel content of less than 10 wt%, which was lower than those of MA grafting

onto NR in the molten state at a high temperature of 135 °C [26] and in the solution state using toluene as the solvent [32], which was about 50 wt%. Therefore, to prepare a graft copolymer of MA on DPNR with no gel fraction in the grafts, the recommended optimal grafting temperature should not be higher than 60 °C.

5.5.2.5 Reaction Time

The effect of reaction time over the range of 1 – 8 h was investigated using 7 wt% BPO, 9 wt% MA, and a MA addition rate of 0.6 ml/min at 60 °C and the results are shown in Figure 5.9.

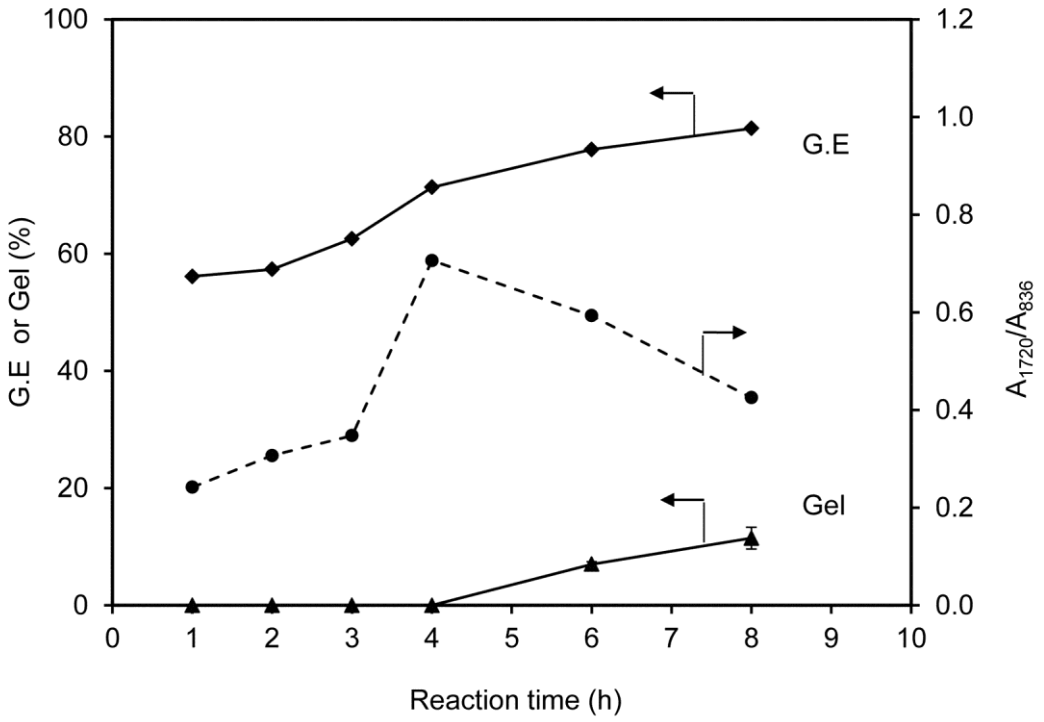

Figure 5.9 Effect of reaction time on grafting efficiency (G.E), gel content, and absorbance ratio (A_{1720}/A_{836}) of graft copolymers. (Grafting conditions: 7 wt% BPO, 9 wt% MA, and grafting temperature of 60 °C; feeding rate of MA of 0.6 ml/min)

It can be seen that the G.E increased with increasing reaction time. The reason is probably that at a long reaction time, a greater possibility of more collisions between excited MA molecules and rubber macroradicals takes place to increase the graft copolymerization. However, the A_{1720}/A_{836} went through a maximum at a reaction time of 4 h and thereafter decreased. It is possible that at longer reaction times, the competition of side reactions such as intermolecular reactions to form crosslinked polymer may occur. Due to a high grafted MA content (i.e., A_{1720}/A_{836}) with no gel content in the grafts was obtained at 4 h. Therefore a grafting time of 4 h should be appropriate for MA grafting onto the DPNR.

5.5.3 Performance of Styrene-Assisted Grafting of MA onto DPNR

The grafting reaction in the presence of styrene at various mole ratios of ST-to-MA (i.e., ST/MA = 1:1, 2:1, 3:1, and 4:1) was carried out under the conditions of 7 wt% BPO and 9 wt% MA at 60 °C for 4 h. The MA addition rate of 0.6 ml/min was used and the results are shown in Figure 5.10. It was found that the G.E is remarkably higher in the presence of styrene than in its absence, and the G.E increased with an increase in the ratio of ST/MA. An increase of grafting efficiency for the styrene-assisted grafting reaction could be elucidated as follows. Styrene can act as an electron donor to activate the carbon-carbon double bond of the MA molecule by creating a charge transfer complex (CTC) between them, which highly activates the weakly reactive double bond of MA towards the rubber macroradicals [30-32, 34, 35]. As a result, the MA was grafted onto the DPNR backbone simultaneously with styrene in the form of the CTC leading to an increase in grafting efficiency. Unfortunately, a small amount of gel content of about 1 – 12 wt% for styrene-assisted grafting was found and it increased with increasing ST/MA mole ratios over the range of 1 – 4. However, this observed gel fraction is relatively low compared to the graft copolymers synthesized in the solution state (~50 wt%) [26, 32].

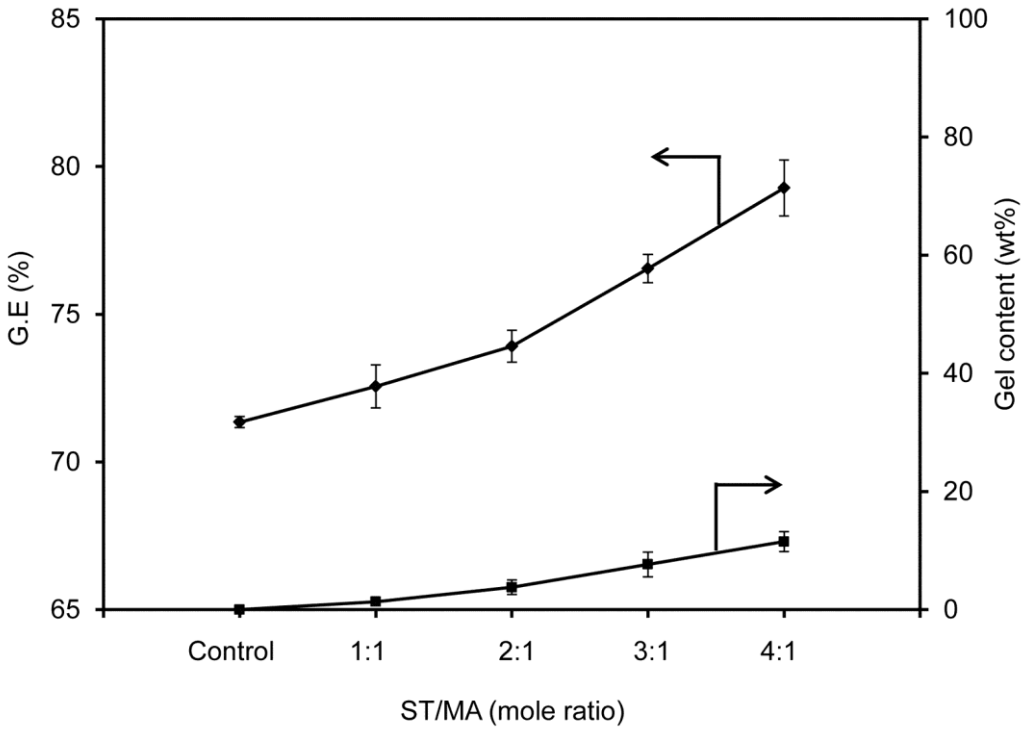

Figure 5.10 Effect of the ST/MA ratio on grafting efficiency (G.E) and gel content of graft copolymers. (Grafting conditions: MA grafting without ST (control reaction): 7 wt% BPO, 9 wt% MA, and feeding rate of MA of 0.6 ml/min at 60 °C; Styrene-assisted grafting reaction: 7 wt% BPO, 9 wt% MA, and ST/MA mole ratio of 1:1, 2:1, 3:1, 4:1 at 60 °C for 4 h; feeding rate of MA of 0.6 ml/min)

The gel formed during the styrene-assisted grafting of MA onto DPNR is probably due to the formation of crosslinked polymer via one of three routes: (i) a recombination reaction of styryl macroradicals; (ii) the interaction between succinyl macroradical and styryl macroradical; and/or (iii) the interaction between rubber macroradical and styryl macroradical [36]. The chemical structures of the crosslinked polymers obtained from each route are shown in Figure 5.11. It should be noted that the gel content constantly increased with an increase in the mole ratio of ST/MA over the range of 1 – 4 and a further increase in the ST/MA ratio beyond 4 would be expected to promote more gel formation.

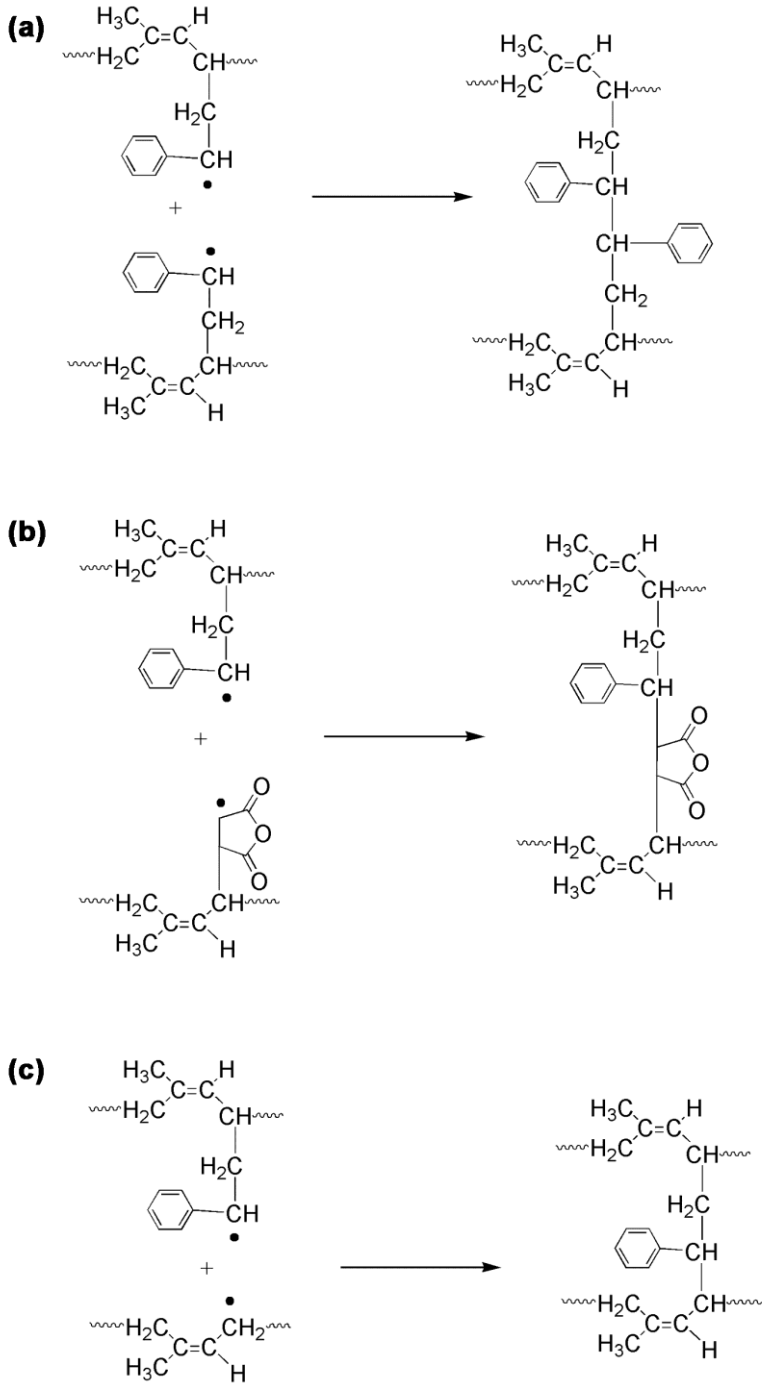

Figure 5.11 Schematic illustrations of the proposed crosslinking mechanisms for grafting of MA onto DPNR in the presence of ST comonomer.

At a high concentration of styrene, part of the ST reacts with MA to produce the CTC while others may preferentially react with rubber macroradicals to form the styryl macroradicals [31]. Due to the stability of the styryl macroradicals, their further reaction with MA or CTC would be difficult, and hence, the recombination reaction of styryl macroradicals to form gel may be more pronounced. Therefore, to obtain a high grafting efficiency with reduced gel content to less than 12 wt%, the recommended optimal ST/MA ratio should not be higher than 4.

A number of reports have shown that the maximum grafting degree of MA grafting onto PP [30, 31], iPB-1 [34], PE [35], and HDPE [96] was observed at a ST/MA ratio of 1:1. However, the present study showed that the optimum ST/MA ratio of 4:1. It should be noted that the former grafting systems were carried out by a melt-mixing process at high reaction temperature while the latter (this work) was carried out in latex form under a very mild grafting condition. Therefore, different mechanisms of MA grafting onto the DPNR backbone may be one reason. Moreover, a new grafting mechanism should involve at higher mole ratio of styrene to MA (See section 5.5.4). However, for the case of ST/MA ratio of 1:1, it was found that the reaction rate of graft copolymerization of MA grafting onto DPNR is much lower than that grafting at the high ST/MA ratio (i.e., 4:1) (See Chapter VI). For a reasonable reaction rate, a ST/MA ratio of 4:1 was therefore used to assist grafting activity of MA on DPNR.

For the grafting content obtained from XPS analysis, G.E, and A_{1720}/A_{836} ratio for the grafting reaction in the presence and absence of styrene as presented in Table 5.5, showed that the addition of styrene with a ratio of ST/MA of 4:1 provided higher grafting content, G.E, and A_{1720}/A_{836} ratio compared to grafting without styrene. The grafting content for styrene-assisted grafting reaction and the MA grafting onto DPNR without styrene were found to be 34.2% and 23.5%, respectively. The obtained results agreed well with the surface elemental compositions of the graft copolymers obtained by XPS (See Table 5.4). The compositions of both CO and COO that contributed to the grafted MA in the case of DPNR-*g*-(MA-*co*-ST) were higher than the compositions for DPNR-*g*-MA. The results obtained clearly show that the inclusion of styrene in the grafting process could help increase grafting efficiency of

MA onto DPNR and it is thus concluded that styrene can be an effective comonomer for promoting grafting activity of MA on DPNR.

Table 5.5 Grafting efficiency, gel content, absorbance ratio, and grafting content of DPNR-*g*-MA and DPNR-*g*-(MA-*co*-ST).

Graft copolymer	G.E (%)	Gel (wt%)	A_{1720}/A_{836} ratio	Grafting content (%)[a]
DPNR-*g*-MA[b]	71.4 ± 0.2	No gel	0.706	23.5
DPNR-*g*-(MA-*co*-ST)[c]	79.3 ± 1.0	11.5 ± 1.6	1.894	34.2

[a] Calculated by equation (5.2).

[b] Grafting conditions: 7 wt% BPO and 9 wt% MA at 60 °C for 4 h; feeding rate of MA of 0.6 ml/min.

[c] Grafting conditions: 7 wt% BPO, 9 wt% MA, and ST/MA mole ratio of 4:1at 60 °C for 4 h; feeding rate of MA of 0.6 ml/min.

5.5.4 Mechanism of Styrene-Assisted Grafting of MA onto DPNR

To gain a deeper understanding of the various grafting behaviors of MA grafting onto DPNR in the presence and absence of styrene, reaction mechanisms for both grafting systems were proposed as shown in Figure 5.12. The mechanism of MA grafted DPNR without ST is presented as reaction route *a*. As described earlier in Chapter IV, a free radical species ($R^{\bullet}$) could generate the rubber macroradicals ($DPNR^{\bullet}$) as the active sites for grafting with MA later reacting with $DPNR^{\bullet}$ to produce succinyl radicals (DPNR-*g*-$MA^{\bullet}$). The DPNR-*g*-MA (1) is obtained by a termination of succinyl radicals with another rubber chain through a chain transfer reaction or hydrogen abstraction. DPNR-*g*-MA (2) is also produced by a disproportionation reaction.

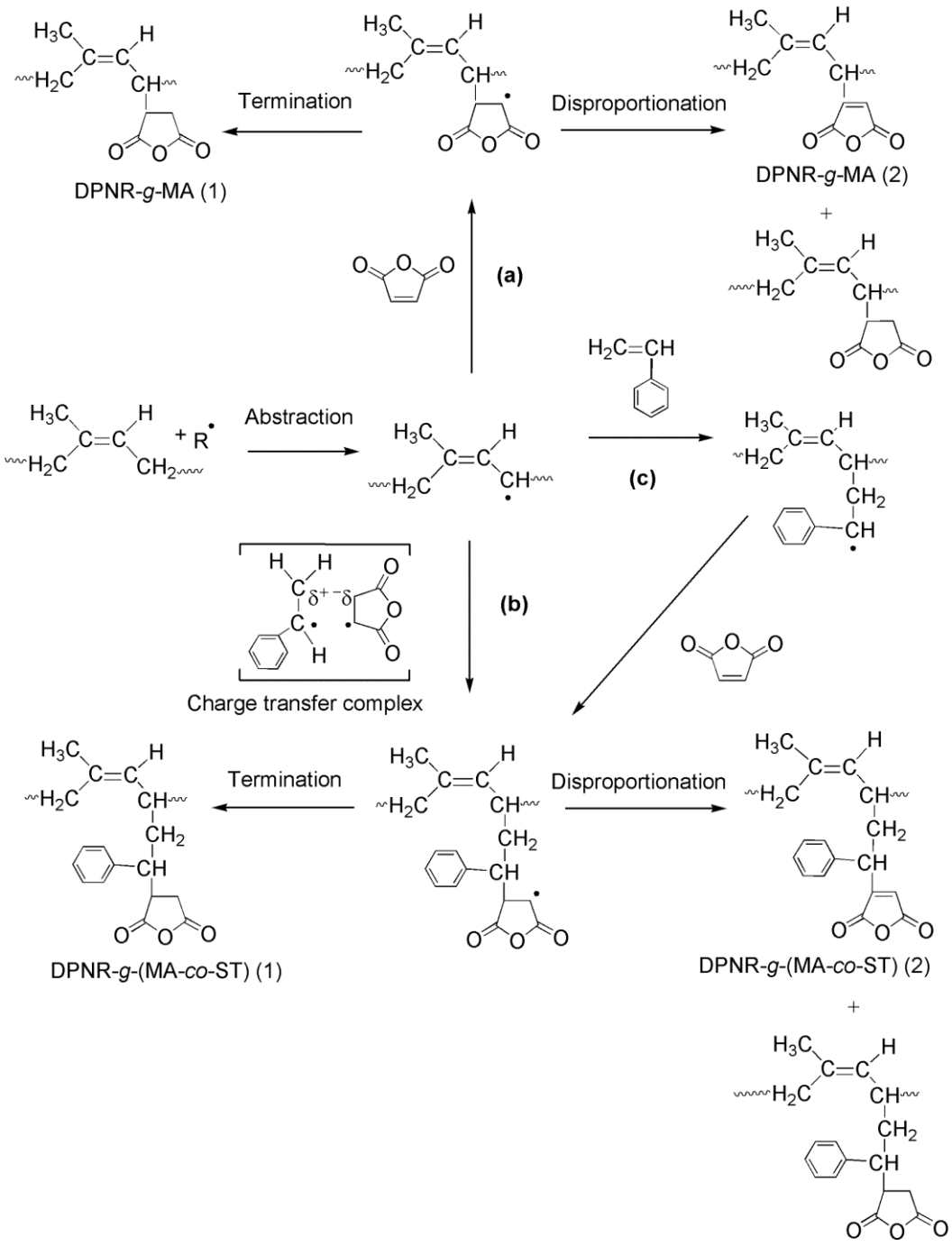

Figure 5.12 Schematic illustration of the proposed free radical mechanism of styrene-assisted grafting of MA onto DPNR.

A number of reports have been carried out to investigate the styrene-assisted grafting of MA onto polyolefins and different grafting mechanisms have also been proposed [30, 31, 34, 35, 97]. In the present work, two possible reaction routes are proposed (Figure 5.12). In reaction route *b*, a charge transfer complex (CTC) between ST and MA can be formed by an electron transfer from the ST donor to the MA acceptor [30, 34, 35]. This CTC is stabilized by the partial electron transfer between the electron-donor and electron-acceptor species. The superior reactivity of CTC therefore reacts preferentially with the rubber macroradicals (DPNR$^{\bullet}$) to form succinyl macroradicals (DPNR-*g*-(MA-*co*-ST$^{\bullet}$). The graft copolymer structures of DPNR-*g*-(MA-*co*-ST) (1) and DPNR-*g*-(MA-*co*-ST) (2) are then obtained by termination and disproportionation reactions, respectively. On the other hand, in reaction route *c*, due to a higher reactivity of ST than MA, ST reacts first with DPNR$^{\bullet}$ to produce more stable styryl macroradicals (DPNR-*g*-ST$^{\bullet}$). However, due to a steric effect, only one ST molecule could be attached onto one isoprene unit. Then MA reacts with DPNR-*g*-ST$^{\bullet}$ to produce a branched structure (i.e., DPNR-*g*-(MA-*co*-ST$^{\bullet}$). This grafting route is preferable especially when the concentration of styrene was high. A similar mechanism has been proposed for styrene-assisted grafting of MA onto PP [31] and grafting of GMA onto PE [36] and PP [38].

The effect of ST/MA ratio on the formation of the charge transfer complex (CTC) can be explained as follows. When the ST/MA ratio = 1:1, it is expected that all the ST and MA monomers can form CTCs, and therefore MA was grafted onto DPNR mainly in the form of the CTC. It has also been expected that the CTC becomes dominant with an increasing ratio of ST/MA. At a high concentration of styrene (i.e., ST/MA ratio > 1:1), not only the CTC can be formed but also styryl macroradicals (DPNR-*g*-ST$^{\bullet}$). That is, part of the ST reacts with MA to form the CTC while the other part of ST may preferentially react with DPNR$^{\bullet}$ to form DPNR-*g*-ST$^{\bullet}$. Therefore, the styrene-assisted grafting mechanism of MA onto DPNR depends on the ratio of ST/MA. It conforms to the melt free-radical grafting of MA onto poly(β-hydroxybutyrate) in the presence of styrene [97].

The chemical structure of the DPNR-*g*-(MA-*co*-ST) graft copolymer could be predicted using the reactivity ratios (r_1 and r_2) of the MA/ST pair [98]. The r_1 and r_2

values for the MA and ST monomers are 0.005 and 0.05, respectively. This demonstrates that MA has little tendency to homopolymerize but readily forms an alternating copolymer with ST. In addition, the product of the reactivity ratio ($r_1 \cdot r_2$) is near zero (2.5 x 10^{-4}), indicating that alternating copolymers should be obtained. Therefore, it is feasible to conclude that the formation of the donor/acceptor complex (CTC) is a precursor for the styrene-assisted grafting of MA onto the DPNR backbone.

5.5.5 Particle Size and Morphology

DLS plots of the DPNR, DPNR-*g*-MA, and DPNR-*g*-(MA-*co*-ST) are compared in Figure 5.13. Two different populations of the particles for the DPNR latex were found at 210 nm and 700 nm. On the other hand, the particle sizes of DPNR-*g*-MA latex showed two different populations with diameters of 230 nm and 870 nm and the DPNR-*g*-(MA-*co*-ST) latex showed different populations with diameters of 260 nm and 880 nm. Compared to the DPNR particles, the larger diameters of the DPNR-*g*-MA and DPNR-*g*-(MA-*co*-ST) were observed which confirmed that MA and/or ST were grafted at the surface of the DPNR particles and the results are strongly supported on the basis of TEM analysis.

Figure 5.14 shows a comparison of TEM micrographs of the DPNR, DPNR-*g*-MA, and DPNR-*g*-(MA-*co*-ST). The TEM micrograph of DPNR showed that rubber particles were spherical in shape with a smooth surface while DPNR-*g*-MA and DPNR-*g*-(MA-*co*-ST) contained a darker core area of natural rubber encompassed by a lighter shell area of the grafted MA and/or ST. Therefore, the morphologies of the DPNR-*g*-MA and DPNR-*g*-(MA-*co*-ST) are core-shell type particles.

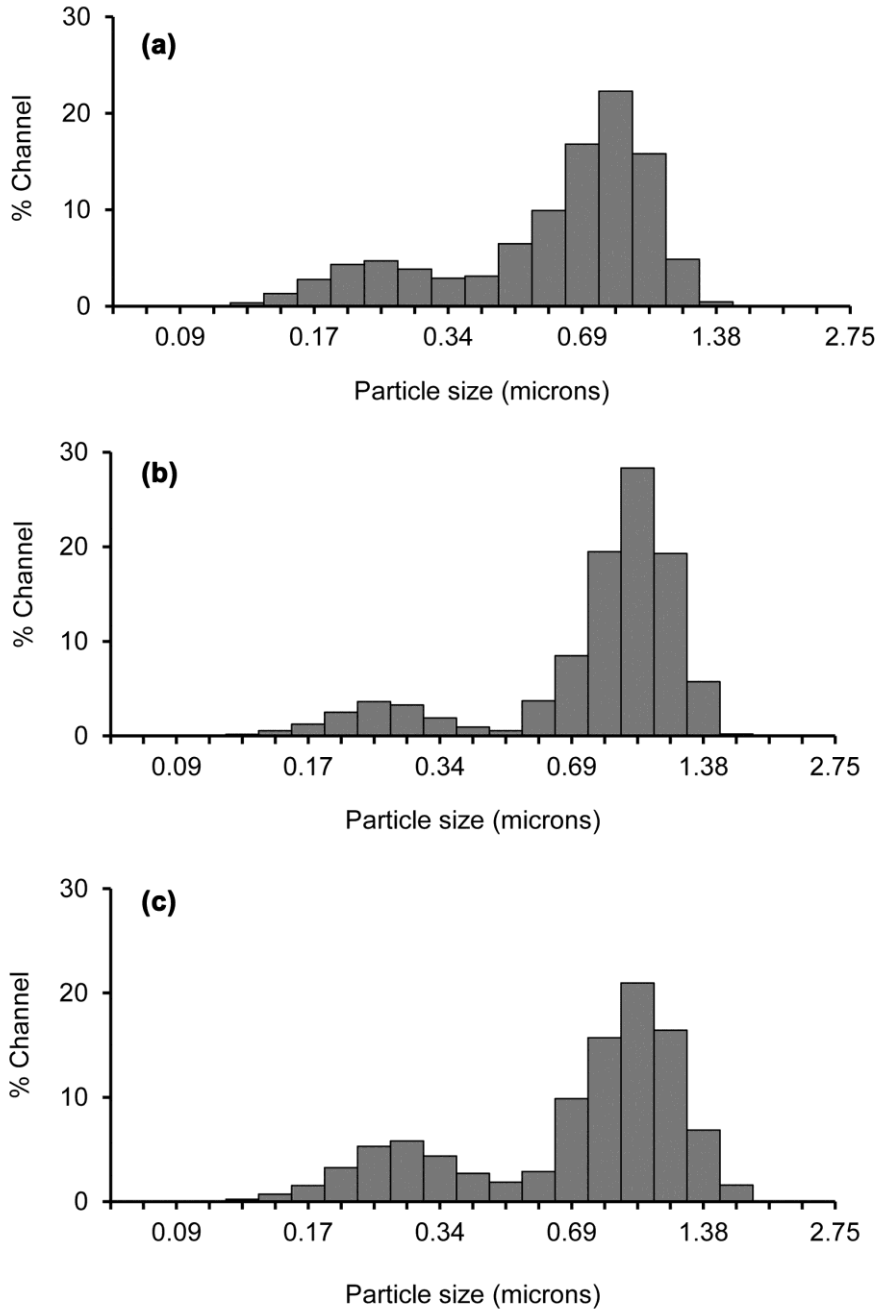

Figure 5. 13 DLS plot of (a) DPNR, (b) DPNR-*g*-MA, and (c) DPNR-*g*-(MA-*co*-ST). (Grafting conditions: DPNR-*g*-MA: 7 wt% BPO, 9 wt% MA, and feeding rate of MA of 0.6 ml/min at 60 °C for 4 h; DPNR-*g*-(MA-*co*-ST): 7 wt% BPO, 9 wt% MA, ST/MA mole ratio of 4:1, and feeding rate of MA of 0.6 ml/min at 60 °C for 4 h)

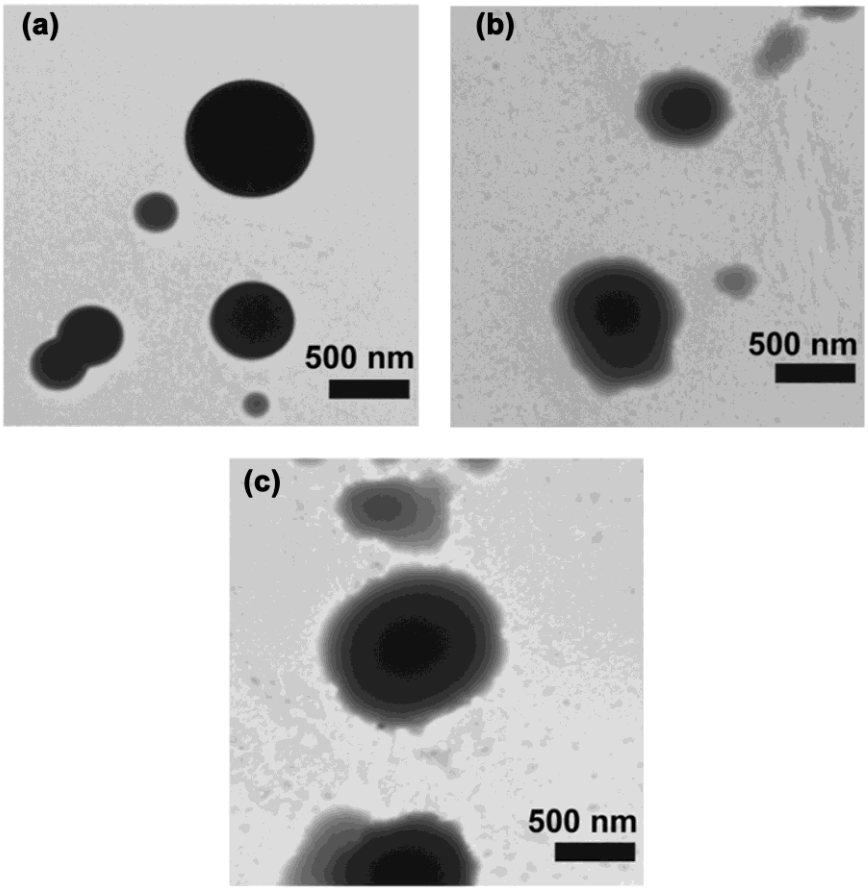

Figure 5.14 TEM micrographs of (a) DPNR, (b) DPNR-*g*-MA, and (c) DPNR-*g*-(MA-*co*-ST). (Grafting conditions: DPNR-*g*-MA: 7 wt% BPO, 9 wt% MA, and feeding rate of MA of 0.6 ml/min at 60 °C for 4 h; DPNR-*g*-(MA-*co*-ST): 7 wt% BPO, 9 wt% MA, ST/MA mole ratio of 4:1, and feeding rate of MA of 0.6 ml/min at 60 °C for 4 h)

5.5.6 Thermal Analysis

Thermal properties of the DPNR, DPNR-*g*-MA, and DPNR-*g*-(MA-*co*-ST) were investigated by DSC and TGA. The DSC curves are shown in Figure 5.15.

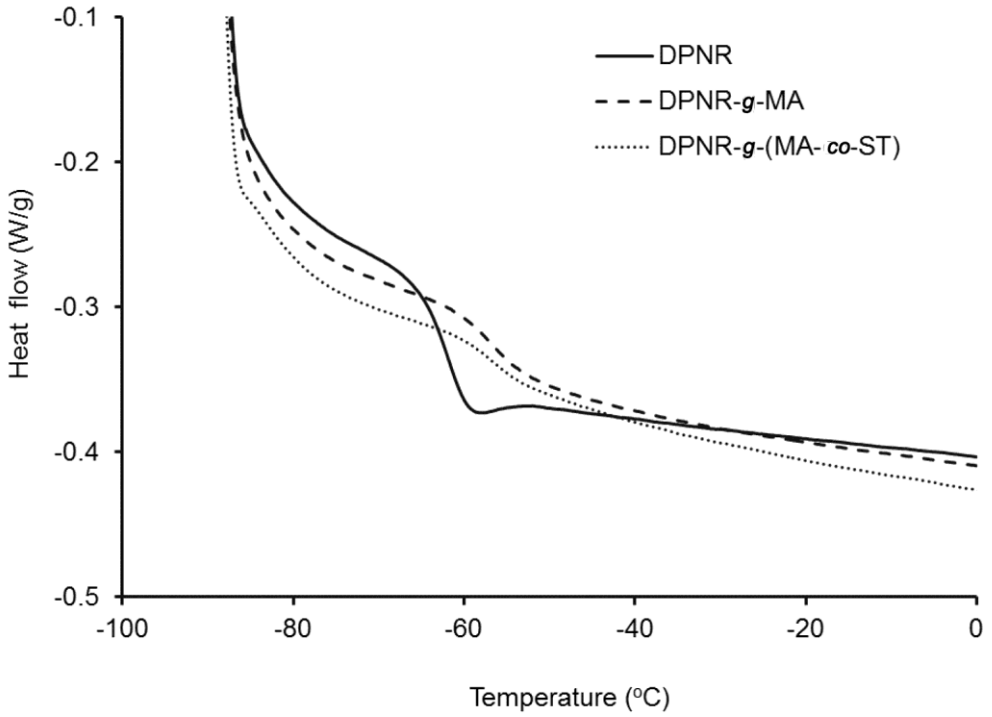

Figure 5.15 DSC curves of DPNR, DPNR-*g*-MA, and DPNR-*g*-(MA-*co*-ST).(Grafting conditions: DPNR-*g*-MA: 7 wt% BPO, 9 wt% MA, and feeding rate of MA of 0.6 ml/min at 60 °C for 4 h; DPNR-*g*-(MA-*co*-ST): 7 wt% BPO, 9 wt% MA, ST/MA mole ratio of 4:1, and feeding rate of MA of 0.6 ml/min at 60 °C for 4 h)

The glass transition temperature (T_g) for the DPNR was -62.6 ºC while the graft copolymers of DPNR-*g*-MA and DPNR-*g*-(MA-*co*-ST) were -56.2 and -56.5 ºC, respectively. It can be seen that both DPNR-*g*-MA and DPNR-*g*-(MA-*co*-ST) had higher T_g than DPNR. Generally, T_g is affected by the size of the side groups and the

mobility of the chain. The increase in T_g of DPNR-*g*-MA and DPNR-*g*-(MA-*co*-ST) is due to chain stiffening because of the presence of MA and/or ST molecules or the increased interchain interaction between polar functional groups of the graft copolymers. However, a slight shift in T_g values of DPNR-*g*-(MA-*co*-ST) (about -57 °C) and DPNR-*g*-MA (about -56 °C) was observed, indicating that a graft copolymer with styrene could not effectively affect the free volume available to the backbone motion.

Figures 5.16 displays the TGA curves of the DPNR, DPNR-*g*-MA, and DPNR-*g*-(MA-*co*-ST). A single decomposition temperature (T_d) for DPNR was observed at 381.5 °C while both DPNR-*g*-MA, and DPNR-*g*-(MA-*co*-ST) showed two decomposition temperatures at 381.5 °C and 436.1 °C. The first step is attributed to the degradation temperature of natural rubber while the second one at the higher decomposition temperature is related to the degradation temperature caused by the grafted MA and/or ST molecules onto the rubber backbone. Similar thermal degradation behavior has been observed for graft copolymers obtained by MA grafting onto PE [94] and styrene-assisted grafting of MA onto poly(β-hydroxybutyrate) [97]. The results obtained indicate that grafting of MA could help increase the thermal stability of the DPNR. However, the degradation temperature of the graft copolymer obtained by MA grafting onto DPNR in the presence of ST did not indicate any marked changes, implying that the grafting comonomer could hardly affect the thermal stability of grafted DPNR.

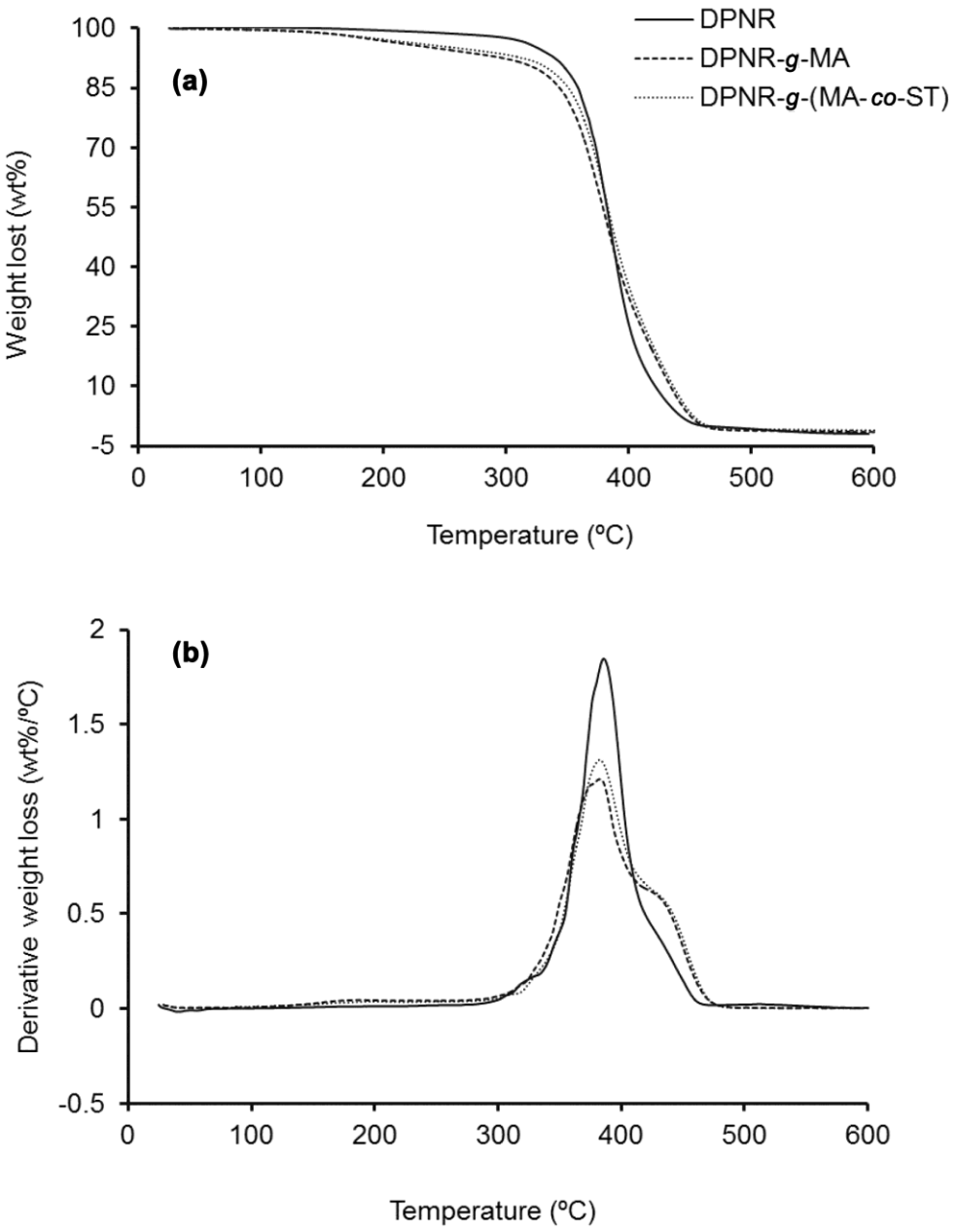

Figure 5.16 TGA curves of DPNR, DPNR-*g*-MA, and DPNR-*g*-(MA-*co*-ST): (a) weight lost versus temperature; and (b) derivative weight loss versus temperature. (Grafting conditions: DPNR-*g*-MA: 7 wt% BPO, 9 wt% MA, and feeding rate of MA of 0.6 ml/min at 60 °C for 4 h; DPNR-*g*-(MA-*co*-ST): 7 wt% BPO, 9 wt% MA, ST/MA mole ratio of 4:1, and feeding rate of MA of 0.6 ml/min at 60 °C for 4 h)

5.6 Conclusions

Styrene-assisted grafting of MA onto the DPNR was successfully carried out by the DMP technique. The results showed that the G.E and gel content were influenced by the initiator and monomer amount, reaction temperature, reaction time, monomer addition rate, and ST/MA ratio. High gel content at a high monomer addition rate was observed. Based on the results obtained, the graft copolymerization system changes from a differential microemulsion system to a conventional emulsion system when the rate of monomer addition is greatly increased. The G.E is remarkably higher in the presence of the styrene comonomer than in its absence. The G.E increased with an increase in the ratio of ST/MA, however, the gel content was more pronounced at a high ST/MA ratio. The appropriate condition for styrene-assisted grafting was 7 wt% BPO, 9 wt% MA, ST/MA mole ratio of 4:1, and addition rate of MA of 0.6 ml/min at 60 °C for 4 h. The grafting content of the graft copolymer synthesized with a ST/MA ratio of 4:1 was 34.2%, which was higher than that of the graft copolymer synthesized without the styrene conmonomer (23.5%). The introduction of copolymerizing styrene in the grafting process showed increased grafting efficiency and grafting content as a result of creating a charge transfer complex (CTC) for the graft copolymerization. This indicates that styrene is an effective comonomer for promoting the efficiency of MA grafting onto DPNR.

CHAPTER VI: GRAFTING KINETICS OF MALEIC ANHYDRIDE ONTO DEPROTEINIZED NATURAL RUBBER IN PRESENCE OF STYRENE COMONOMER

This chapter focuses on the grafting kinetics of MA onto DPNR in the presence and absence of styrene comonomer. The effect of ST/MA ratio on polymerization kinetics of MA grafting onto DPNR was investigated. The monomer conversion was calculated by a gravimetric method. The monomer conversion as a function of reaction time and graft copolymerization rate of MA grafting onto DNPR under the influences of styrene comonomer are discussed in this chapter.

6.1 Preparation of Grafting of MA onto DPNR in Presence of Styrene

Grafting kinetics of MA onto DPNR without styrene was investigated under grafting condition of a fixed 7 wt% BPO, 9 wt% MA, and feeding rate of MA = 0.6 ml/min at 60 °C. Reaction kinetics of the styrene-assisted grafting with various ST/MA ratios were investigated. Two types of grafting conditions were studied: (i) at a fixed amount of MA (i.e., ST/MA mole ratio = 1:1, 2:1, 3:1, and 4:1); and (ii) at a fixed amount of ST (i.e., ST/MA mole ratio = 4:0.5, 4:1, 4:1.5, and 4:2). The experiments were carried out under the same grafting condition as for MA grafting. The experimental procedure for the graft copolymerization in the presence and absence of styrene was the same as previously described in Chapters IV and V, and the monomer conversions under the mentioned conditions were carried out and analyzed.

6.2 Determination of Monomer Conversion

The monomer conversion was determined by a gravimetric method. The graft copolymerization latex was sampled at different reaction times and hydroquinone was immediately added to each sample to stop the polymerization. Afterwards, the sample was coagulated with hot formic acid and the coagulum product was later washed with deionized water, and then dried in a vacuum oven at 50 °C to a constant weight. The weight of each sample before and after drying was recorded. The conversion was calculated as follows:

$$\text{Conversion (\%)} = \frac{\text{Weight of monomer consumed}}{\text{Weight of monomer charged}} \text{x } 100 \qquad (6.1)$$

6.3 Results and Discussion

The content of this section is divided into two parts. The first part relates to the monomer conversion and the second part to the graft copolymerization rate of MA grafting onto DPNR either in the presence or absence of styrene comonomer.

6.3.1 Monomer Conversion

Monomer conversion is defined as the fraction of monomers (i.e., MA and ST) at time *t*, which has been converted to polymers (i.e., graft copolymers, free copolymers, and homopolymers). Figure 6.1 shows conversion versus time curves for MA grafting onto DPNR either in the presence or absence of styrene comonomer. Time-conversion curves for the grafting reaction with a fixed amount of MA (ST/MA ratio = 1:1, 2:1, 3:1, and 4:1) and grafting reaction with a fixed amount of ST (ST/MA ratio = 4:0.5, 4:1, 4:1.5, and 4:2) are shown in Figure 6.1 (a) and (b), respectively.

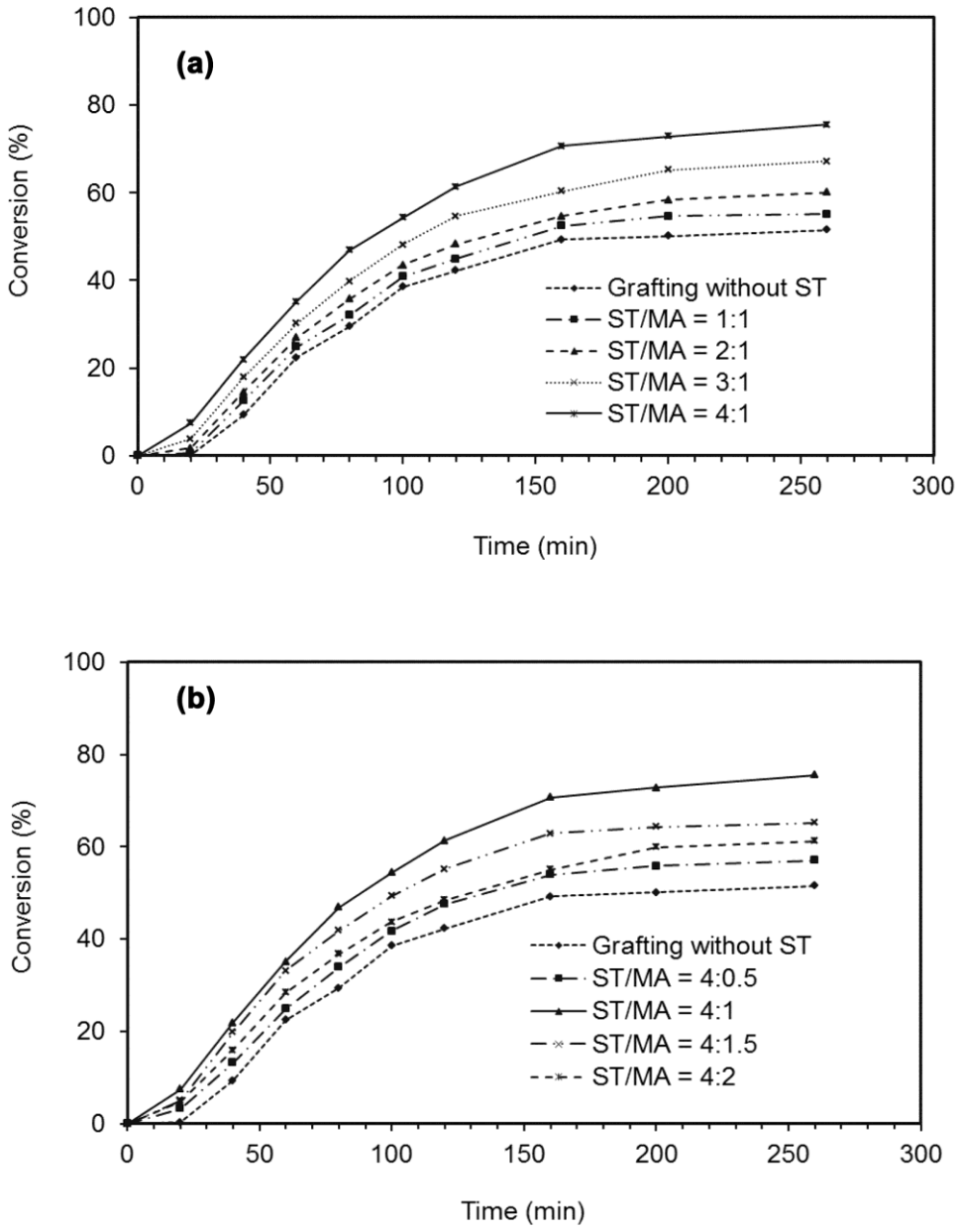

Figure 6.1 Conversion versus time curves of MA grafting onto DPNR in the presence and absence of styrene: (a) grafting reaction with a fixed amount of MA using ST/MA mole ratio of 1:1, 2:1, 3:1, and 4:1; and (b) grafting reaction with a fixed amount of ST using ST/MA mole ratio of 4:0.5, 4:1, 4:1.5, and 4:2. (Grafting conditions: MA grafting without ST (control reaction): 7 wt% BPO, 9 wt% MA, and feeding rate of MA of 0.6 ml/min at 60 °C; Styrene-assisted grafting reaction: 7 wt% BPO and feeding rate of MA of 0.6 ml/min at 60 °C)

It was found that the monomer conversion increased greatly up to 200 min and thereafter it was constant. Compared to the MA grafting onto DPNR without styrene, a higher total monomer conversion of the styrene-assisted grafting reaction was observed and the conversion increased on increasing the ST/MA mole ratios from 1 – 4. This is attributed in that ST formed the charge transfer complex (CTC) with MA, and/or ST was polymerized or copolymerized with MA to generate new polymeric radicals, and they were then grafted at the surface of the rubber particles. In addition, when the amount of ST in the grafting system increased, a more favorable condition resulted to produce more graft copolymers (i.e., DPNR-*g*-MA, DPNR-*g*-ST, and DPNR-*g*-(MA-*co*-ST)), free copolymers (i.e., poly(ST-*co*-MA)), and/or homopolymers (i.e., ungrafted polystyrene) [13, 21]. As a result, an increase in monomer conversion for the styrene-assisted grafting of MA onto DPNR was obtained.

6.3.2 Graft Copolymerization Rate

The reaction rate of graft copolymerization is defined as the ratio of the percentage of monomer conversion to reaction time. Figure 6.2 shows the plots of reaction rate versus conversion for MA grafting onto DPNR at various ST/MA ratios. It can be seen that the reaction rate-conversion curves showed three main intervals of the graft copolymerization process. That is the ascending-period (particle nucleation), followed by the steady-period (particle growth) with constant reaction rate, and finally the falling-period (reduction of monomer concentration in particles towards zero) with the reaction rate tending to zero. The results obtained are consistent with a typical emulsion polymerization [99].

As seen in Figure 6.2, the reaction rate increases rapidly with increasing monomer conversion in the first stage of graft copolymerization (i.e., low conversions). Afterwards, at conversion intervals from approximately 20% to 50%, the reaction rate becomes constant in which large monomer droplets exist with a continuous supply of monomer to all particles in the system.

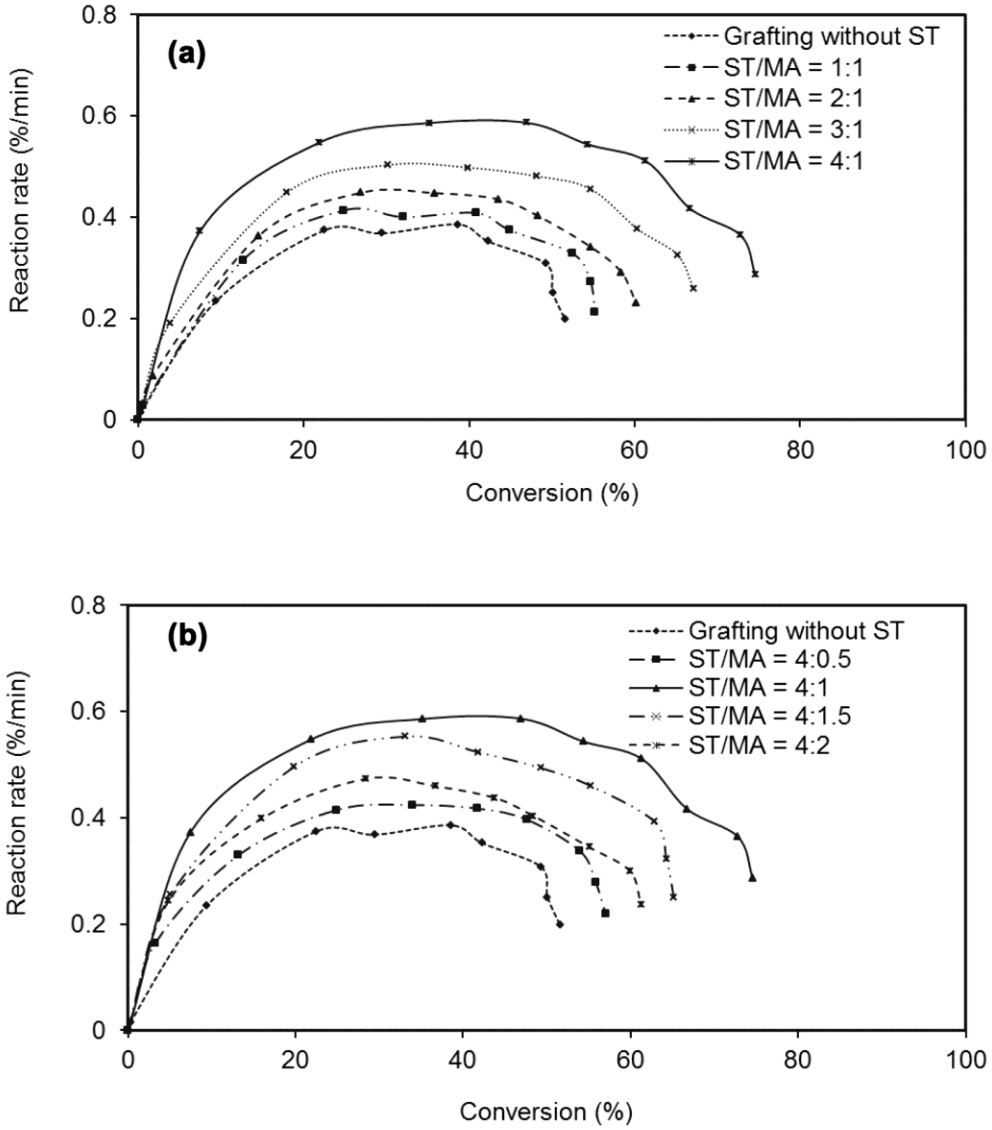

Figure 6.2 Reaction rate as a function of the monomer conversion for MA grafting onto DPNR in the presence and absence of styrene: (a) grafting reaction with a fixed amount of MA using ST/MA mole ratio of 1:1, 2:1, 3:1, and 4:1; and (b) grafting reaction with a fixed amount of ST using ST/MA mole ratio of 4:0.5, 4:1, 4:1.5, and 4:2. (Grafting conditions: MA grafting without ST (control reaction): 7 wt% BPO, 9 wt% MA, and feeding rate of MA of 0.6 ml/min at 60 °C; Styrene-assisted grafting reaction: 7 wt% BPO and feeding rate of MA of 0.6 ml/min at 60 °C)

Therefore, in this stage, the monomer concentrations in the homopolymer (i.e., homopolystyrene) and grafted rubber particles were constant. Finally, at high conversions (i.e., beyond 50%), the reaction rate decreases and it tends to zero. This contributes to the effect of diffusion-controlled phenomena on the propagation reaction and the reduced mobility of monomer molecules (i.e., MA and ST) to find a macro-radical and react.

The initial rate of graft copolymerization (R_p) was determined from the slope of the conversion-time curve during the period of the initial stage of reaction (i.e., 0 – 120 min) as shown in Figures 6.3 and 6.4. The coefficient of correlation (R^2) for each curve during that interval time is greater than 0.9, indicative of a strong linear relationship between conversion and time. The R_p for MA grafting onto DPNR in the absence and presence of styrene at different ST/MA ratios are presented in Figure 6.5.

As seen in Figure 6.5 (a), when the amount of MA was fixed (i.e., ST/MA mole ratio = 1:1, 2:1, 3:1, and 4:1), the R_p of styrene-assisted grafting system for all experiments was higher than that of MA grafting in the absence of styrene. It was found that the R_p increased on increasing the ratio of ST/MA over the range investigated (i.e., ST/MA mole ratio = 1 – 4). It can be seen that the R_p for the styrene-assisted grafting reaction with a ST/MA ratio of 4:1 (0.5409 %/min) was higher than that of the grafting reaction without styrene (0.3577 %/min), indicating that styrene can enhance the rate of graft copolymerization of MA onto DPNR. This behavior is attributed to the formation of a charge transfer complex (CTC) for graft copolymerization as mentioned earlier in that the superior reactivity of the CTC can react preferentially with the DPNR$^{\bullet}$ to form DPNR-*g*-(MA-*co*-ST$^{\bullet}$). In addition, due to a higher reactivity of ST than MA, ST can react first with the DPNR$^{\bullet}$ to generate the DPNR-*g*-ST$^{\bullet}$ and then it reacts with MA to produce the graft copolymers. This grafting route is preferable especially when the amount of styrene was high (i.e., ST/MA mole ratio = 4:1). Therefore, an increase in the graft copolymerization rate on increasing the ratio of ST/MA was observed. The results obtained indicate that the styrene comonomer plays an important role in the final monomer conversion and the polymerization kinetics of MA grafting onto DPNR.

When the amount of styrene was fixed (i.e., ST/MA mole ratio = 4:0.5, 4:1, 4:1.5, and 4:2), as shown in Figure 6.5 (b), the R_p increased with increasing MA content and reached a maximum at a ST/MA mole ratio = 4:1 and thereafter decreased. The phenomena may be associated with the surface reaction. Since MA and DPNR are relatively immiscible, the grafting reaction occurs largely on the surface of the rubber particles and therefore the rate of graft copolymerization depends on the diffusion rate of MA and/or ST into the DPNR phase. At a higher amount of MA, more MA molecules can diffuse onto the rubber phase for grafting and therefore provide a higher graft copolymerization rate. However, a further increase in MA content beyond a ST/MA mole ratio of 4:1, results in a decrease in R_p. At a high concentration of MA (i.e., ST/MA mole ratio = 4:1.5 and 4:2), the grafting reaction may be retarded by phase separation between MA and DPNR leading to a decrease in total monomer conversion and reaction rate. Furthermore, an increase in MA may decrease the amount of excited MA molecules as the excited MA is quenched by the MA ground state and hence less excited MA molecules are available for grafting and therefore result in a lower rate of graft copolymerization. It can be seen that the conversion curves (i.e., R_p) of grafting reactions change caused by adding of styrene with various ST/MA ratios. This indicates that the graft copolymerization rates were dependent on the ratio of ST/MA.

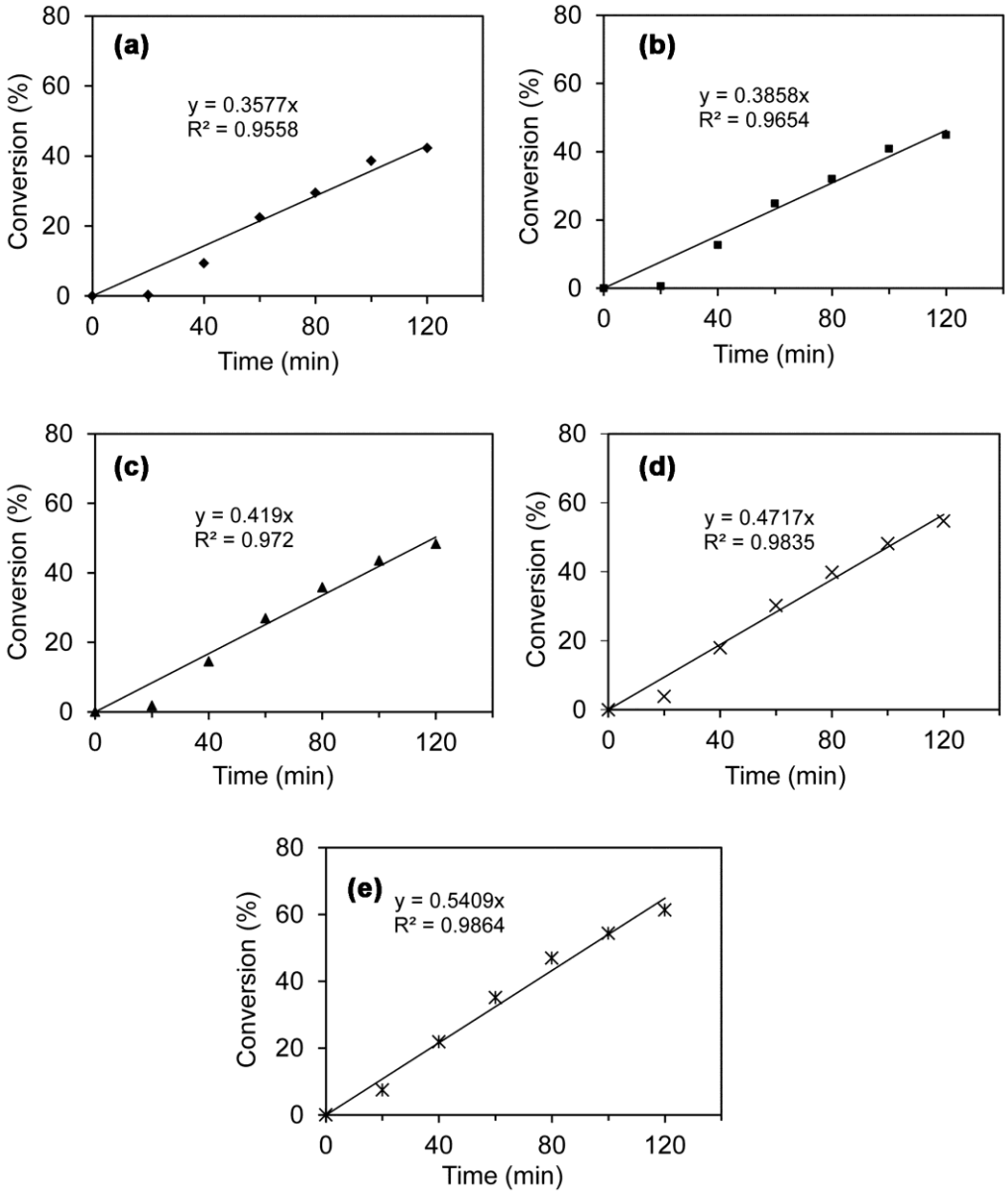

Figure 6.3 Plots of conversion as a function of reaction time during 0 – 120 min for MA grafting onto DPNR in the presence and absence of styrene: (a) control reaction; and (b) – (e) grafting reaction with a fixed amount of MA using ST/MA mole ratio of 1:1, 2:1, 3:1, and 4:1, respectively. (Grafting conditions: MA grafting without ST (control reaction): 7 wt% BPO, 9 wt% MA, and feeding rate of MA of 0.6 ml/min at 60 °C; Styrene-assisted grafting reaction: 7 wt% BPO and feeding rate of MA of 0.6 ml/min at 60 °C)

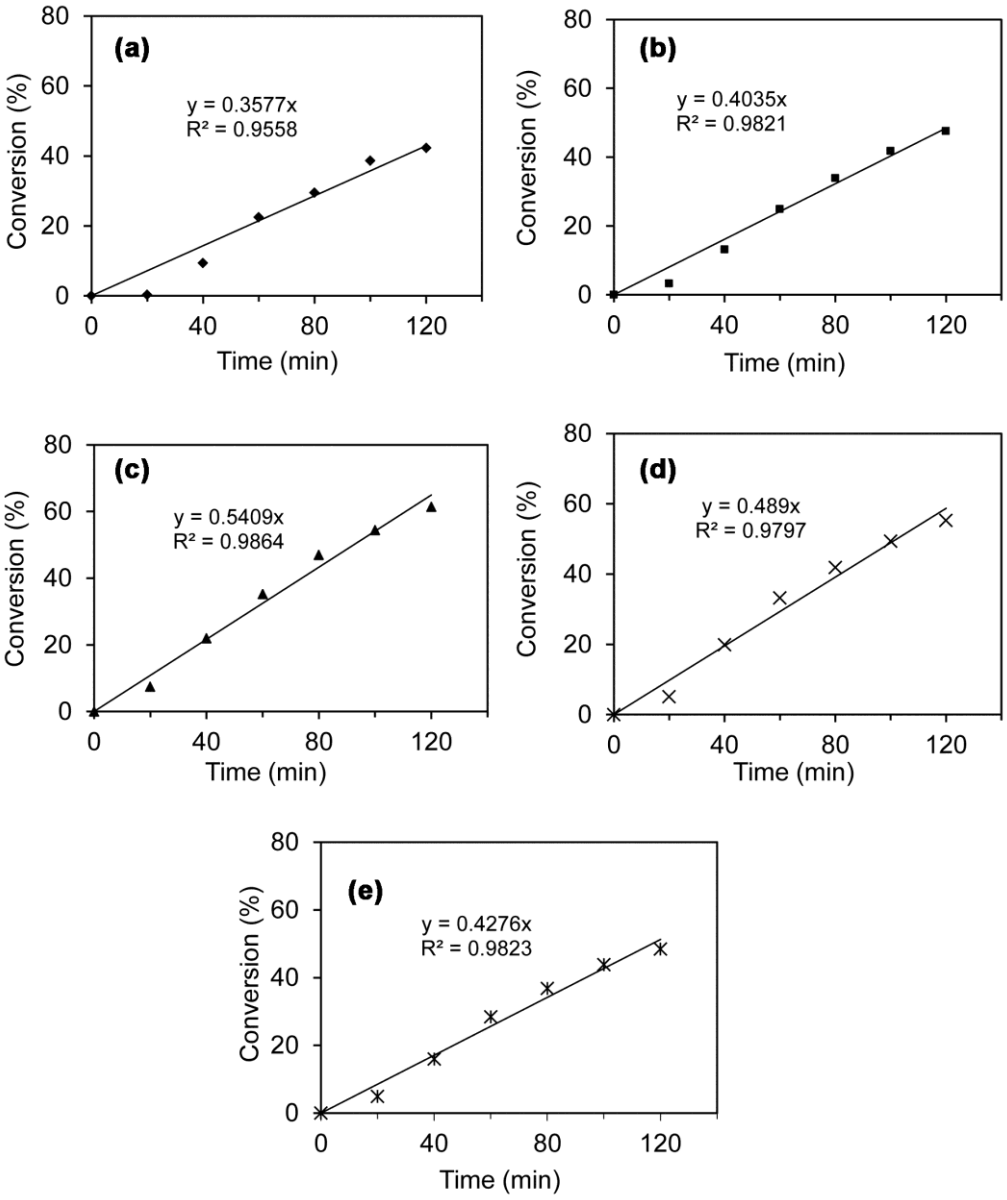

Figure 6.4 Plots of conversion as a function of reaction time during 0 – 120 min for MA grafting onto DPNR in the presence and absence of styrene: (a) control reaction; and (b) – (e) grafting reaction with a fixed amount of ST using ST/MA mole ratio of 4:0.5, 4:1, 4:1.5, and 4:2, respectively. (Grafting conditions: MA grafting without ST (control reaction): 7 wt% BPO, 9 wt% MA, and feeding rate of MA of 0.6 ml/min at 60 °C; Styrene-assisted grafting reaction: 7 wt% BPO and feeding rate of MA of 0.6 ml/min at 60 °C)

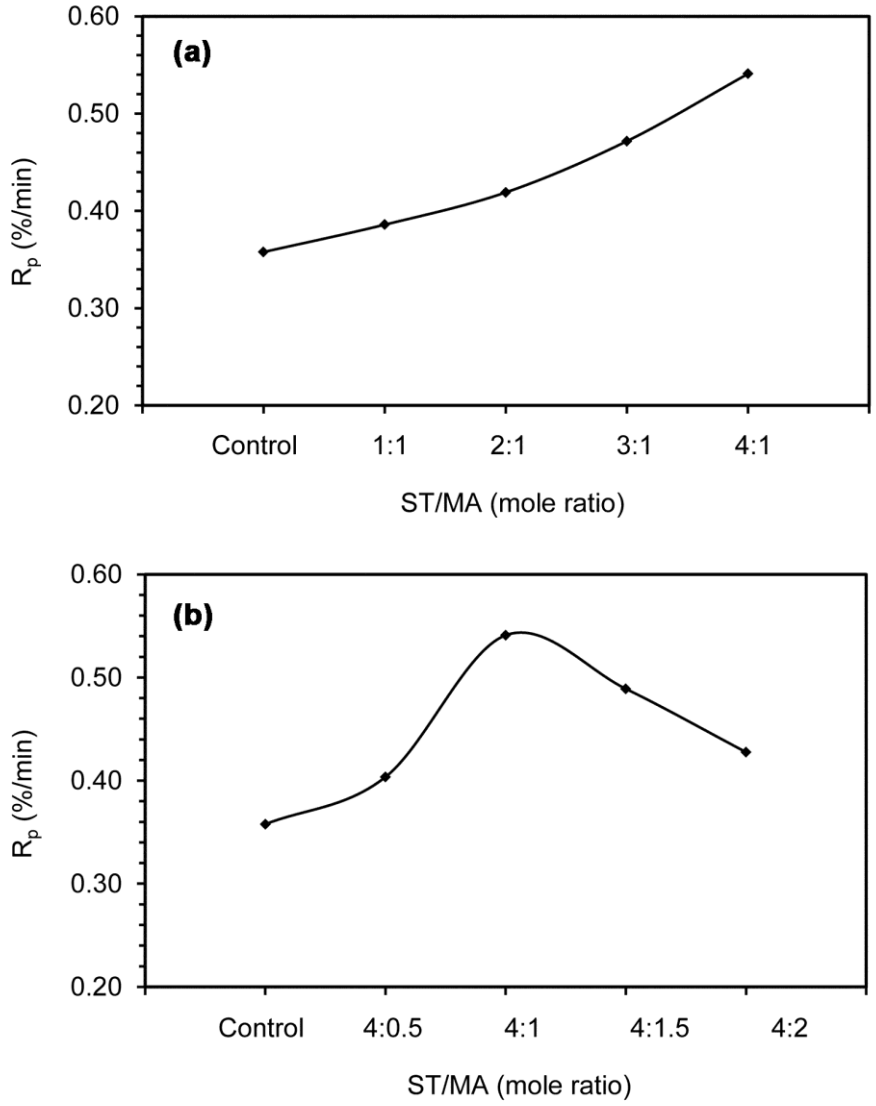

Figure 6.5 Graft copolymerization rate (R_p) of MA grafting onto DPNR in the presence and absence of styrene: (a) grafting reaction with a fixed amount of MA using ST/MA mole ratio of 1:1, 2:1, 3:1, and 4:1; and (b) grafting reaction with a fixed amount of ST using ST/MA mole ratio of 4:0.5, 4:1, 4:1.5, and 4:2. (Grafting conditions: MA grafting reaction without ST (control reaction): 7 wt% BPO, 9 wt% MA, and feeding rate of MA of 0.6 ml/min at 60 °C; Styrene-assisted grafting reaction: 7 wt% BPO and feeding rate of MA of 0.6 ml/min at 60 °C)

6.4 Conclusions

Grafting kinetics of MA onto DPNR in the presence and absence of styrene were investigated. When the amount of MA was fixed (i.e., ST/MA mole ratio = 1:1, 2:1, 3:1, and 4:1), a higher monomer conversion and graft copolymerization rate of styrene-assisted grafting reaction than that of grafting reaction without styrene were observed. The conversion and the graft copolymerization rate of the styrene-assisted grafting reaction increased with increasing the ST/MA mole ratio. This behavior can be attributed to the formation of a charge transfer complex (CTC) for graft copolymerization. This indicates that the styrene comonomer plays an important role in the monomer conversion and the polymerization kinetics of MA grafting onto DPNR. When the amount of styrene was fixed (i.e., ST/MA mole ratio = 4:0.5, 4:1, 4:1.5, and 4:2), the graft copolymerization rate increased with increasing MA content and reached a maximum at a ST/MA ratio of 4:1 and thereafter decreased. At a high concentration of MA (i.e., ST/MA ratio = 4:1.5 and 4:2), the grafting reaction may be retarded by phase separation between MA and DPNR leading to a decrease in conversion and reaction rate. It was found that the graft copolymerization rate (R_p) for the styrene-assisted grafting with ST/MA ratio of 4:1 (R_p = 0.5409 %/min) was higher than that of grafting reaction without styrene (R_p = 0.3577 %/min) and therefore it could be concluded that styrene can enhance the rate of graft copolymerization of MA onto DPNR.

CHAPTER VII: APPLICATION OF GRAFT COPOLYMER AS COMPATIBILIZER FOR VULCANIZED NATURAL RUBBER AND ACRYLONITRILE-BUTADIENE-STYRENE BLENDS

In this chapter, graft copolymers of DPNR-*g*-MA and DPNR-*g*-(MA-*co*-ST) were used as compatibilizers for vulcanized NR/ABS blends using a phenolic resin as a curing agent by a melt mixing process. The effects of the blend proportions, phenolic curative content, and graft copolymer on mechanical, morphological and the related properties of the vulcanized NR/ABS blends were investigated. Curing characteristics of the NR vulcanizates were characterized using an Oscillating Disk Rheometer. Tensile testing was performed using a Hounsfield Tensometer. Hardness of the blends was measured using a Shore A durometer. Izod impact strength of the blends was measured using a Pendulum Impact Tester. Dynamic properties were investigated using a moving die processability tester. Thermal properties of T_d of the blends were investigated using TGA. Morphology of the blends was investigated by SEM.

7.1 Materials

Natural rubber (NR, STR 5L) was provided by Yala Latex Industry Co., Ltd., Thailand. Acrylonitrile-butadiene-styrene (ABS, SP200) was manufactured by the IRPC Public Co., Ltd., Rayong, Thailand. The ABS having a weight ratio of acrylonitrile: butadiene: styrene of 24:19:57 is an injection molding grade with a melt flow index (MFI) of 17 g/10 min (10 kg loads at 220 °C). The general physical properties of ABS are summarized in Appendix B (Table B-1). Hydroxymethylol phenolic resin (HRJ-10518) was manufactured by the Schenectady International Inc., New York, USA. This contains 6 – 9% active hydroxymethyl (methylol) groups. Stannous chloride ($SnCl_2.2H_2O$) was purchased from Qrec (New Zealand). Stearic acid and zinc oxide were purchased from Loba Chemie (India). 2,2,4-trimethyl-1,2-

dihydroquinoline (TMQ) was provided by Topflight Co., Ltd., Thailand. Tetrahydrofuran (THF) was manufactured by Labscan (Ireland).

7.2 Preparation of NR Compound and Vulcanized NR/ABS Blends

NR compound was first prepared before blending with ABS. The mixing was carried out using an internal mixer (Brabender GmbH & Co.KG, Duisburg, Germany). The capacity of the mixing chamber is 50 cm^3. The mixing was carried out at 50 °C with a rotor speed of 60 rpm. The formulations and mixing schedule used for compounding NR at various concentrations of the phenolic resin are shown in Table 7.1. The NR compound was carried out according to the following steps. NR was first introduced into the mixing chamber and the other chemical ingredients were then sequentially added. After dumping the mixture from the mixing chamber, the NR compound was sheeted out using a laboratory mill and left at room temperature for at least 12 h before blending with ABS.

Table 7.1 Formulations and mixing schedule used for NR compound.

Ingredients	Quantities (phr) at condition			Mixing time (min)	Cumulative mixing time (min)
	1	2	3		
NR	100	100	100	3	3
Zinc oxide	5	5	5	1	4
Stearic acid	1	1	1	1	5
TMQ[a]	1	1	1	1	6
$SnCl_2.2H_2O$[b]	3	3	3	1	7
HRJ-10518[c]	10	15	20	3	10

[a] 2, 2, 4-Trimethyl-1,2-dihydroquinoline; [b] Stannous chloride; [c] Hydroxymethylol phenolic resin.

The vulcanization of NR/ABS blends with a NR/ABS blend ratios of 50/50, 60/40, and 70/30 were carried out using the same internal mixer at 180 °C with a rotor

speed of 60 rpm. ABS was dried in a hot air oven at 80 °C for at least 5 h. Dried ABS was first mixed in the mixing chamber for 2 min and followed by mixing the NR compound. The mixing was further continued for 4 min until a plateau torque was obtained. For the blends with the graft copolymer, the NR compound with various amounts of graft copolymer was first prepared and later used for blending with ABS using the same procedure as previously described.

7.3 Testing and Characterization

7.3.1 Curing Characteristics

Curing characteristics of the NR vulcanizates were characterized using an Oscillating Disk Rheometer (ODR2000, Monsanto, America) at 180 °C for 30 min. The minimum (M_L) and maximum (M_H) torques, scorch time (T_{s1}), and the optimum cure time (T_{c90}) were measured based on the curing curve. The cure rate index (CRI) is defined as presented in equation (7.1):

$$\mathrm{CRI} = \frac{100}{T_{C90} - T_{S1}} \tag{7.1}$$

7.3.2 Mechanical Properties

Thin sheets of 2 mm thickness of the samples for mechanical testing were prepared by compression molding at 180 °C for 5 min. The dumbbell shaped specimens were prepared by cutting the molded sheet using a die C, according to ASTM D412. Tensile testing was performed using a Hounsfield Tensometer (H10KS, Hounsfield Test Equipment, UK) at a crosshead speed of 500 mm/min according to ISO 37. Hardness of the samples was measured using a Shore A durometer according to ASTM D2240. Izod impact strength was measured according to ASTM D256 using a Pendulum Impact Tester (Resil Impactor 21130, Italy). Five specimens of each sample were tested and the average values were reported.

7.3.3 Dynamic Properties

Dynamic properties were investigated using a moving die processability tester (RheoTech MDPT, Tech-Pro Inc, USA). The experiment was carried out using a frequency sweep mode at a constant strain of 3% at 180 °C which was assumed to be in the linear viscoelastic (LVE) range.

7.3.4 Thermal Properties

Thermogravimetric Analysis (TGA) was performed on a Perkin Elmer STA600 (Perkin Elmer Inc., USA) using a heating rate of 20 °C/min under a nitrogen atmosphere and a temperature scan from 30 to 800 °C.

7.3.5 Morphological Properties

Morphology was investigated by scanning electron microscopic method (SEM, JSM-5800 LV, Japan). Molded samples of the NR/ABS vulcanizates were cryogenically cracked in liquid nitrogen to avoid any possibility of phase deformation. The ABS phase was extracted from the blended product using hot THF for 15 min and dried in a vacuum oven at 50 °C. The dried samples were later sputter-coated with gold for SEM investigation. The solubility parameter (δ) is used to explain the effectiveness of THF in extracting the ABS phase from the blended products. The δ of the NR and THF were obtained from existing literature [100, 101]. The δ of the ABS in the present work was approximated using the Hansen solubility parameters [101] for comparison purposes as presented in equations (7.2) – (7.5):

$$\delta_t^2 = \delta_d^2 + \delta_p^2 + \delta_h^2 \tag{7.2}$$

where δ_t is the total solubility parameter and δ_d, δ_p, δ_h, are the dispersive component, polar component, and hydrogen-bonding component, respectively. The δ_d, δ_p, and δ_h are defined as follows:

$$\delta_d = w_1\delta_{d1} + w_2\delta_{d2} + w_3\delta_{d3} \tag{7.3}$$

$$\delta_p = w_1\delta_{p1} + w_2\delta_{p2} + w_3\delta_{p3} \quad (7.4)$$

$$\delta_h = w_1\delta_{h1} + w_2\delta_{h2} + w_3\delta_{h3} \quad (7.5)$$

where w_1, w_2, and w_3 are the weight fractions of acrylonitrile, butadiene, and styrene in ABS, respectively. The subscripts "1", "2", and "3" for each δ represent the components of polyacrylonitrile, polybutadiene, and polystyrene, respectively.

7.4 Results and Discussion

7.4.1 Mixing Torque of Vulcanized NR/ABS Blends

Torque-time curves of the vulcanized NR/ABS blends at three NR/ABS blend ratios of 50/50, 60/40, and 70/30 are shown in Figure 7.1. The NR compound with 15 phr HRJ-10518 was used to blend with ABS. In the early stage (before 2 min of ABS processing), it can be seen that the mixing torque sharply rose when the rotor started to work because of resistance exerted on the rotor by the un-molten ABS. At this stage, the mixing torque increased with increasing content of ABS. This is attributed to the high loading of hard material (ABS) which gave higher resistance exerted on the rotor and therefore resulted in higher mixing torque. A decrease in torque was later observed because ABS was molten as a result of mechanical shear. When the NR compound was introduced, the mixing torque rose sharply again which was caused by the resistance of un-molten components and thereafter the mixing torque decreased. Then the mixing torque dramatically rose again due to the vulcanization during the melt mixing process. The mixing was further continued until a plateau torque was obtained. It was found that the levels of the final mixing torque increased with increasing content of the NR compound. Therefore, 70/30 NR/ABS blends gave the highest final mixing torque. This is attributed to an influence of the higher viscosity of the vulcanized NR than that of the neat ABS. At a higher proportion of NR, a crosslinking reaction of the rubber with the curing agent was more pronounced and that might be another reason for the increasing trend of the mixing torque.

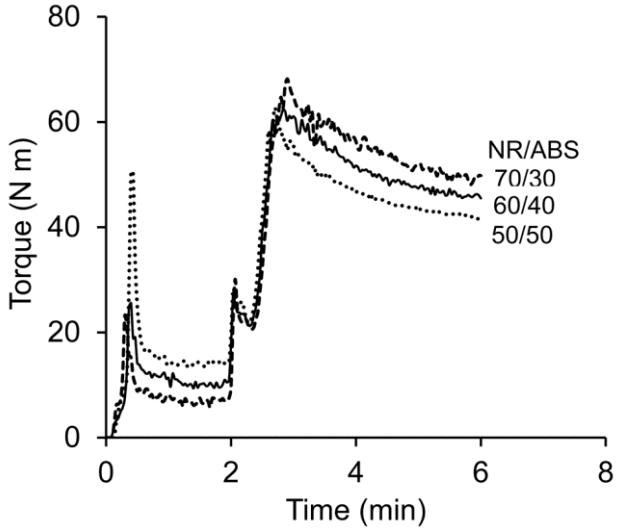

Figure 7.1 Torque-time curves of vulcanized NR/ABS blends at three ratios of 50/50, 60/40, and 70/30. (Conditions of the blends: NR compound with 15 phr HRJ-10518; mixing temperature of 180 °C)

7.4.2 Effect of Blend Proportions on Properties of Vulcanized NR/ABS Blends

7.4.2.1 Mechanical Properties

The mechanical properties in terms of tensile strength, elongation at break, hardness, and impact strength of the neat ABS, cured NR, and NR/ABS vulcanizates prepared using a NR compound with 15 phr HRJ-10518 are presented in Table 7.2. It is seen that the vulcanized NR gave excellent elasticity while the neat ABS provided good tensile strength, hardness, and impact strength but poor elongation. ABS is synthesized by graft copolymerization of styrene and acrylonitrile monomers onto polybutadiene. The rubber particles are grafted with styrene-*co*-acrylonitrile (SAN) and thus the properties of ABS depend on the compositions of its constituents. In the present work, ABS contains an acrylonitrile: butadiene: styrene weight ratio of 24:19:57. Polystyrene gives the strength and rigidity while the polybutadiene provides the toughness and impact strength. The polar nitrile groups from neighboring chains can attract each other and bind the chains together, making ABS stronger than pure polystyrene.

Table 7.2 Mechanical properties of neat ABS, cured NR, and NR/ABS vulcanizates.

Samples	Tensile strength (MPa)	Elongation at break (%)	Hardness (Shore A)	Impact strength (J/m)
ABS[a]	35.0 ± 0.5	25.7 ± 1.5	96.3 ± 0.3	379.8 ± 2.4[c]
Cured NR	16.4 ± 0.8	570.0 ± 9.8	38.3 ± 0.5	-
NR/ABS vulcanizates[b]				
50/50	12.1 ± 0.3	77.2 ± 1.9	94.8 ± 0.3	245.9 ± 2.8[d]
60/40	10.3 ± 0.2	107.3 ± 2.7	92.2 ± 0.3	313.8 ± 6.7[d]
70/30	6.5 ± 0.3	105.4 ± 9.3	86.6 ± 0.6	NA[e]

[a] Acrylonitrile: butadiene: styrene weight ratio is 24:19:57; [b] Vulcanized NR/ABS blends using NR compound with 15 phr HRJ-10518; [c] Failure type is a C-complete break; [d] Failure type is a P-partial break; [e] NA-unbreakable, very flexible.

As seen in in Table 7.2, ABS showed excellent strength and hardness properties; it is thus a favorable polymer for blending with NR to improve the elongation of the ABS thermoplastic. The results showed that tensile strength and hardness properties of vulcanized NR/ABS blends increased with increasing ABS content. That is, the strength and hardness of the blends were controlled by the thermoplastic component. On the other hand, elongation of the blends increased with increasing rubber content, indicating that the vulcanized NR is an essential component for improving elongation of the blends. It was found that the cured NR with the phenolic curing agent exhibited higher tensile strength than that of the vulcanized NR/ABS blends because the former was fully crosslinked while the latter was crosslinked only in the NR part. Furthermore, higher impact strength of the vulcanized 60/40 NR/ABS blends than that of the vulcanized 50/50 NR/ABS blends was obtained. However, the vulcanized 70/30 NR/ABS blends are very flexible

(unbreakable) and therefore one cannot determine its impact strength. It can be seen that the vulcanized 60/40 NR/ABS blends showed well-balanced mechanical properties. These mechanical properties are consistent with the morphology of the blends (SEM analysis shall be discussed in the next section). The obtained results demonstrate that vulcanization of NR/ABS blends could provide a new material with superior mechanical properties. These products can be used in protective bumper applications and other appliances where high impact strength and elasticity are needed.

7.4.2.2 Morphological Properties

The fractured surfaces of the vulcanized NR/ABS blends were investigated by SEM. The ABS phase was extracted from the blended products using THF. The effectiveness of THF in extracting the ABS phase could result from the solubility parameters (δ) of THF and ABS as shown in Table 7.3. The dispersive component (δ_d), polar component (δ_p), and total solubility parameter (δ_t) of THF (9.50 $cal^{1/2}/cm^{3/2}$) are very close to ABS (10.04 $cal^{1/2}/cm^{3/2}$), indicating that THF can better dissolve ABS than NR (8.17 $cal^{1/2}/cm^{3/2}$). This could be demonstrated by the basic principle of solubility parameter theory in that "like dissolves like". The morphology of the blends is shown in Figure 7.2. The phase morphology of the vulcanized 60/40 NR/ABS blends without extracting the ABS phase from the blended product is presented in Figure 7.2 (a). It was found that no difference between ABS and NR phases can be observed. Thus the ABS phase was preferentially extracted from the blended products using THF. Appearance of the etched, fractured surfaces of the vulcanized NR/ABS blends at three ratios of 50/50, 60/40, and 70/30 is presented in Figure 7.2 (b) – (d). The ABS phase was etched from the sample surfaces, while the vulcanized NR domains remained undissolved and adhered to the surfaces. SEM micrographs of the three blends showed a two-phase morphology system (i.e., vulcanized rubber phase and thermoplastic phase). That is, ABS particles are dispersed in the NR matrix for all the vulcanized NR/ABS blends under study.

Table 7.3 Hansen solubility parameters of solvent and polymers.

Samples	Hansen solubility parameter ($cal^{1/2}/cm^{3/2}$)[a]			
	δ_d	δ_p	δ_h	δ_t
Tetrahydrofuran (THF)[b]	8.20	2.78	3.90	9.50
Polyacrylonitrile[b]	10.59	6.88	4.44	13.39
Polybutadiene[b]	8.54	1.12	1.66	8.77
Polystyrene[b]	9.03	2.20	1.42	9.40
ABS[c]	9.31	3.12	2.19	10.04
NR[d]	-	-	-	8.17

[a] δ_t is the total solubility parameter and δ_d, δ_p, δ_h, are dispersive component, polar component, and hydrogen-bonding component, respectively;

[b] Data obtained from Ref. [101];

[c] Data calculated using equations (7.2) – (7.5);

[d] Data obtained from Ref. [100].

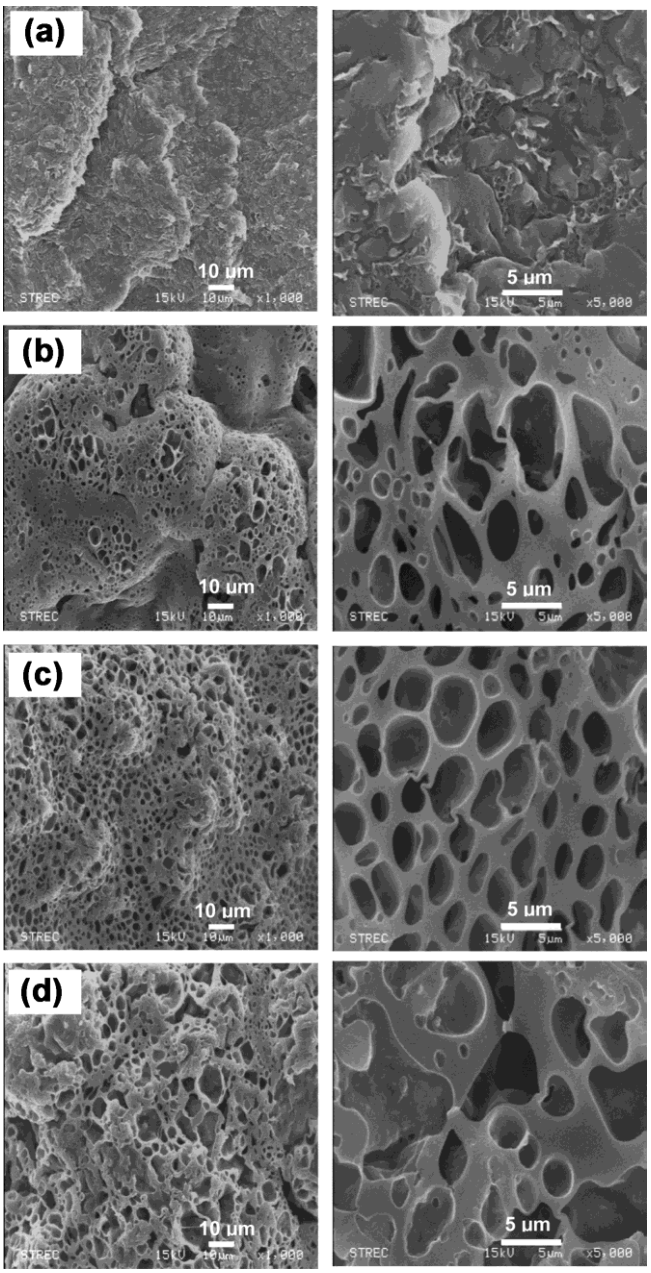

Figure 7.2 SEM micrographs of the vulcanized NR/ABS blends: (a) fractured surface of 60/40 NR/ABS blends without etching ABS phase; and (b)-(d) etched, fractured surfaces of 50/50, 60/40 and 70/30 NR/ABS blends, respectively. The left column is the micrographs at low magnification (x 1,000) and the right column is the micrographs at high magnification (x 5,000). (Conditions of the blends: NR compound with 15 phr HRJ-10518; mixing temperature of 180 °C)

Besides the difference in molecular weights of the two polymers, the immiscibility of the vulcanized NR/ABS blends could be caused by the difference in the solubility parameters of NR and ABS, i.e., $|\delta_1 - \delta_2 = 10.04 - 8.17 = 1.87$ ($cal^{1/2}/cm^{3/2}$)$|$ indicates that the blends are relatively immiscible. As a matter of fact, the molecular weight of NR is normally much higher than that of ABS; based on this important point, the extent of difference in solubility parameter to achieve a good miscibility of these two polymers must be very much smaller than 1.87 $cal^{1/2}/cm^{3/2}$. Therefore, a phase separation and a two-phase morphology of the blends undoubtedly resulted. Among the three blends, the finer ABS phases with smaller cavity sizes were observed for the vulcanized 60/40 NR/ABS blends. Smaller ABS particles provide higher surface areas to promote the dispersion between NR and ABS phases and therefore resulted in superior mixing properties. The non-uniformly vulcanized NR and ABS phases and some irregular structures were observed at a high proportion of NR (i.e., 70/30 NR/ABS), presumably due to the incompatibility and immiscibility between the two components of rubber and thermoplastic [71]. Also, increasing the rubber proportion in the vulcanized NR/ABS blends caused coalescence of the ABS domains dispersed in the NR matrix. Larger size of the dispersed ABS domains having lower surface areas provided poorer dispersion of cured NR and ABS phases resulting in lower mechanical strength. It can be seen that the morphology of vulcanized NR/ABS blends is related to the mechanical properties. Thus the morphological analysis indicates that the mechanical properties of vulcanized NR/ABS blends are mainly controlled by the phase morphology of the blend system.

7.4.2.3 Dynamic Properties

The storage modulus (G′) and loss modulus (G″) of the neat ABS, cured NR, and NR/ABS vulcanizates as a function of frequency are shown in Figure 7.3. The G′ increased with an increase of frequency. At a given frequency, the vulcanized NR gave the highest and nearly stable storage modulus while the neat ABS provided the lowest value and increased with increasing frequency. The vulcanized NR/ABS blends showed intermediate values of the storage modulus with a slight increase in

their values with increasing frequency. The high G′ of the NR vulcanizate is attributed to the formation of stably and chemically crosslinked macromolecular networks of high elasticity. It can be seen that G′of the blends increased with an increase in the vulcanized rubber component. This is attributed to a higher content of crosslinked polymers in the blended product. Therefore, the vulcanized 70/30 NR/ABS blends gave the highest G′. Furthermore, the G′ of the blends was higher than the G″ over the frequency range investigated, indicating that they were more elastic than viscous.

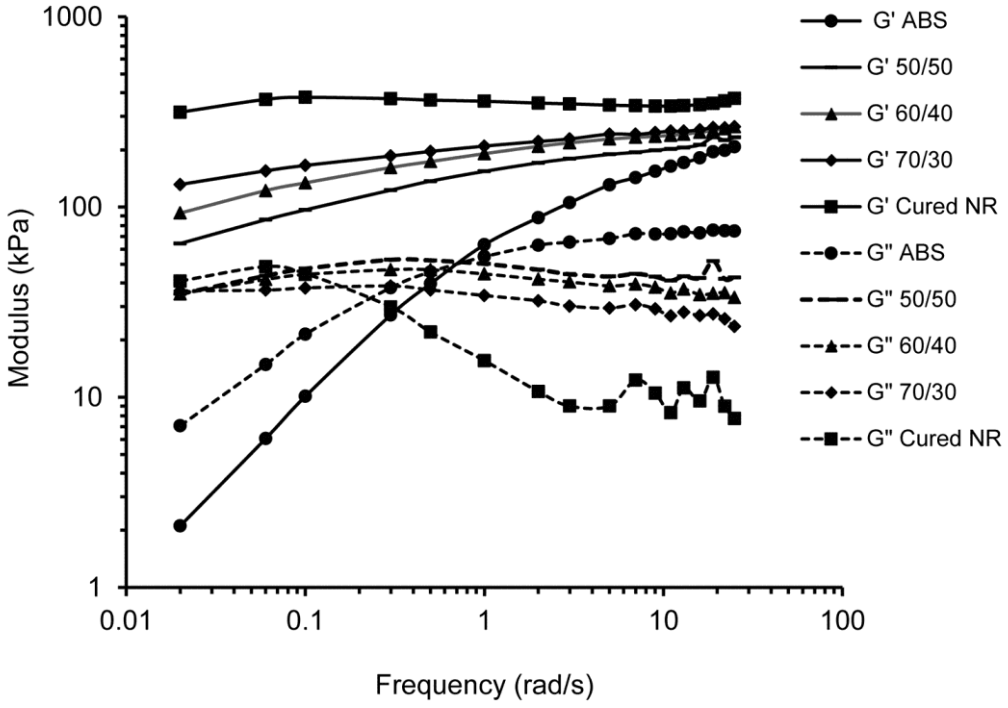

Figure 7.3 Storage modulus (G′) and loss modulus (G″) as a function of frequency of the neat ABS, cured NR, and vulcanized NR/ABS blends at various blend ratios. (Conditions of the blends: NR compound with 15 phr HRJ-10518; mixing temperature of 180 °C)

The relationship between tan δ and frequency is shown in Figure 7.4. Tan δ is a ratio of the loss modulus to storage modulus (i.e., tan δ = G″/G′). It can be seen that

the vulcanized NR showed the lowest tan δ whilst the highest value was found for neat ABS. The tan δ of the vulcanized NR/ABS blends for various blend ratios was lower than 1 and that of the neat ABS as well which had frequency dependence. A decrease in tan δ at high loadings of rubber was observed. This means that the blends exhibited a greater elastic response than that of the neat ABS, particularly for the blends with NR/ABS ratios of 60/40 and 70/30. In other words, the ABS behaved in a liquid-like manner under frequency sweep while those of vulcanized NR/ABS blends were solid-like materials.

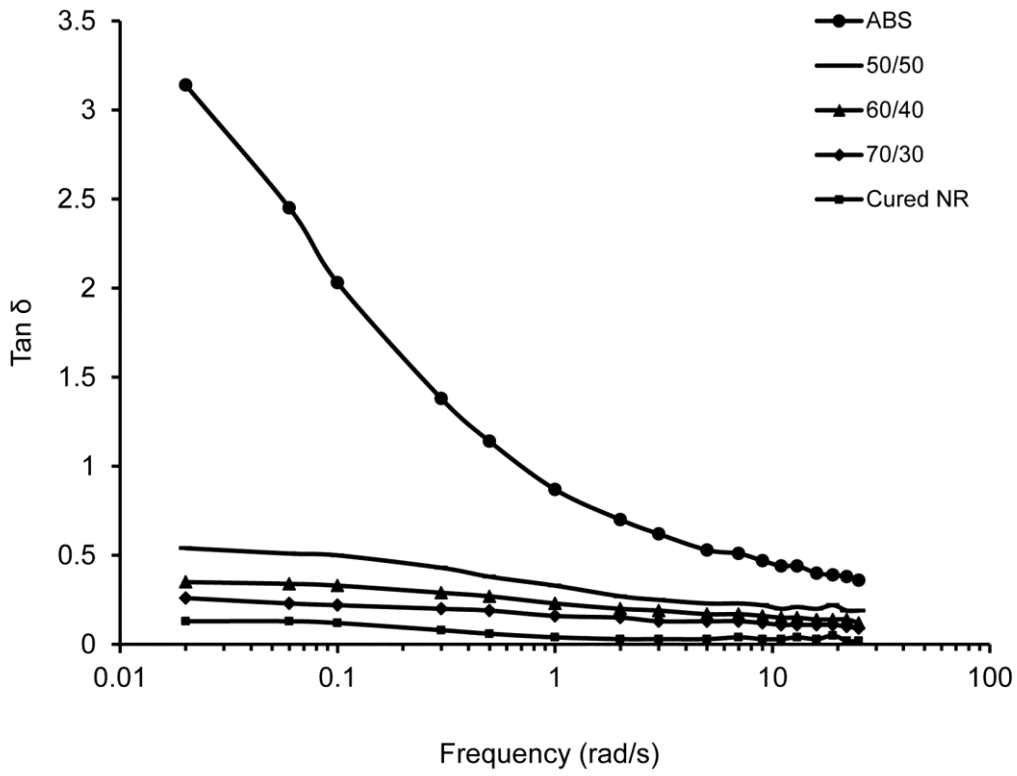

Figure 7.4 Tan δ as a function of frequency of the neat ABS, cured NR, and vulcanized NR/ABS blends at various blend ratios. (Conditions of the blends: NR compound with 15 phr HRJ-10518; mixing temperature of 180 °C)

The relationship between phase angle and frequency is shown in Figure 7.5. The phase angle is generally referred to as a shift between the deformation (G″) and response (G′) curves. The NR/ABS vulcanizates at all blend ratios showed lower phase angles (from a few degrees to about 30 degrees) indicating higher viscous materials while the phase angle of ABS was relatively high (about 80 degrees) at low frequency sweep and decreased with increasing frequency to a lower phase angle becoming a highly viscous material. This implies that the vulcanized NR/ABS blends are relatively stable and solid-like materials under the effect of frequency sweep.

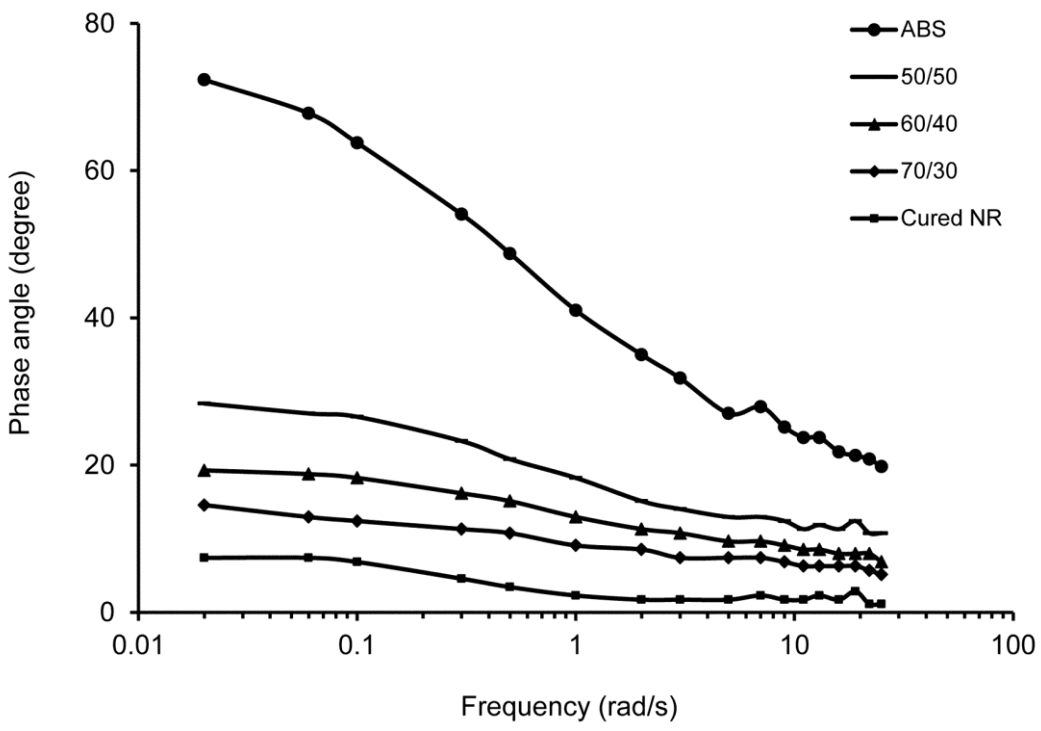

Figure 7.5 Phase angle as a function of frequency of the neat ABS, cured NR, and vulcanized NR/ABS blends at various blend ratios. (Conditions of the blends: NR compound with 15 phr HRJ-10518; mixing temperature of 180 °C)

The dynamic viscosity as a function of frequency sweep is presented in Figure 7.6. The viscosity decreased with increasing frequency sweeps, suggesting that the vulcanized NR/ABS blends and ABS exhibited shear-thinning behavior (i.e., pseudoplasticity). Similar behavior has been observed for the blending of maleated NR with PP [27]. At a given frequency, higher complex viscosity was observed for the NR/ABS vulcanizates prepared with a higher content of the rubber. Therefore, the vulcanized 70/30 NR/ABS blends showed the highest complex viscosity while the lowest value was observed at a blend ratio of 50/50 due to the content of ABS providing a lower complex viscosity.

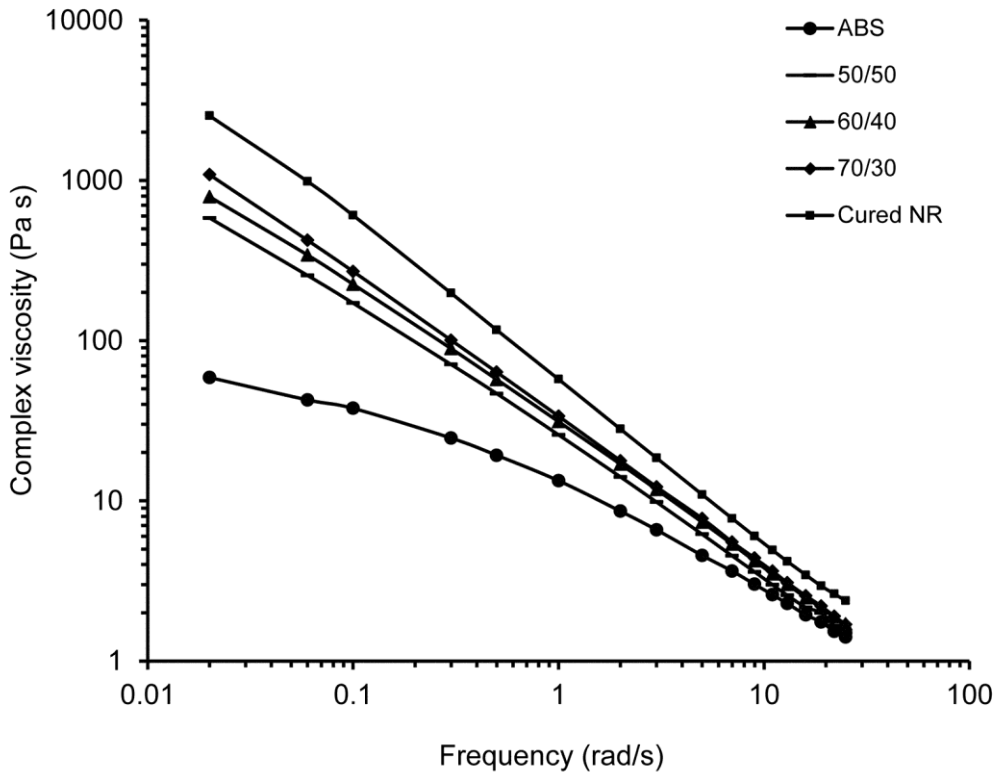

Figure 7.6 Complex viscosity as a function of frequency of the neat ABS, cured NR, and vulcanized NR/ABS blends at various blend ratios. (Conditions of the blends: NR compound with 15 phr HRJ-10518; mixing temperature of 180 °C)

It should be noted that both NR and ABS are viscoelastic materials differing in the magnitude of viscous and elastic responses. Based on the results obtained, the rheological characteristics of vulcanized NR/ABS blends (i.e., modulus, phase angle, tan δ, and complex viscosity) showed the intermediate values between the neat NR and ABS. The blending of ABS with NR provided lower tan δ and phase angle but the complex viscosity was higher than that of neat ABS. This demonstrates that rheological properties of vulcanized NR/ABS blends are contributed to the blend component.

7.4.2.4 Thermal Properties

TGA curves for ABS, NR, and NR/ABS vulcanizates prepared using an NR compound with 15 phr HRJ-10518 are shown in Figure 7.7 and the thermal properties are summarized in Table 7.4. The decomposition temperature was obtained from the peak maxima of the derivative of the TGA curves. It can be seen that a single decomposition temperature of the neat NR and ABS were observed at 386 °C and 441 °C, respectively. That is, the thermal stability of the thermoplastic is better than that of the natural rubber. The vulcanized NR moiety does not melt but it decomposes before melting under heat. The decomposition temperature of the vulcanized NR/ABS blends increased with increasing content of ABS. That is, the thermoplastic component accounts for the thermal stability of the NR/ABS vulcanizates. The improved thermal stability could be explained by a protective effect, that is, the rubber phase can be protected under thermal conditions by the thermoplastic phase. Concerning the remaining residues, it can be seen that neat NR and ABS were almost degraded at 600 °C, i.e., only approximately 0.7 – 0.8 wt% residues were left. At this temperature, the char residues of vulcanized NR/ABS blends were 10.8 – 11.9 wt%, which were higher than that of the neat NR and ABS. The small amount of char residue remained above 600 °C of NR is attributed to the insoluble and intractable materials which were linked to the cyclized rubber while the residue of ABS could be the ash of partially crosslinked polybutadiene. On the other hand, the higher char residues of the three blends might correspond to the degradation of the carbonaceous residue of stable crosslinked rubber in the blends. It was found that there is little

difference in char residue at 600 °C of the vulcanized NR/ABS blends at the three blend ratios. However, the amount of char residue of the three blends was higher than that of the neat NR, suggesting that the thermal properties of the NR/ABS vulcanizates were better.

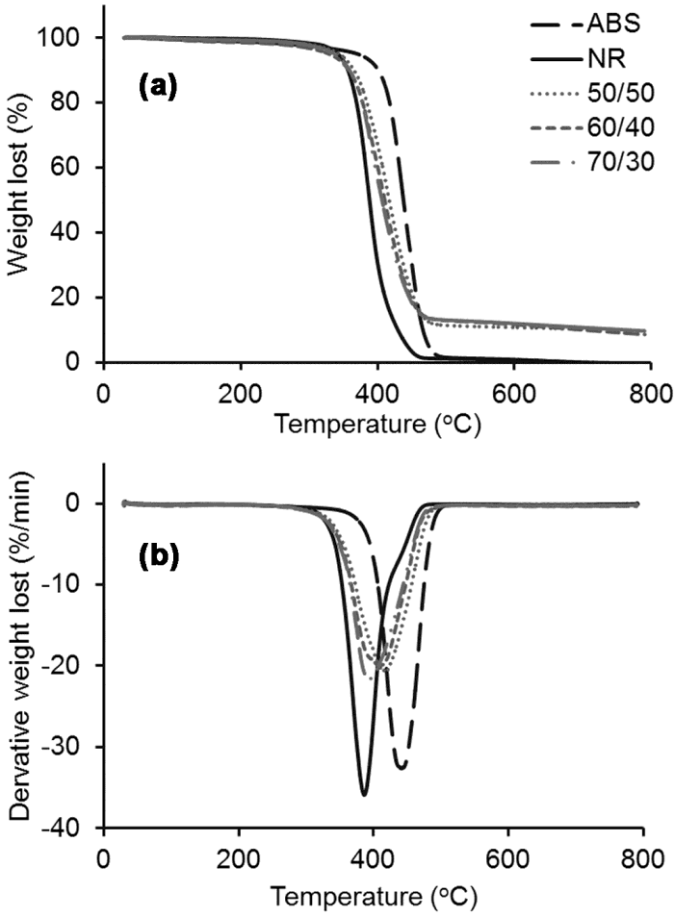

Figure 7.7 TGA curves for the neat ABS, cured NR, and vulcanized NR/ABS blends at various blend ratios: (a) weight loss versus temperature; (b) derivative weight loss versus temperature. (Conditions of the blends: NR compound with 15 phr HRJ-10518; mixing temperature of 180 °C)

Table 7.4 TGA data of the neat ABS, NR, and NR/ABS vulcanizates.

Sample	Decomposition temperature (°C)	Char residue at 600 °C (wt%)
NR	386.1	0.7
ABS	440.6	0.8
NR/ABS vulcanizates[a]		
50/50	418.2	10.8
60/40	411.0	11.7
70/30	391.2	11.9

[a] Conditions of the blends: NR compound with 15 phr HRJ-10518; mixing temperature of 180 °C.

7.4.3 Effect of Phenolic Curative Content on Mechanical and Morphological Properties of Vulcanized NR/ABS Blends

7.4.3.1 Mechanical Properties

The effect of phenolic curative content over the range of 10-20 phr HRJ-10518 on the mechanical properties of the NR/ABS vulcanizates at three ratios of 50/50, 60/40, and 70/30 is shown in Figure 7.8. At a given blend proportion, the tensile strength and elongation at break of the blends increased with an increase in the concentration of phenolic resin up to 15 phr and thereafter decreased. This is attributed to the influence of vulcanization via the phenolic curative molecules which thereafter resulted in stronger materials. At a given phenolic resin concentration, the hardness of the blends decreased with an increase in the NR ratio of the blends. This is due to an increase in NR portion as the soft phase of the blends. However, at a given blend proportion, there is little difference in the hardness between these materials, indicating that the loading level of the phenolic curative did not play a significant role on the magnitude of the hardness.

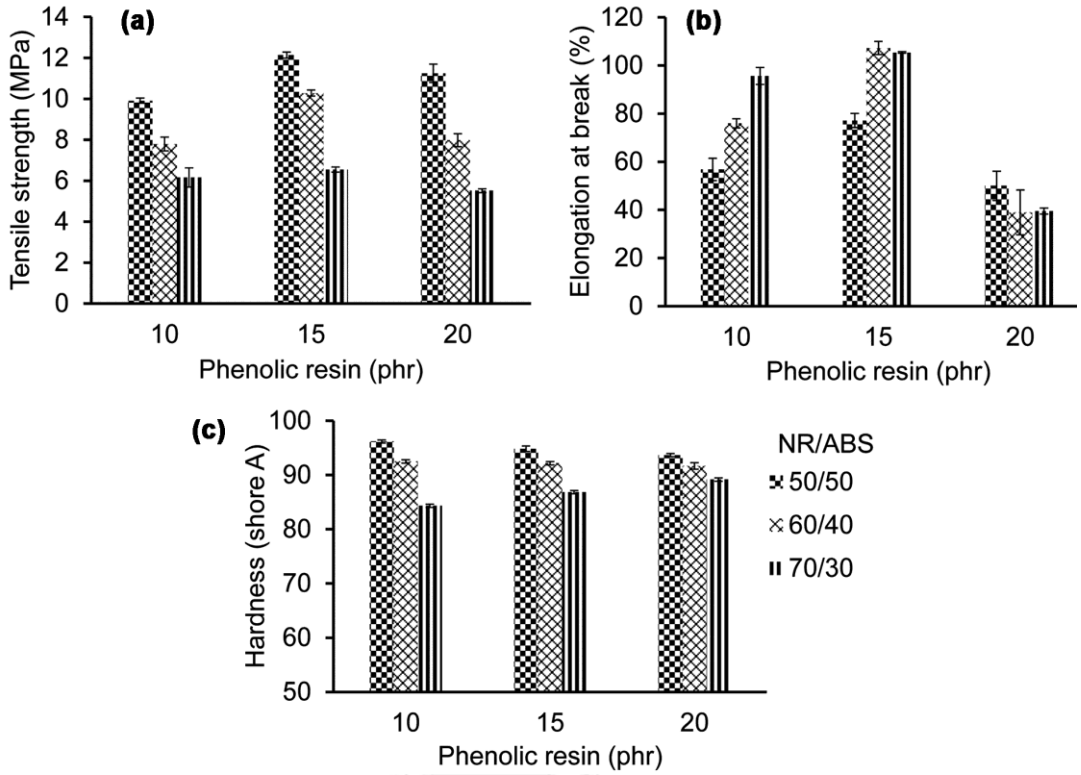

Figure 7.8 Effect of phenolic curative content on mechanical properties of vulcanized NR/ABS blends at three ratios of 50/50, 60/40, and 70/30: (a) tensile strength; (b) elongation at break; and (c) hardness. (Conditions of vulcanized NR/ABS blends: NR compound with 10, 15, and 20 phr HRJ-10518; mixing temperature of 180 °C).

In order to achieve a better understanding of the chemical reaction involved with vulcanization of the NR/ABS blends using various concentrations of phenolic resin, it is essential to know the vulcanization characteristics of the pure NR compounds without any ABS. Curing curves of vulcanization of NR with various amounts of phenolic resin is shown in Figure 7.9 and the results are summarized in Table 7.5. The M_H and M_L are the minimum and maximum torques, respectively. The M_L is a measure of the stiffness of the non-vulcanized rubber by taking the lowest

point of the curing curve while the M_H is a measure of the stiffness of the fully vulcanized NR at the vulcanizing temperature. It was found that the M_H increased with increasing loadings of the phenolic resin. The delta torque (M_H-M_L) correlates with the crosslinking efficiency of the curing agent. An increase in M_H-M_L with increasing levels of the phenolic curative was observed. Therefore, the NR compound with 20 phr HRJ-10518 gave the highest value of M_H and M_H-M_L. This indicated that the crosslink density was more pronounced at high concentrations of the curing agent. This could be explained by the vulcanization reaction in that the crosslinking reaction occurs through the reactive functional groups of phenolic resin (i.e., methylol and hydroxyl groups) with the unsaturation in the NR molecules to form the Chroman ring structure [61] as shown in Figure 7.10.

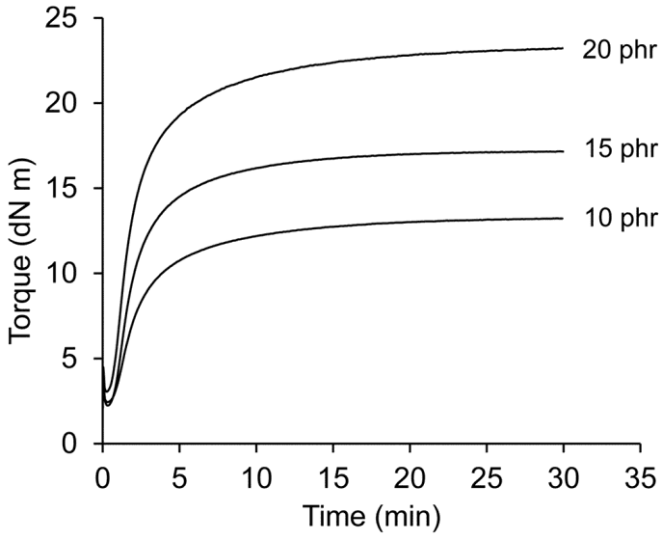

Figure 7.9 Curing curves of vulcanization of NR with various amounts of phenolic resin of 10, 15, and 20 phr HRJ-10518 at the curing temperature of 180 °C.

Table 7.5 Curing characteristics of NR vulcanizates at three concentrations of phenolic curing agent.

Phenolic resin (phr)	M_L (dN m)	M_H (dN m)	$M_H - M_L$ (dN m)	T_{s1} (min)	T_{c90} (min)	CRI (1/min)
10	2.45	13.23	10.78	0.57	9.45	11.26
15	2.25	17.16	14.91	0.49	7.42	14.43
20	3.10	23.22	20.12	0.40	8.55	12.27

M_L = minimum torque; M_H = maximum torque; T_{s1} = scorch time; T_{c90} = optimum cure time; and CRI = cure rate index.

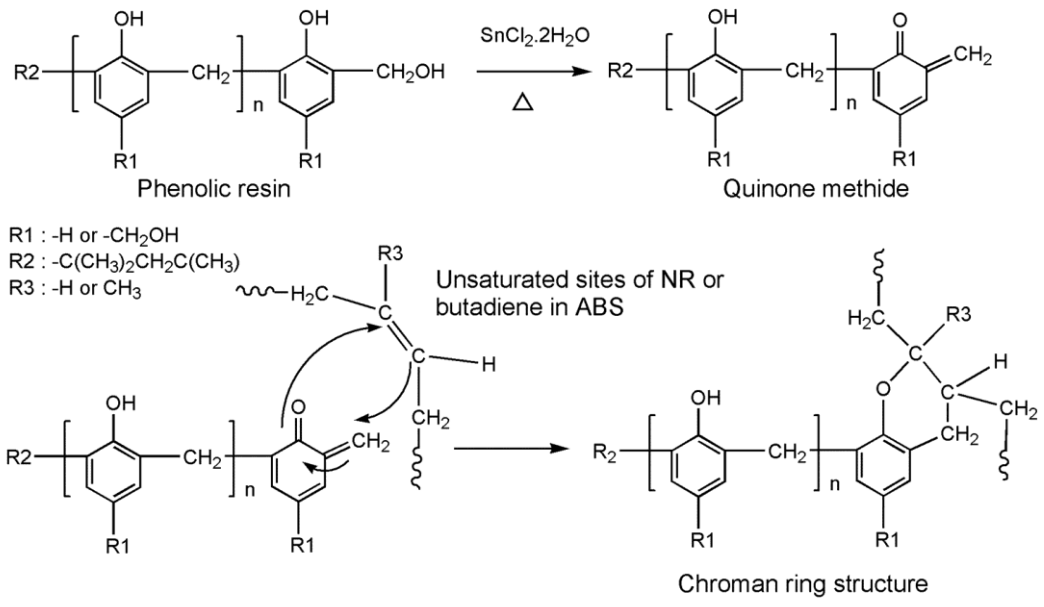

Figure 7.10 Schematic representation of the proposed crosslinking reaction of natural rubber or butadiene in ABS using a phenolic resin in the presence of stannous chloride [61].

During curing at a high temperature of 180 °C, quinone methides have been proposed as key intermediates. Then the Chroman ring structure can be formed by the interaction of the quinone methide and double bonds in the rubber molecules. It clearly indicated that increasing the phenolic concentration allowed more methylol and hydroxyl groups to be available for the reaction, which basically leads to a higher extent of crosslinking sites in the NR phase. A decrease in scorch time (T_{s1}) with increasing cure loadings was also caused by similar reasons. These results are in a good agreement with the data previously reported in the literature [64, 102]. It was found that the M_H-M_L of maleated ethylene propylene rubber (m-EPM) at different concentrations of dicumyl peroxide (i.e., 0 – 3 phr) as a curing agent was directly proportional to the crosslink density [102]. The cure rate index (CRI) is basically a measure of the rate of vulcanization. Among various phenolic curative contents, the amount of 15 phr gave a short scorch time and cure time, that is, the highest CRI was obtained.

As seen in Figure 7.8, the improved tensile strength and elongation at break of vulcanized NR/ABS blends at higher levels of the phenolic curative (i.e., 15 phr HRJ-10518) for a given blend ratio are consistent with the delta torque ($M_H - M_L$) of NR vulcanizates. Higher $M_H - M_L$ generated by a crosslinking reaction through the reactive functional groups of the phenolic resin with the double bonds presented in the NR chains, as previously discussed, contributes to the improvement of the mechanical properties of the blends. Similar behavior has been observed for vulcanized NR/HDPE [64] and m-EPM/PP [102] blends. It was found that the increased crosslink density at higher cure loadings caused improved tensile strength and elongation at break of the blends. However, in the present work, when the concentration of phenolic resin was greater than 15 phr, decreases in mechanical properties of the blends were obtained. At a very high loading of the curing agent (20 phr HRJ-10518), a high curing reaction occurs. In addition, phenolic resins can also self-condense with heat (180 °C) to form a crosslinked phenolic network by a polycondenzation reaction as shown in Figure 7.11. In these crosslinked phenolic polymers, the clusters linked by methylene and dimethylene ether bridges; result in a hard substance embedded in the blended product which caused the vulcanized NR/ABS products to become a brittle

material (i.e., low elasticity). As a result, the lowest elongation at break of the blends at three NR/ABS ratios of 50/50, 60/40, and 70/30 was observed when using NR compound with 20 phr HRJ-10518. Thus compounding NR with 15 phr HRJ-10518 was appropriate for blending with ABS.

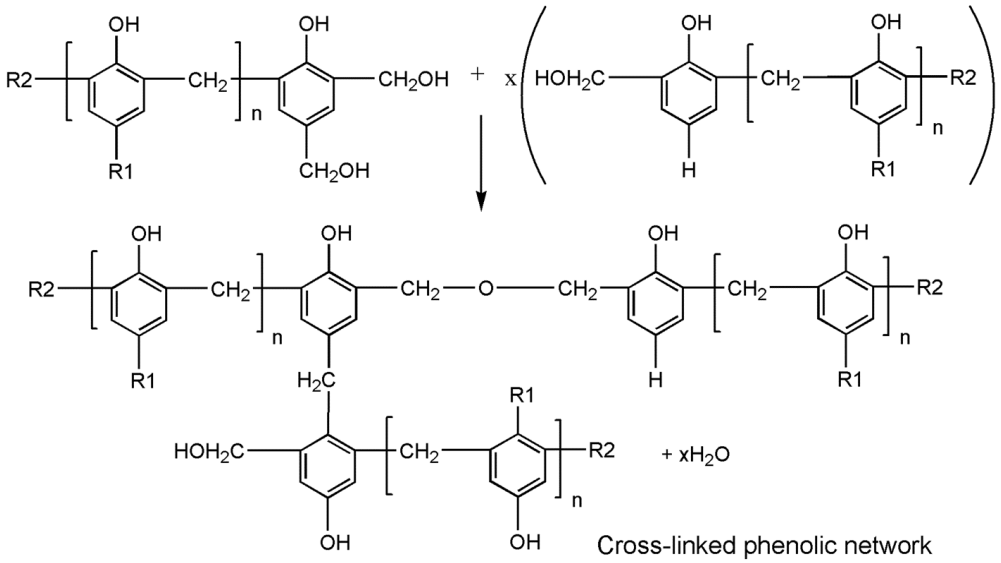

Figure 7.11 Schematic representation of the proposed polycondenzation reaction of phenolic resin to form a crosslinked phenolic network.

It is inevitably seen that the mechanical properties of vulcanized NR/ABS blends were influenced by the phenolic curative content. It should be noted that the ABS in this study consists of three components of acrylonitrile, butadiene, and styrene with a weight ratio of 24:19:57. During the vulcanization process, the reactive functional groups of the phenolic curing agent can also interact with the remaining double bonds of 2,3-polybutadiene in the virgin ABS (Figure 7.10). However, for a given blend proportion, the number of unsaturated sites in ABS are much smaller than that within the NR. For example, the 70/30 NR/ABS blend system is composed of 70 wt% NR and 5.7 wt% butadiene. Thus the possibility of chemical interaction between

the functional groups of HRJ-10518 and the double bonds of polybutadiene in ABS is less than that in NR, suggesting that the vulcanization reaction occurs mainly in the NR phase. Therefore, it can be concluded that the mechanical properties of the blends were influenced by the phenolic resin through crosslinking reactions not only by the chemical interactions of the methylol and hydroxyl groups of the phenolic resin with the double bonds in the NR (major) but also with the remaining double bonds of polybutadiene in the ABS (minor), and they accounted for the elongation of the vulcanized NR/ABS blends.

It should be noted that the reasons for using a phenolic cure system to crosslink the rubber phase of the NR/ABS blends was not only to obtain superior mechanical properties of the blends but also to overcome the unpleasant smell of the finished products and thermoplastic degradation (i.e., by sulfur and peroxide cure systems). The results are consistent with those previously reported [63]. It was found that vulcanized ENR/PP blends using a phenolic cure system exhibited higher mechanical and dynamic properties than those of the blends obtained by sulfur, peroxide, and mixed sulfur-peroxide cure systems. The phenolic cure system provided smaller vulcanized rubber domains dispersed in the PP matrix and the absence of PP degradation and therefore provided superior properties of the blends.

7.4.3.2 Morphological Properties

The effect of the phenolic curative content on the morphological properties of the vulcanized NR/ABS blends was investigated as showed in Figure 7.12. A NR/ABS blend ratio of 60/40 was selected to investigate the effect of phenolic curative at different contents of 10, 15, 20 phr HRJ-10518. SEM micrographs of the etched, fractured surfaces of the vulcanized 60/40 NR/ABS blends at various phenolic curative contents showed a two-phase morphology system. Among the three conditions, large numbers of small and uniformly distributed ABS phases were observed for the blends with 15 phr HRJ-10518. The non-uniformly vulcanized NR and ABS phases with some irregular structures were observed for the blends with 10 and 20 phr HRJ-10518. These morphologies of the blends are consistent with the

mechanical properties of the NR/ABS vulcanizates, in that the blends with 15 phr HRJ-10518 exhibited higher tensile strength and elongation at break than those of the blends with 10 and 20 phr (Figure 7.8). This change in mechanical properties of the blends is a result of the morphology changes [64, 67].

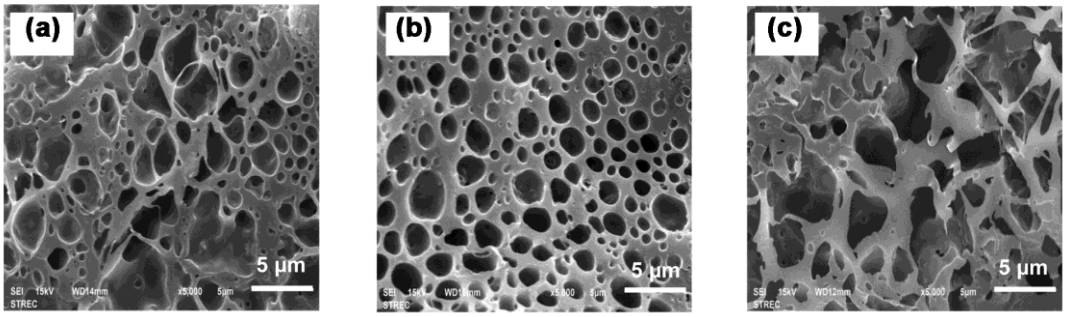

Figure 7.12 SEM micrographs of the etched, fractured surfaces of vulcanized 60/40 NR/ABS blends at various amounts of phenolic resin: (a) 10 phr HRJ-10518; (b) 15 phr HRJ-10518: and (c) 20 phr HRJ-10518. (Conditions of the blends: NR compound with 10, 15, and 20 phr HRJ-10518; mixing temperature of 180 °C)

The well-balanced mechanical properties of vulcanized NR/ABS blends with 15 phr HRJ-10518 were attributed to the uniformly crosslinked rubber and ABS phases which gave better dispersion between the two phases of the blends and thus provided superior mixing properties. On the other hand, it can be seen that the coalescence of the ABS domains dispersed in the NR matrix was observed when using NR compound with a high phenolic curative content (20 phr HRJ-10518) as shown in Figure 7.12 (c).The broad size distribution of ABS particles was obtained. As described earlier, larger dispersed ABS domains with lower interfacial areas give poorer dispersion of cured NR and ABS phases and resulted in lower mechanical strength. The non-uniformly vulcanized NR and ABS phases might be caused by different rates of the vulcanization reaction. An increase in the amount of the phenolic

curative in the rubber compound caused increasing torque of the curing curves (See Figure 7.9). Thus the viscosity of the rubber compound during vulcanization with ABS was also increased. Inevitably, under these conditions, the coalescence of the ABS particles were formed, resulting in poorer mechanical properties of the vulcanized 60/40 NR/ABS blends with 20 phr HRJ-10518. SEM analysis supports that the mechanical and morphological properties of vulcanized NR/ABS blends were influenced by the phenolic curative content.

Based on Figure 7.6 and comparing the complex viscosity between ABS and the blends containing the cured NR, ABS with the overall lower viscosity could elongate its molecules to give small droplets and dispersed in the higher viscosity cured NR at each blend proportion, as shown in Figure 7.13.

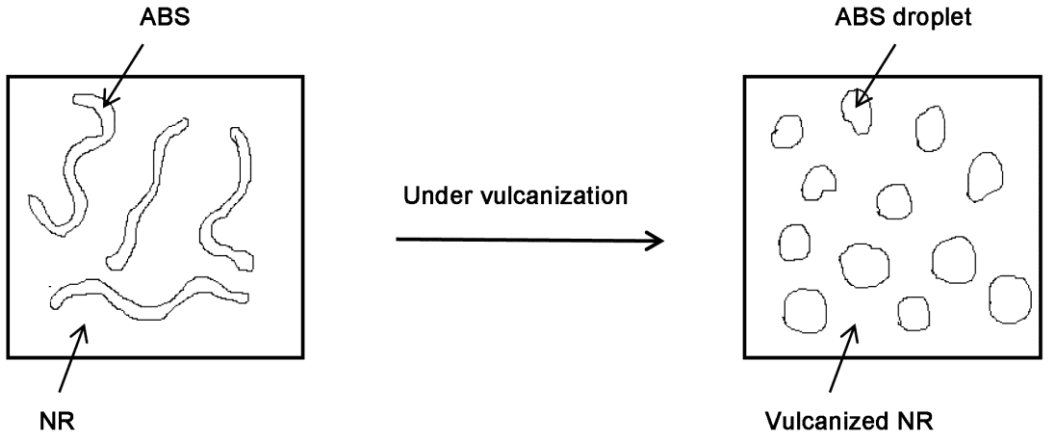

Figure 7.13 The morphology development of vulcanization of NR/ABS blends during melt blending process (ABS chains were dispersed in NR and became the dispersed domain and cured NR was the matrix).

7.4.4 Effect of Graft Copolymers on Mechanical and Morphological Properties of Vulcanized NR/ABS Blends

The graft copolymers of DPNR-*g*-MA and DPNR-*g*-(MA-*co*-ST) with grafting contents of 23.5 and 34.2%, respectively, were used as compatibilizers for the immiscible NR/ABS blends. The experiment was carried out with a fixed NR/ABS blend ratio of 60/40 using NR compound with 15 phr HRJ-10518. Various amounts of graft copolymer of 4, 8, 12, and 16 wt% of NR were used. The effects of graft copolymers on mechanical and morphological properties of vulcanized NR/ABS blends were investigated. The mechanical properties in terms of tensile strength, elongation at break, hardness, and impact strength of 60/40 NR/ABS vulcanizates with various amounts of the graft copolymer are shown in Table 7.6. At a given amount of graft copolymer, the vulcanized NR/ABS blends with graft copolymer of DPNR-*g*-(MA-*co*-ST) gave the best mechanical properties (i.e., tensile strength, elongation at break, and impact strength) than that of the blends with DPNR-*g*-MA. This is due to that DPNR-*g*-(MA-*co*-ST) has a high grafting efficiency and contains more reactive functional groups (i.e., grafted MA and ST molecules), providing more chemical interactions of the functional groups in the grafted segments with the polar functional groups in the ABS molecules. That is, the interfacial adhesion between the different phases of the blends is enhanced and therefore the mechanical properties of the blends with DPNR-*g*-(MA-*co*-ST) were better.

The proposed chemical interactions of graft copolymers of DPNR-*g*-MA or DPNR-*g*-(MA-*co*-ST) with NR and ABS are shown in Figure 7.14. During the mixing process, the DPNR-*g*-MA or DPNR-*g*-(MA-*co*-ST) molecules were forced to locate at the interface of NR and ABS. The nonpolar DPNR segments in the DPNR-*g*-MA or DPNR-*g*-(MA-*co*-ST) molecules are wetted by the NR component, while the polar functional groups of the graft copolymer could only interact with the polar functional groups in ABS molecules. The chemical interactions of hydrogen bonding of carboxylic groups (–COOH) of the grafted MA with nitrile groups (–CN) of ABS and the dipole–dipole force of carbonyl groups (–CO) of grafted MA with –CN groups of ABS molecules could occur.

Table 7.6 Mechanical properties of 60/40 NR/ABS vulcanizates with various amounts of graft copolymer.

Graft copolymer amount (wt%)[a]	Tensile strength (MPa)	Elongation at break (%)	Hardness (Shore A)	Impact strength (J/m)
0[b]	10.3 ± 0.2	107.3 ± 2.7	92.2 ± 0.3	313.8 ± 6.7
DPNR-*g*-MA[c]				
4	8.6 ± 0.4	91.2 ± 3.5	92.0 ± 0.5	306.1 ± 2.7
8	9.9 ± 0.8	101.4 ± 4.7	91.3 ± 0.3	310.6 ± 5.1
12	9.4 ± 0.5	89.4 ± 2.4	90.1 ± 0.5	295.1 ± 3.4
16	8.3 ± 0.2	58.1 ± 1.8	88.3 ± 0.3	289.5 ± 1.9
DPNR-*g*-(MA-*co*-ST)[c]				
4	10.2 ± 0.2	98.6 ± 2.2	92.2 ± 0.5	308.3 ± 2.4
8	10.5 ± 0.7	110.0 ± 2.8	92.8 ± 0.3	319.2 ± 1.1
12	9.7 ± 0.2	100.0 ± 1.5	90.2 ± 0.6	315.7 ± 1.2
16	8.6 ± 0.6	89.7 ± 3.1	89.3 ± 0.3	305.2 ± 0.8

[a] Percent by weight of NR.

[b] Vulcanized NR/ABS blends without graft copolymer using NR compound with 15 phr HRJ-10518.

[c] Vulcanized NR/ABS blends with various amounts of graft copolymer using NR compound with 15 phr HRJ-10518. The mixing temperature is 180 °C.

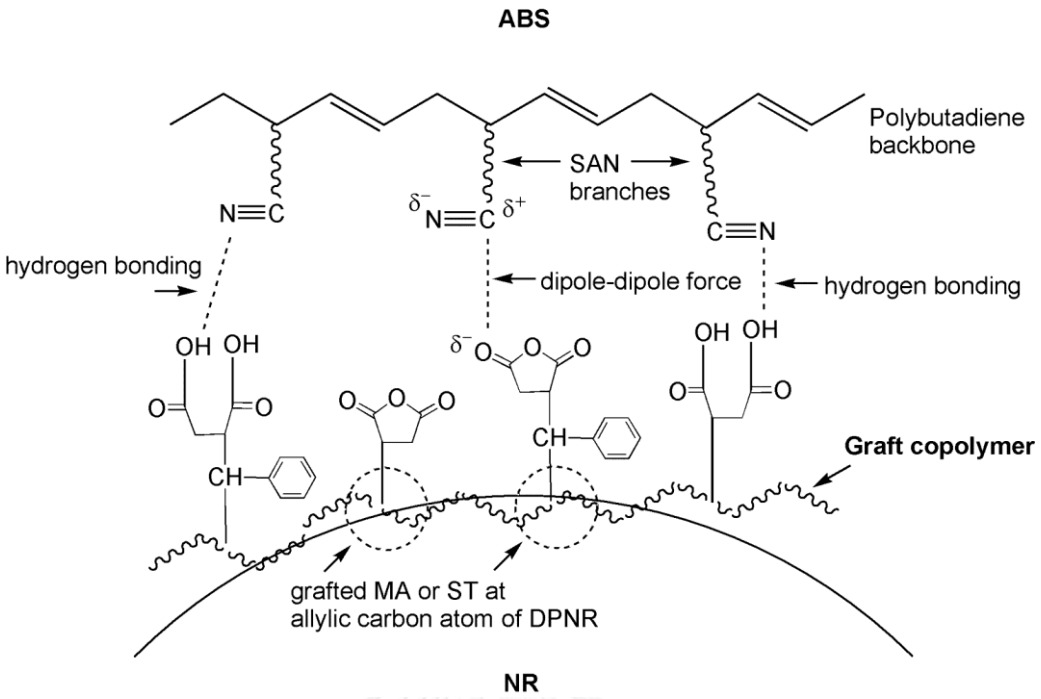

Figure 7.14 The proposed chemical interactions of graft copolymers of DPNR-*g*-MA or DPNR-*g*-(MA-*co*-ST) with NR and ABS during melt blending process.

As seen in Table 7.6, the hardness of the blends slightly decreased with an increase in the graft copolymer amount. This is due to an increase in the graft copolymer portion as the soft phase of the blends.

It is expected that an introduction of graft copolymers of DPNR-*g*-MA or DPNR-*g*-(MA-*co*-ST) should enhance the compatibility of the NR/ABS blends and therefore improve the mechanical properties. Unfortunately, it shows somewhat poorer mechanical properties for higher graft copolymers. That is, it can be seen that the vulcanized NR/ABS blends with the graft copolymer gave similar (i.e., blends with a graft copolymer = 8 wt%) or poorer mechanical properties (i.e., blends with graft copolymer > 8 wt%) compared to the blends without the graft copolymer. These results imply that these graft copolymers may not be fully compatible with NR and ABS, which was confirmed by SEM analysis as shown in Figure 7.15.

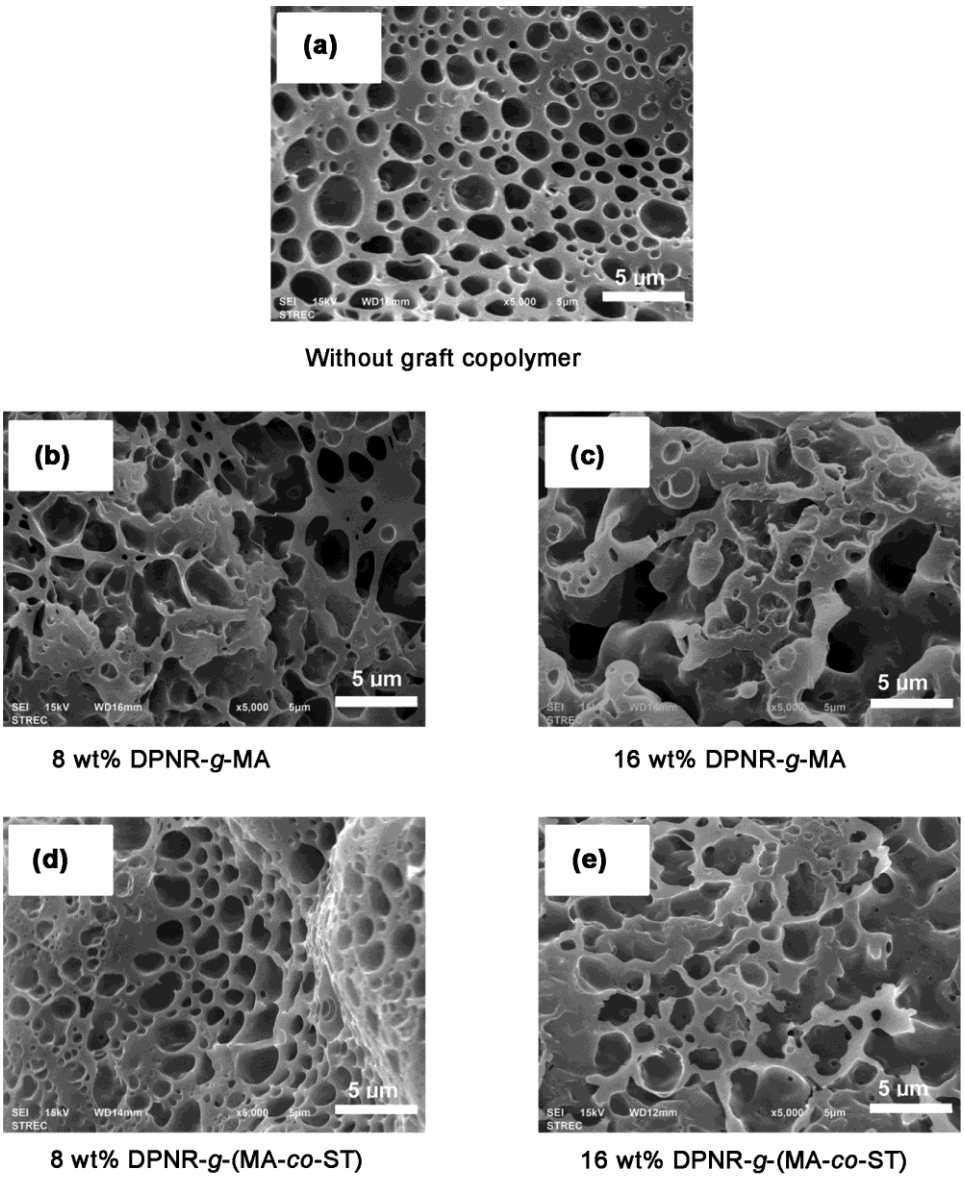

Figure 7.15 SEM micrographs of the etched, fractured surfaces of vulcanized 60/40 NR/ABS blends at various amounts of graft copolymer: (a) without graft copolymer; (b) 8 wt% DPNR-*g*-MA; (c) 16 wt% DPNR-*g*-MA; (d) 8 wt% DPNR-*g*-(MA-*co*-ST); and (e) 16 wt% DPNR-*g*-(MA-*co*-ST). (Conditions of the blends: NR compound with 15 phr HRJ-10518 and mixing temperature of 180 °C)

These lower mechanical properties of the blends with the graft copolymer are correlated with the morphology of the blends. It is seen that non-uniformly vulcanized NR and ABS phases were obtained for the blends with the graft copolymer, especially at high amounts of the graft copolymer (16 wt%). Under these conditions, the broad size distribution of ABS particles was observed. This might be due to the coalescence of the ABS particles in the blends.

The reasons for the poorer mechanical properties of the blends with these graft copolymers might be explained as follows. Firstly, based on the chemical interaction of DPNR-*g*-MA or DPNR-*g*-(MA-*co*-ST) with NR and ABS as proposed in Figure 7.14, the mechanical properties should improve. However, it did not improve which might be attributed to the removal of proteins from the NR latex. In fact, the green strength of NR is attributed to the presence of non-rubber components in the latex, such as lipids and proteins. It has been reported that the tensile strength and green strength of NR were reduced after deproteinization [44, 103-105]. Thus this might be a reason for the poorer mechanical properties of the NR/ABS blends with these graft copolymers. However, in the literature, it has been reported that graft copolymers of NR-*g*-MA, NR-*g*-PMMA, and NR-*g*-PDMMMP are effective compatibilizers for immiscible blends [16, 23, 24]. These mentioned graft copolymers enhance interfacial adhesion between the different phases of the blends and therefore improve the mechanical properties of the blends. Secondly, a decrease in mechanical properties of vulcanized NR/ABS blends with higher amounts of graft copolymer than 8 wt% may be attributed to the formation of micelles of the graft copolymer in the blends and that these small droplets of micelles can act as a lubricant in the blended products during the mixing process. This phenomenon has also been observed for vulcanized NR/EVA blends with a high amount of graft copolymer as compatibilizer [16]. Third, the ABS having a high portion of polystyrene of 57 wt% (acrylonitrile: butadiene: styrene weight ratio = 24:19:57) is very rigid in nature. Therefore, the ABS blended NR with these graft copolymers can hardly exhibit good tensile strength due to the characteristics of the constituent (ABS) of the blend systems. The results so obtained imply that these graft copolymers of DPNR-*g*-MA and DPNR-*g*-(MA-*co*-ST) might

not be suited for the blending of NR and ABS. Recommendations for a suitable application of these graft copolymers are given in Chapter VIII.

7.5 Conclusions

Vulcanization of NR/ABS blends using a phenolic curing agent was successfully carried out by a melt mixing process. The effects of blend proportions, phenolic curative content, and graft copolymers of DPNR-*g*-MA and DPNR-*g*-(MA-*co*-ST) on mechanical, morphological and other related properties of vulcanized NR/ABS blends were investigated. It was found that the mechanical, dynamic, thermal and morphological properties of the blends were influenced by the blend proportions. The curing characteristics of NR vulcanizates, the mechanical and morphological properties of the blends were also influenced by the phenolic curative content. The elongation at break of vulcanized NR/ABS blends increased with an increase in NR content while the tensile strength and hardness decreased, indicating that strength and hardness properties of the blends were attributed by the thermoplastic component and the vulcanized NR is an essential component for improving elongation of the blends. The storage modulus of the blends increased with increasing rubber content. This is due to a higher content of crosslinked rubbers in the blended product. These blends showed a greater elastic response than that of neat ABS. The thermal stability of the blends increased with increasing ABS content. SEM micrographs of vulcanized NR/ABS blends showed a two-phase morphology system. The morphology of the blends was influenced by phenolic curative content and NR/ABS ratio. The vulcanized 60/40 NR/ABS blends using NR compound with 15 phr of phenolic curative showed finer ABS particles dispersed in the NR phase which gave better dispersion between the two different phases of the blends and thus provided superior mixing properties. The results showed that the vulcanized NR/ABS blends with the graft copolymers of DPNR-*g*-MA or DPNR-*g*-(MA-*co*-ST) gave similar (i.e., blends with graft copolymer = 8 wt%) or poorer mechanical properties (i.e., blends with graft copolymer > 8 wt%) compared to the blends without the graft copolymer. The results imply that these graft copolymers may not be fully compatible

with NR and ABS which is confirmed by SEM analysis. The addition of graft copolymer as blend compatibilizer caused changes of morphology of the blends to give non-uniformly vulcanized NR and ABS phases which affected the mechanical properties of the blends, implying that these graft copolymers might not be suitable for the vulcanized NR/ABS blends.

CHAPTER VIII: SUMMARY AND RECOMMENDATIONS

8.1 Summary

An extremely low protein containing NR (0.0787 wt%), DPNR, was obtained by urea treatment under the conditions of 0.2 wt% urea and 1.0 wt% SDS at 30 °C for 60 min. The nitrogen content of the treated NR significantly decreased after the deproteinization which confirmed that proteins were removed. This demonstrates that most proteins in NR latex are attached on the surface of the rubber particles with weak attractive force interactions and they can be disturbed or changed in their conformation by urea and then all the proteins were removed by centrifugation. After removing the proteins, no gel content was found in the DPNR, indicating that the formation of gel or a branched network in NR may be attributed to non-rubber components present in NR latex such as proteins. The DPNR latex was later used as a preferred substrate for MA grafting.

The grafting of MA onto DPNR with high G.E and low gel content in the grafts was obtained using a DMP technique. The G.E and gel content were influenced by initiator and monomer amount, reaction temperature, and reaction time. A high grafting efficiency of more than 90% and a 21% of grafted MA onto DPNR can be achieved at a grafting condition of 7 wt% BPO, 9 wt% MA, and feeding rate of MA of 0.2 ml/min at 80 °C for 8 h. A low gel content of about 6 wt% was obtained at a low grafting temperature of 60 °C. The removal of proteins from the NR latex showed different characteristics for the grafting behavior of MA onto NR and DPNR substrates. Grafting onto DPNR provided higher G.E and lower gel content compared to grafting onto NR, indicating that DPNR is a preferred substrate for MA grafting. The graft copolymers obtained by the DMP method provided much better results with respect to the G.E and the grafted MA content compared to conventional emulsion polymerization, indicating that the DMP is an effective method for synthesizing graft copolymers of natural rubber.

To increase the efficiency of MA grafting onto DPNR, styrene as a comonomer was used. The introduction of styrene to the grafting system improved both the grafting efficiency and grafting content. An appropriate condition was 7 wt% BPO, 9 wt% MA, ST/MA mole ratio of 4:1, and MA addition rate of 0.6 ml/min at 60 °C for 4 h. The grafting content of the graft copolymer synthesized with a ST/MA ratio of 4:1 was 34.2 %, which was higher than that of a graft copolymer synthesized without the presence of the styrene comonomer (23.5 %). This improvement in grafting efficiency and grafting content of the styrene-assisted grafting reaction was attributed to the formation a charge transfer complex (CTC) for graft copolymerization. It was proposed that, with a ST/MA ratio of 1:1, it is expected that all the ST and MA monomers can form CTC, and therefore MA was grafted onto DPNR mainly in the form of the CTC. When the concentration of styrene was high, ST not only can form the CTC with MA but also reacts with rubber macroradicals to produce styryl macroradicals, which can later react with MA or CTC to produce the graft copolymer. Therefore, the grafting efficiency increased with an increase in the ST/MA ratio. The results obtained indicate that styrene is an effective comonomer for promoting the grafting of MA onto DPNR.

Grafting kinetics of MA onto DPNR in the presence and absence of the styrene comonomer were investigated. The monomer conversion and graft copolymerization rate of the grafting reaction with styrene at various ST/MA ratios were higher than that of grafting reaction without styrene. This demonstrates that the styrene comonomer plays an important role in conversion and the polymerization kinetics of MA grafting onto DPNR. The graft copolymerization rate (R_p) for the styrene-assisted grafting with an ST-to-MA ratio of 4:1 (R_p = 0.5409 %/min) was higher than that of the grafting reaction without styrene (R_p = 0.3577 %/min). This demonstrates that the introduction of styrene to the grafting system could enhance the graft copolymerization rate of MA grafting onto DPNR.

The graft copolymers of DPNR-*g*-MA and DPNR-*g*-(MA-*co*-ST) were used as compatibilizers for vulcanized NR/ABS blends. The results showed that the mechanical, morphological, and other related properties of the blends were influenced by blend proportions, phenolic curative content and, graft copolymers. Tensile

strength and hardness of vulcanized NR/ABS blends increased with increasing ABS content while elongation at break decreased. These blends showed a greater elastic response than that of neat ABS. Thermal stability of the blends increased with an increase in the ABS component. SEM micrographs of vulcanized NR/ABS blends showed a two-phase morphology system. Finer ABS phases with smaller cavity sizes were observed for vulcanized 60/40 NR/ABS blends using NR compound with 15 phr HRJ-10518. This provides for better interfacial adhesion between the two phases and therefore resulted in superior mixing properties. Blending of NR and ABS with DPNR-*g*-MA or DPNR-*g*-(MA-*co*-ST) as a blend compatibilizer gave similar or poorer mechanical properties compared to the blends without the graft copolymer. The results obtained imply that these graft copolymers may not be fully compatible with NR and ABS which is confirmed by SEM analysis. Adding the graft copolymer as a blend compatibilizer produced a non-uniform vulcanized NR and ABS phase morphology that affected the mechanical properties.

8.2 Recommendations

A further study of this research work should be concerned with the following aspects:

1. Investigation on an improvement of grafting efficiency

To increase the efficiency of MA grafting onto DPNR, other grafting parameters should be further studied as follows: (i) type of initiator such as ammonium persulfate (APS), 2,2'-azoisobutyronitrile (AIBN), and a redox initiator of cumene hydroperoxide (CHPO) and tetraethylenepentamine (TEPA) should be investigated for comparing the results with benzoyl peroxide (BPO); and (ii) type of comonomer such as vinyl acetate and acrylonitrile should be investigated for comparing the results with styrene.

2. Investigation on a suitable application of DPNR latex

An extremely low proteins containing NR as DPNR latex is very attractive in the medical sector. The DPNR latex could be used as a good starting material for

medical applications such as latex surgical gloves and condoms being safer for patients who fall into anaphylactic reactions because of the latex-allergies.

3. Investigation on a suitable application of graft copolymers of DPNR-*g*-MA and DPNR-*g*-(MA-*co*-ST)

Since the hydrophilicity of NR is increased by grafting with MA, a graft copolymer of DPNR-*g*-MA can be used in the area of reactive blending as a blend compatibilizer or blend composition with some polar polymers. In addition, the graft copolymer so obtained with a high grafting efficiency by introducing styrene to the grafting system (DPNR-*g*-(MA-*co*-ST)) is more attractive as it has more reactive functional groups (i.e., grafted MA and ST molecules), which could be used as an efficient material for compatibilizing immiscible polymer blends. These graft copolymers do enhance adhesion between the two different phases of the blends and therefore it is expected that they could improve the mechanical properties of the blends.

It should be noted that the graft copolymers of the present study were synthesized by grafting of MA or MA with ST onto highly deproteinized natural rubber. Therefore, it would be better to blend these graft copolymers with other polymers which do not contain any protein. Poly($_L$-lactide) (PLLA) has attracted much attention because it is produced from renewable recourses and is biodegradable. However, it is difficult to use PLLA alone for industrial applications due to some inferior properties such as its rigid and brittle nature. To overcome these advantages, the PLLA is recommended to blend with a biodegradable soft polymer such as graft copolymers of DPNR-*g*-MA or DPNR-*g*-(MA-*co*-ST) to produce toughened products. It has been reported that liquid epoxidized DPNR (LEDPNR) is more effective for blending with PLLA than commercial epoxidized NR (ENR) containing proteins [106]. The oxirane group of ENR may not react with the ester group of PLLA due to the presence of proteins. To make the chemical interaction of the oxirane group of ENR with the ester group of PLLA, it is very important to remove the proteins from NR. Therefore, it is expected that the blends of PLLA with DPNR-*g*-MA or DPNR-*g*-(MA-*co*-ST) should be compatible not only due to the removal of proteins from NR

but also the total solubility parameter (δ_t) of rubber = 8.2 $cal^{1/2}/cm^{3/2}$ [100] and those for PLLA; dispersive component (δ_d) = 8.6 $cal^{1/2}/cm^{3/2}$, polar component (δ_p) = 2.6 $cal^{1/2}/cm^{3/2}$, hydrogen-bonding component (δ_h) = 2.8 $cal^{1/2}/cm^{3/2}$ that makes the total solubility parameter (δ_t) = 9.4 $cal^{1/2}/cm^{3/2}$ [107].

REFERENCES

1. Raquez J-M, Deléglise M, Lacrampe M-F, Krawczak P. Thermosetting (bio)materials derived from renewable resources: A critical review. *Progress in Polymer Science* 2010,**35**:487-509.
2. Satyanarayana KG, Arizaga GGC, Wypych F. Biodegradable composites based on lignocellulosic fibers-An overview. *Progress in Polymer Science* 2009,**34**:982-1021.
3. Mark HF. Encyclopedia of polymer science and engineering, Wiley, New York, 1970, p. 492.
4. Natural rubber statistics 2012–Malaysian Rubber Board. http://www.lgm.gov.my/nrstat/nrstats.pdf (accessed April 30, 2014).
5. Amerongen GJV, Koningsberger C, Salomon G. Chlorination of natural rubber. I. Preparation and properties of chlorinated rubber. *Journal of Applied Polymer Science* 1950,**5**:639-652.
6. Zhong J-P, Li S-D, Wei Y-C, Peng Z, Yu H-P. Study on preparation of chlorinated natural rubber from latex and its thermal stability. *Journal of Applied Polymer Science* 1999,**73**:2863–2867.
7. Chuayjuljit S, Yaowsang C, Na-Ranong N, Potiyaraj P. Oil resistance and physical properties of *in situ* epoxidized natural rubber from high ammonia concentrated latex. *Journal of Applied Polymer Science* 2006,**100**:3948-3955.
8. Nair MNR, Biju PK, Thomas GV, Nair MRG. Blends of PVC and epoxidized liquid natural rubber: Studies on impact modification. *Journal of Applied Polymer Science* 2009,**111**:48-56.
9. Tanrattanakul V, Wattanathai B, Tiangjunya A, Muhamud P. In Situ epoxidized natural rubber: Improved oil resistance of natural rubber. *Journal of Applied Polymer Science* 2003, **90**:261-269.
10. Thitithammawong A, Noordermeer JWM, Kaesaman A, Nakason C. Influence of compatibilizers on the rheological, mechanical, and morphological properties of epoxidized natural rubber/polypropylene thermoplastic vulcanizates. *Journal of Applied Polymer Science* 2008,**107**:2436-2443

11. Mahittikul A, Prasassarakich P, Rempel GL. Noncatalytic hydrogenation of natural rubber latex. *Journal of Applied Polymer Science* 2007,**103**:2885-2895.

12. Tangthongkul R, Prasassarakich P, Rempel GL. Hydrogenation of natural rubber with $Ru(CH=CH(Ph))Cl(CO)(PCy_3)_2$ as a catalyst. *Journal of Applied Polymer Science* 2005,**97**:2399-2406.

13. Arayapranee W, Rempel GL. Factorial experimental design for grafting of vinyl monomers onto natural rubber latex. *Journal of Applied Polymer Science* 2004,**93**:455-463.

14. Fukushima Y, Kawahara S, Tanaka Y. Synthesis of graft copolymers from highly deproteinised natural rubber. *Journal of Rubber Research* 1998,**1**:154-166.

15. Hinchiranan N, Suppaibulsuk B, Promprayoon S, Prasassarakich P. Improving properties of modified acrylic sheet via addition of graft natural rubber. *Materials Letters* 2007,**61** 3951–3955.

16. Intharapat P, Derouet D, Nakason C. Dynamically cured natural rubber/EVA blends: influence of NR-*g*-poly(dimethyl (methacryloyloxymethyl)phosphonate) compatibilizer. *Polymers for Advanced Technologies* 2010,**21**:310-321.

17. Kangwansupamonkon W, Gilbert RG, Kiatkamjornwong S. Modification of natural rubber by grafting with hydrophilic vinyl monomers. *Macromolecular Chemistry and Physics* 2005,**206**:2450-2460.

18. Kawahara S, Kawazura T, Sawada T, Isono Y. Preparation and characterization of natural rubber dispersed in nano-matrix. *Polymer* 2003,**44** 4527–4531.

19. Kongparakul S, Prasassarakich P, Rempel GL. Catalytic hydrogenation of styrene-*g*-natural rubber (ST-*g*-NR) in the presence of $OsHCl(CO)(O_2)(PCy_3)_2$. *European Polymer Journal* 2009,**45**:2358-2373.

20. Nakason C, Kaesaman A, Yimwan N. Preparation of graft copolymers from deproteinized and high ammonia concentrated natural rubber latices with methyl methacrylate. *Journal of Applied Polymer Science* 2003,**87**:68-75.

21. Songsing K, Vatanatham T, Hansupalak N. Kinetics and mechanism of grafting styrene onto natural rubber in emulsion polymerization using cumene hydroperoxide–tetraethylenepentamine as redox initiator. *European Polymer Journal* 2013,**49**:1007-1016.

22. Thiraphattaraphun L, Kiatkamjornwong S, Prasassarakich P, Damronglerd S. Natural rubber-*g*-methyl methacrylate/poly(methyl methacrylate) blends. *Journal of Applied Polymer Science* 2001,**81**:428–439.

23. Nakason C, Kaesman A, Homsin S, Kiatkamjornwong S. Rheological and curing behavior of reactive blending. I. Maleated natural rubber–Cassava starch. *Journal of Applied Polymer Science* 2001,**81**:2803-2813.

24. Kalkornsurapranee E, Vennemann N, Kummerlöwe C, Nakason C. Novel thermoplastic natural rubber based on thermoplastic polyurethane blends: influence of modified natural rubbers on properties of the blends. *Iranian Polymer Journal* 2012,**21**:689-700.

25. Nakason C, Kaesaman A, Samoh Z, Homsin S, Kiatkamjornwong S. Rheological properties of maleated natural rubber and natural rubber blends. *Polymer Testing* 2002,**21**:449–455.

26. Nakason C, Saiwaree S, Tatun S, Kaesaman A. Rheological, thermal and morphological properties of maleated natural rubber and its reactive blending with poly(methyl methacrylate). *Polymer Testing* 2006,**25**:656-667.

27. Nakason C, Saiwari S, Kaesaman A. Rheological properties of maleated natural rubber/polypropylene blends with phenolic modified polypropylene and polypropylene-*g*-maleic anhydride compatibilizers. *Polymer Testing* 2006,**25**:413-423.

28. Russell KE. Free radical graft polymerization and copolymerization at higher temperatures. *Progress in Polymer Science* 2002,**27**:1007-1038.

29. Shi D, Yang J, Yao Z, Wang Y, Huang H, Jing W, *et al.* Functionalization of isotactic polypropylene with maleic anhydride by reactive extrusion: mechanism of melt grafting. *Polymer* 2001,**42**:5549-5557.

30. Bettini SHP, Filho ACR. Styrene-assisted grafting of maleic anhydride onto polypropylene by reactive processing. *Journal of Applied Polymer Science* 2008,**107**:1430-1438.

31. Li Y, Xie X-M, Guo B-H. Study on styrene-assisted melt free-radical grafting of maleic anhydride onto polypropylene. *Polymer* 2001,**42**:3419-3425.

32. Saelao J, Phinyocheep P. Influence of styrene on grafting efficiency of maleic anhydride onto natural rubber. *Journal of Applied Polymer Science* 2005,**95**:28-38.

33. Chen X, Wu H, Yu J, Guo S, Luo Z. Maleic anhydride/styrene melt grafting and crosslinking onto ethylene-octene copolymer. *Polymer Engineeing and Science* 2008,**48**:2289-2296.

34. Zhao Y, Ma Y, Yao W, Huang B. Styrene-assisted grafting of maleic anhydride onto isotactic poly butene-1. *Polymer Engineering and Science* 2011,**51**:2483-2489.

35. Samay G, Nagy T, White JL. Grafting maleic anhydride and comonomers onto polyethylene. *Journal of Applied Polymer Science* 1995,**56**:1423-1433.

36. Cartier H, Hu G-H. Styrene-assisted free radical grafting of glycidyl methacrylate onto polyethylene in the melt. *Journal of Polymer Science: Part A: Polymer Chemistry* 1998,**36**:2763-2774.

37. Torres N, Robin JJ, Boutevin B. Functionalization of high-density polyethylene in the molten state by glycidyl methacrylate grafting. *Journal of Applied Polymer Science* 2001,**81**:581-590.

38. Cartier H, Hu G-H. Styrene-assisted melt free radical grafting of glycidyl methacrylate onto polypropylene. *Journal of Polymer Science Part A: Polymer Chemistry* 1998,**36**:1053-1063.

39. Carone Jr E, Kopcak U, Gonçalves MC, Nunes SP. In situ compatibilization of polyamide 6/natural rubber blends with maleic anhydride. *Polymer* 2000,**41**:5929-5935.

40. Nakason C, Kaesaman A, Supasanthitikul P. The grafting of maleic anhydride onto natural rubber. *Polymer Testing* 2004,**23**:35–41.

41. Visconte LLY, Andrade CT, Azuma C. Photosensitivity of modified natural polyisoprenes as function of the alipathic side chain. *Polymer Bulletin* 1991,**25**:217-223.

42. Kawahara S, Klinklai W, Kuroda H, Isono Y. Removal of proteins from natural rubber with urea. *Polymers for Advanced Technologies* 2004,**15**:181-184.

43. Klinklai W, Saito T, Kawahara S, Tashiro K, Suzuki Y, Sakdapipanich JT, *et al.* Hyperdeproteinized natural rubber prepared with urea. *Journal of Applied Polymer Science* 2004,**93**:555-559.

44. Nawamawat K, Sakdapipanich JT, Ho CC. Effect of deproteinized methods on the proteins and properties of natural rubber latex during storage. *Macromolecular Symposia* 2010,**288**:95-103.

45. Sansatsadeekul J, Sakdapipanich J, Rojruthai P. Characterization of associated proteins and phospholipids in natural rubber latex. *Journal of Bioscience and Bioengineering* 2011,**11**: 628-634.

46. Tarachiwin L, Sakdapipanich J, Ute K, Kitayama T, Bamba T, Fukusaki E-i, *et al.* Structural characterization of α-terminal group of natural rubber. 1. Decomposition of branch-points by lipase and phosphatase treatments. *Biomacromolecules* 2005,**6**:1851-1857.

47. Tarachiwin L, Sakdapipanich J, Ute K, Kitayama T, Tanaka Y. Structural characterization of α-terminal group of natural rubber. 2. Decomposition of branch-points by phospholipase and chemical treatments. *Biomacromolecules* 2005,**6**:1858-1863.

48. Yunyongwattanakorn J, Sakdapipanich JT, Kawahara S, Hikosaka M, Tanaka Y. Effect of gel on crystallization behavior of natural rubber after accelerated storage hardening test. *Journal of Applied Polymer Science* 2007,**106**:455-461.

49. He G, Pan Q. Synthesis of polystyrene and polystyrene/poly(methyl methacrylate) nanoparticles. *Macromolmolecula Rapid Communications* 2004,**25**:1545-1548.

50. He G, Pan Q, Rempel GL. Synthesis of poly(methyl methacrylate) nanosize particles by differential microemulsion polymerization. *Macromolecular Rapid Communications* 2003,**24**:585–588.

51. He G, Pan Q, Rempel GL. Modeling of differential microemulsion polymerization for synthesizing nanosized poly(methyl methacrylate) particles. *Industrial & Engineering Chemistry Research* 2007,**46**:1682-1689.

52. Norakankorn C, Pan Q, Rempel GL, Kiatkamjornwong S. Synthesis of poly(methyl methacrylate) nanoparticles initiated by 2,2'-azoisobutyronitrile via differential microemulsion polymerization. *Macromolecular Rapid Communications* 2007,**28**:1029–1033.

53. Taenghom T, Pan Q, Rempel G, Kiatkamjornwong S. Synthesis and characterization of nano-sized poly((butyl acrylate)-*co*-(methyl methacrylate)-*co*-(methacrylic acid)) latex via differential microemulsion polymerization. *Colloid and Polymer Science* 2013,**291**:1365-1374.

54. Wang H, Pan Q, Rempel GL. Micellar nucleation differential microemulsion polymerization. *European Polymer Journal* 2011,**47**:973-980.

55. Hassan A, Wahit MU, Chee CY. Mechanical and morphological properties of PP/NR/LLDPE ternary blend-effect of HVA-2. *Polymer Testing* 2003,**22**:281-290.

56. Mohanty S, Nando GB, Vijayan K, Neelakanthan NR. Mechanical and dynamic mechanical properties of miscible blends of epoxidized natural rubber and poly(ethylene-*co*-acrylic acid). *Polymer* 1996,**37**:5387-5394.

57. Oommen Z, Thomas S, Premalatha CK, Kuriakose B. Melt rheological behaviour of natural rubber/poly(methyl methacrylate)/natural rubber-*g*-poly(methyl methacrylate) blends. *Polymer* 1997,**38**:5611-5621.

58. Coran AY, Patel RP. Rubber-thermoplastic compositions. Part V. Selecting polymers for thermoplastic vulcanizates. *Rubber Chemistry and Technology* 1982,**55**:116-136.

59. John B, Varughese KT, Oommen Z, Potschke P, Thomas S. Dynamic mechanical behavior of high-density polyethylene/ethylene vinyl acetate copolymer blends: The effects of the blend ratio, reactive compatibilization, and dynamic vulcanization. *Journal of Applied Polymer Science* 2003,**87**:2083-2099.

60. Mousa A, Ishiaku US, Ishak ZAM. Oil-resistance studies of dynamically vulcanized poly(vinyl chloride)/epoxidized natural rubber thermoplastic elastomer. *Journal of Applied Polymer Science* 1998,**69**:1357-1366.

61. Nakason C, Nuansomsri K, Kaesaman A, Kiatkamjornwong S. Dynamic vulcanization of natural rubber/high-density polyethylene blends: Effect of

compatibilization, blend ratio and curing system. *Polymer Testing* 2006,**25**:782-796.

62. Nakason C, Wannavilai P, Kaesaman A. Effect of vulcanization system on properties of thermoplastic vulcanizates based on epoxidized natural rubber/polypropylene blends. *Polymer Testing* 2006,**25**:34-41.
63. Nakason C, Worlee A, Salaeh S. Effect of vulcanization systems on properties and recyclability of dynamically cured epoxidized natural rubber/polypropylene blends. *Polymer Testing* 2008, **27**:858-869.
64. Pechurai W, Sahakaro K, Nakason C. Influence of phenolic curative on crosslink density and other related properties of dynamically cured NR/HDPE blends. *Journal of Applied Polymer Science* 2009,**113**:1232-1240.
65. Shi Q, Stagnaro P, Cai CL, Yin JH, Costa G, Turturro A. Thermoplastic elastomers based on compatibilized poly(butylene terephthalate) blends: Effect of functional groups and dynamic curing. *Journal of Applied Polymer Science* 2008,**110**:3963-3972.
66. Thitithammawong A, Nakason C, Sahakaro K, Noordermeer JWM. NR/PP thermoplastic vulcanizates: Selection of optimal peroxide type and concentration in relation to mixing conditions. *Journal of Applied Polymer Science* 2007,**106**:2204-2209.
67. Vennemann N, Bökamp K, Bröker D. Crosslink Density of Peroxide Cured TPV. *Macromolecular Symposia* 2006,**245-246**:641-650.
68. Wang Z, Zhang X, Zhang Y. Impact properties of dynamically vulcanized nylon/styrene–acrylonitrile copolymer/nitrile rubber blends. *Polymer Testing* 2002,**21**:577-582.
69. Wei D, Mao C, Li S, Wang Z. Dynamically vulcanized nitrile butadiene rubber/acrylonitrile-butadiene-styrene terpolymer blends compatibilized by styrene-butadiene-styrene block copolymer. *Journal of Macromolecular Science, Part B: Physics* 2014,**53**:601-614.
70. Wei D, Zhao J, Liu T, Wang Z. Mechanical and morphological properties of acrylonitrile–butadiene–styrene terpolymer/nitrile butadiene rubber thermoplastic vulcanizates plasticized by dioctyl phthalate. *Journal of Thermoplastic Composite Materials* 2014:1-15.

71. Pisuttisap A, Hinchiranan N, Rempel GL, Prasassarakich P. ABS modified with hydrogenated polystyrene-grafted-natural rubber. *Journal of Applied Polymer Science* 2013,**129**:94-104.

72. Resing W. Production, processing and properties. *Natural Rubber–1st Quarter* 2000,**17**:2-3.

73. Odian G. Principles of Polymerization, 4th ed, Wiley, New York, 2004, p. 752-753.

74. Mendes PM. Stimuli-responsive surfaces for bio-applications. *Chemical Society Reviews* 2008,**37**:2512-2529.

75. Capek I, Potisk P. Microemulsion polymerization of butyl acrylate, 3. Effect of the monomer concentration. *Macromolecular Chemistry and Physics* 1995,**196**:723-737.

76. Morgan JD, Kaler EW. Particle size and monomer partitioning in microemulsion polymerization. 1. Calculation of the particle size distribution. *Macromolecules* 1998,**31**:3197-3202.

77. Jiang W, Yang W, Zeng X, Fu S. Structure and properties of poly(methyl methacrylate) particles prepared by a modified microemulsion polymerization. *Journal of Polymer Science Part A: Polymer Chemistry* 2004,**42**:733-741.

78. Xu XJ, Chew CH, Siow KS, Wong MK, Gan LM. Microemulsion polymerization of styrene for obtaining high ratios of polystyrene/surfactant. *Langmuir* 1999,**15**:8067-8071.

79. Ramirez AG, Lopez RG, Tauer K. Studies on semibatch microemulsion polymerization of butyl acrylate: Influence of the potassium peroxodisulfate concentration. *Macromolecules* 2004,**37**:2738-2747.

80. Sajjadi S. Nanoparticle formation by monomer-starved semibatch emulsion polymerization. *Langmuir* 2007,**23**:1018-1024.

81. Šebenik U, Krajnc M. Seeded semibatch emulsion copolymerization of methyl methacrylate and butyl acrylate using polyurethane dispersion: effect of soft segment length on kinetics. *Colloids and Surfaces A: Physicochemical and Engineering Aspects* 2004,**233**:51-62.

82. Sosa N, Peralta RD, López RG, Ramos LF, Katime I, Cesteros C, *et al.* A comparison of the characteristics of poly(vinyl acetate) latex with high solid

content made by emulsion and semi-continuous microemulsion polymerization. *Polymer* 2001,**42**:6923-6928.

83. Rubber Research Institute of Malaysia. SMR Bulletin No. 17; 1973.
84. Othman AB, Hepburn C, Hasma H. Influence of non-rubber constituents on elastic properties of natural rubber vulcanizates. *Plastics, Rubber and Composites Processing and Applications* 1993,**19**:185-194.
85. Dafader NC, Haque ME, Akhtar F, Ahmad MU. Study on grafting of different types of acrylic monomers onto natural rubber by γ-rays. *Radiation Physics and Chemistry* 2006,**75**:168-172.
86. Vicente AI, Campos J, Bordado JM, Ribeiro MR. Maleic anhydride modified ethylene–diene copolymers: Synthesis and properties. *Reactive and Functional Polymers* 2008,**68**:519-526.
87. Oliveira PC, Oliveira AM, Garcia A, Barboza JCS, Zavaglia CAC, Santos AM. Modification of natural rubber: A study by ^{1}H NMR to assess the degree of graftization of polyDMAEMA or polyMMA onto rubber particles under latex form in the presence of a redox couple initiator. *European Polymer Journal* 2005,**41**:1883–1892.
88. Tessier M, Marechal E. Synthesis of α-phenyl-ω-anhydride oligoisobutylene and α,ω-dianhydride oligoisobutylene. *European Polymer Journal* 1990,**26**:499-508.
89. Zhang Y, Chen J, Li H. Functionalization of polyolefins with maleic anhydride in melt state through ultrasonic initiation. *Polymer* 2006,**47**:4750–4759.
90. Thompson MR, Tzoganakis C, Rempel GL. Terminal functionalization of propylene via the Alder Ene reaction. *Polymer* 1998,**39**:327-334.
91. Aimin Z, Chao L. Chemical initiation mechanism of maleic anhydride grafted onto styrene–butadiene–styrene block copolymer. *European Polymer Journal* 2003,**39**:1291-1295.
92. Mitov Z, Velichkova R. Modification of styrene-isoprene block copolymers-3. Addition of maleic anhydride-mechanism. *European Polymer Journal* 1993,**29**:597-601.

93. Wang P, Tan KL, Ho CC, Khew MC, Kang ET. Surface modification of natural rubber latex films by graft copolymerization. *European Polymer Journal* 2000,**36**:1323-1331.

94. Huang J-W, Lu W-C, Yeh M-Y, Lin C-H, Tsai I-S. Unusual thermal degradation of maleic anhydride grafted polyethylene. *Polymer Engineering and Science* 2008,**48**:1550-1554.

95. Mehrabzadeh M, Kasaei S, Khosravi M. Modification of fast-cure ethylene–propylene diene terpolymer rubber by maleic anhydride and effect of electron donor. *Journal of Applied Polymer Science* 1998,**70**:1-5.

96. Sheshkali HRZ, Assempour H, Nazockdast H. Parameters affecting the grafting reaction and side reactions involved in the free-radical melt grafting of maleic anhydride onto high-density polyethylene. *Journal of Applied Polymer Science* 2007,**105**:1869-1881.

97. Ma P, Cai X, Lou X, Dong W, Chen M, Lemstra PJ. Styrene-assisted melt free-radical grafting of maleic anhydride onto poly(β-hydroxybutyrate). *Polymer Degradation and Stability* 2014,**100**:93-100.

98. Odian G. Principles of Polymerization, 4th ed, Wiley, New York, 2004, p. 491.

99. Chern CS. Emulsion polymerization mechanisms and kinetics. *Progress in Polymer Science* 2006,**31**:443-486.

100. Andrew JT, Kevin PJ. Blends of Natural Rubber: Novel Techniques for Blending with Speciality Polymers, Chapman & Hall: London, 1988.

101. Hansen CM. Hansen Solubility Parameters A User's Handbook; 2nd ed, CRC Press: Boca Raton, 2007.

102. Chatterjee K, Naskar K. Development of thermoplastic elastomers based on maleated ethylene propylene rubber (m-EPM) and polypropylene (PP) by dynamic vulcanization. *eXPRESS Polymer Letters* 2007,**1**:527-534.

103. Amnuaypornsri S, Sakdapipanich J, Tanaka Y. Highly purified natural rubber by saponificaion of latex: Analysis of green and cured properties. *Journal of Applied Polymer Science* 2010,**118**:3524-3531.

104. Eng AH, Ejiri S, Kawahara S, Tanaka Y. Structural characterization of natural rubber: Role of ester groups. *Journal of Applied Polymer Science: Applied Polymer Symposium* 1994,**53**:5-14.

105. Kawahara S, Kakubo T, Nishiyama N, Tanaka Y, Isono Y, Sakdapipanich JT. Crystallization behavior and strength of natural rubber: Skim rubber, deproteinized natural rubber, and pale crepe. *Journal of Applied Polymer Science* 2000,**78**:1510-1516.

106. Nghia PT, Siripitakchai N, Klinklai W, Saito T, Yamamoto Y, Kawahara S. Compatibility of liquid deproteinized natural rubber having epoxy group (LEDPNR)/Poly ($_L$-Lactide) blend. *Journal of Applied Polymer Science* 2008,**108**:393-399.

107. Agrawal A, Saran AD, Rath SS, Khanna A. Constrained nonlinear optimization for solubility parameters of poly(lactic acid) and poly(glycolic acid)-validation and comparison. *Polymer* 2004,**45**:8603-8612.

APPENDIX

Appendix A

The Overall Compositions in NR Latex

Table A- 1 The overall compositions in NR latex.

Parameters	Unit	Tested results[a]
Total solid content (TSC)	% by mass	61.7005
Dry rubber content (DRC)	% by mass	60.0544
pH value at 25.7 °C	-	10.49
KOH number	% by mass	0.5523
Alkalinity (as ammonia on total weight)	% by mass	0.6896
Alkalinity (as ammonia on water phase)	% by mass	1.8005
Non rubber content (NRC)	% by mass	1.6461
Volatile fatty acid number (VFA)	-	0.0329
Mechanical stability time (MST) at 55% TSC	sec	650
Specific gravity (SG) at 25 °C	-	0.9438
Magnesium (Mg) content	ppm	22.50
Viscosity at 60% TSC spindle no. 1 at 60 rpm	cps.	69.0
Coagulum content (80 mesh)	ppm	24.0

[a] Test are performed by Thai Rubber Latex Corporation (Thailand) Public Company Limited Testing Laboratory. All tested results are performed according to ISO 2004 specification.

Appendix B

The Physical Properties of ABS

Table B- 1 The physical properties of ABS[a].

Physical properties	Method	Unit	Value
Melt flow index (10 kg/220 °C)	ASTM D1238	g/10min	17
Izod Notched Impact (1/4", 23 °C)	ASTM D256	Kg-cm/cm	36
Tensile Strength at Yield (23 °C)	ASTM D638	kg/cm^2	420
Flexural Strength at Yield (23 °C)	ASTM D790	kg/cm^2	570
Flexural Modulus (23 °C)	ASTM D790	$x10^4 kg/cm^2$	2.05
Rockwell Hardness (1/4", 23 °C)	ASTM D785	R-Scale	109

[a]Acrylonitrile-butadiene-styrene (ABS, SP200) is manufactured by the IRPC Public Co., Ltd., Rayong, Thailand. The weight ratio of acrylonitrile: butadiene: styrene is 24:19:57.

VITA

Mr. Pinyo Wongthong was born on March 22, 1979 in Sisaket, Thailand. He received his B.Sc. degree (Second class honors) in Chemistry, Faculty of Science, Khon Kaen University in 2002 and received M.Sc. degree in Chemistry, Faculty of Science, Kasetsart University in 2005. Pinyo joined the doctoral degree program in Petrochemistry Program, Faculty of Science, Chulalongkorn University since 2009 and finished his study in 2014. He received a Royal Golden Jubilee Ph.D. Scholarship (RGJ-Ph.D.) from the Thailand Research Fund (TRF) and Chulalongkorn University.

International Publications:

1. Wongthong, P.; Nakason, C.; Pan, Q.; Rempel, G.L. Kiatkamjornwong, S. Modification of deproteinized natural rubber via grafting polymerization with maleic anhydride. Eur. Polym. J. 2013, 49, 4035–4046.

2. Wongthong, P.; Nakason, C.; Pan, Q.; Rempel, G.L. Kiatkamjornwong, S. Styrene-assisted grafting of maleic anhydride onto deproteinized natural rubber, Eur. Polym. J. 2014, 59, 144–155.

3. Wongthong, P.; Nakason, C.; Pan, Q.; Rempel, G.L. Kiatkamjornwong, S. Effect of NR/ABS ratio on mechanical, dynamical and morphological properties of vulcanized NR/ABS blends, Adv. Mater. Res. 2014, 844, 61–64.

4. Wongthong, P.; Nakason, C.; Pan, Q.; Rempel, G.L. Kiatkamjornwong, S. Influences of phenolic curative content and blend proportions on properties of vulcanized NR/ABS blends, J. Appl. Polym. Sci. 2014, under review.

Patent:

1. Wongthong, P.; Nakason, C.; Pan, Q.; Rempel, G.L.; Kiatkamjornwong, S. Grafting of maleic anhydride onto deproteinized natural rubber via differential microemulsion polymerization technique. Application number 1401001490, Thai patent (March 19, 2014).